



**KTH Industrial Engineering  
and Management**

# **Renewables-driven membrane distillation for drinking water purification: Main Ethiopian Rift Valley case study**

**Andrea Gabaldón Moreno**

**Master of Science Thesis**

KTH School of Industrial Engineering and Management

Energy Technology TRITA-ITM-EX 2018:615

Division of Heat and Power Technology

SE-100 44 STOCKHOLM

**Master of Science Thesis EGI 2018: TRITA-ITM-EX 2018:615**



**KTH Industrial Engineering  
and Management**

**Renewables-driven membrane distillation for  
drinking water purification: Main Ethiopian  
Rift Valley case study**

Andrea Gabaldón Moreno

Approved	Examiner <b>Andrew Martin</b>	Supervisor <b>Imtisal-e Noor</b>
	Commissioner	Contact person

## ABSTRACT

Fluoride is present in all type of water sources, but levels beyond the current World Health Organization guideline of 1.5 mg/L can be very harmful for people's health. Due to the volcanic nature of rocks in the Ethiopian Rift Valley, groundwater is contaminated with fluoride, and studies have even recorded levels up to 26 mg/L. These excessive levels are affecting more than 14 million women and children in Ethiopia. Providing population with safe and clean water could help to achieve the Sustainable Development Goal 6 (i.e. Ensure availability and sustainable management of water and sanitation for all) from the United Nations. Membrane distillation systems have been extensively tested in literature, proving to be effective in removing fluoride, even at higher concentration levels (500 mg/L). Membrane distillation is a heat driven system that works under feed water temperatures below 100 °C. Renewable energy sources such as geothermal, solar or biomass can be used to provide that heat. This report evaluates techno-economically different technologies using TRNSYS: flat plate solar collectors, evacuated tube solar collectors and biogas from animal dung, as heat source for the membrane distillation unit. The size of the hypothetical installations was optimized to cover the demand of 30 households. Several indicators were calculated to compare the different technologies: specific energy demand, water production, and efficiency of the systems. Investment costs and operation and management costs were considered to calculate total costs and payback period of the different installations. The results show that the best techno-economic option to be installed is a hybrid model that includes a combined heat and power unit powered by biogas and evacuated tube collectors, as can meet the demand with one membrane distillation unit and also supplies electricity and biogas for cooking. However, depending on the specific location, the availability of solar radiation and manure can vary, and consequently the best option will change. In case the existence of livestock is limited, three membrane distillation units coupled with 85 m<sup>2</sup> of evacuated tube collectors can cover the demand. If the availability of sun is limited one membrane unit coupled with a standalone biogas unit can be considered. Flat plate collectors are never the best option, as they require the biggest investment cost. Nevertheless, the existence of local manufacturers can decrease the costs.

**Master of Science Thesis EGI 2018: TRITA-ITM-EX 2018:615**



**KTH Industrial Engineering  
and Management**

**Förnybar energi-driven membrandestillering  
för rening av dricksvatten: Main Ethiopian  
Rift Valley fallstudie**

Andrea Gabaldón Moreno

Approved	Examiner <b>Andrew Martin</b>	Supervisor <b>Imtisal-e Noor</b>
	Commissioner	Contact person

## SAMMANDRAG

Fluor finns i alla typer av vattenkällor, men koncentrationer som ligger över nuvarande Världshälsoorganisationens riktlinjer (max 1.5 mg/L) kan vara skadlig för hälsan. Grundvatten vid Ethiopian Rift Valley innehåller höga fluorhalter på grund av geologiska orsaker, och studier har visat nivåer upp till 26 mg/L. Sådana höga halter påverkar över 14 miljoner Etiopiska kvinnor och barn negativt. Att tillgodose befolkningen med säkert och rent dricksvatten skulle bidra till uppfyllelsen av FN:s Hållbarhetsmål nr 6 (Säkerställa tillgång till och hållbar vatten- och sanitetsförvaltning för alla). Membrandestillering har testats grundligt och har visat sig att vara en effektiv teknik för fluorseparatoring även vid höga halter (över 500 mg/L). Membrandestillering är en värmedriven process som utnyttjar källor under 100 °C. Värmen kan fås från förnybara energikällor som geotermisk energi, solenergi och biobränsle. Denna rapport presenterar en tekno-ekonomisk utvärdering av olika teknik med TRNSYS: plan solfångare, vakuumsolfångare och biogas från boskapsgödsel.

Storleken hos de undersökta systemen optimerades för att täcka behovet av 30 hushåll. Flera indikatorer beräknades för att jämföra de olika teknikerna: specifika energibehov, vattenproduktion och systemens verkningsgrader. Investeringskostnaderna och drift- och underhållskostnaderna låg som grund för att bestämma bruttokostnaderna och återbetalningstiderna av de olika systemen. Resultaten visar att den mest fördelaktiga konfigurationen består av en hybrid av biogas och vakuumsolfångare. Detta system tillgodoser vattenbehovet och dessutom levererar el och gas för matlagning. Tillgången till solenergi och gödsel spelar en viktig roll när det gäller systemvalet. Om tillgång till gödsel är begränsad kan efterfrågan täcks genom tre membrandestilleringsenheter kopplade till 85 m<sup>2</sup> vakuumsolfångare. Däremot om solenergin är begränsad kan ett system med en membrandestilleringsenhet kopplade till en biogasanläggning tillgodose vattenbehovet. Plan solfångare är aldrig ett bra alternativ eftersom de kräver höga investeringskostnader. Tillgång till lokal tillverkning kan dock minska sådana kostnader.

## RESUMEN

El flúor está presente en todo tipo de recursos hídricos, pero consumir agua con concentración de flúor por encima del actual límite (1.5 mg/L) de la Organización Mundial de la Salud puede ser muy dañino para la salud de las personas. Debido a la naturaleza volcánica de las rocas en el Valle del Rift de Etiopía, el agua subterránea está contaminada con flúor, y los estudios incluso han registrado niveles de hasta 26 mg/l. Estos niveles excesivos están afectando a más de 14 millones de mujeres y niños de Etiopía. Proporcionar a esa población agua segura y limpia podría ayudar a alcanzar el Objetivo de Desarrollo Sostenible 6 (Garantizar la disponibilidad y la gestión sostenible del agua y el saneamiento para todos) de la ONU. Los sistemas de destilación por membrana han sido probados y han demostrado ser efectivos para eliminar el flúor incluso con agua con concentraciones altas de flúor (500 mg/L). La destilación por membrana es un sistema impulsado por calor que funciona con temperaturas por debajo de los 100 °C. Fuentes de energía renovables como geotermia, solar o biomasa pueden usarse para proporcionar ese calor. Esta tesis evalúa tecno-económicamente diferentes tecnologías usando TRNSYS: colectores planos, colectores de tubos de vacío y biogás a partir de estiércol animal, como fuente de calor para la unidad de destilación por membrana. El tamaño de las instalaciones se optimizó para cubrir la demanda de 30 hogares. Se calcularon varios indicadores para comparar las diferentes tecnologías: consumo térmico específico, producción de agua y la eficiencia de los sistemas. Se consideraron los costes de inversión y los costes de operación y mantenimiento para calcular los costes totales de la instalación y el período de amortización de las diferentes instalaciones. Los resultados muestran que la mejor opción tecno-económica es un modelo híbrido que combina colectores de tubos de vacío y una unidad de producción de calor y electricidad alimentada con biogás. Ésta puede satisfacer no solo la demanda con una unidad de destilación de membrana sino también suministrar electricidad y biogás para cocinar. Sin embargo, dependiendo de la ubicación específica de la instalación, la disponibilidad de radiación solar y el estiércol puede variar y, en consecuencia, la mejor opción cambiará. En caso de que la existencia de ganado sea limitada, tres unidades de destilación de membrana junto con 85 m<sup>2</sup> de colectores de tubo evacuados pueden cubrir la demanda. Si la disponibilidad de sol es limitada, se puede considerar dos unidades de destilación por membrana con una unidad de biogás autónoma. Los colectores planos nunca son la mejor opción, ya que requieren el coste de inversión más alto. Sin embargo, la existencia de fabricantes locales puede disminuir los costes.

## ACKNOWLEDGEMENTS

I would like to thank all those who have helped me in carrying out the master thesis. First, I would like to express my very great appreciation to Imtisal-e Noor for her incredible support, friendship and advice that provided me while conducting this master thesis, and for supervising me from the very beginning. To my examiner, Dr. Andrew Martin at KTH, for the support to conduct this project. To Scarab Development AB for giving me the great opportunity to work with them; the assistance provided by Daniel Woldemariam is greatly appreciated.

Last, but by far not least, I would like to thank all my friends who provided me with very valuable support. I would like to make a special mention of Alberto, for supporting me and standing by my side from the beginning to the end of this thesis, it would not have been possible without you. Finally, special gratitude to my family who motivated me all these years to finish my studies and gave me the opportunity to go abroad twice.

## TABLE OF CONTENTS

Abstract.....	2
Resumen.....	3
Acknowledgements.....	4
Table of Contents.....	5
List of Figures.....	6
List of Tables.....	7
Abbreviations.....	8
Nomenclature.....	8
1 Introduction.....	9
1.1 Context.....	9
1.2 Objectives.....	11
1.3 Methodology.....	11
2 Background.....	13
2.1 Ethiopia.....	13
2.1.1 Introduction to Ethiopia.....	13
2.1.2 Climate in Ethiopia.....	15
2.1.3 Fluoride problem in Ethiopia.....	15
2.1.4 Renewable energy potential in Ethiopia.....	16
2.2 Membrane distillation.....	21
2.2.1 Membrane distillation review.....	21
2.2.2 HVR and Scarab Development AB.....	23
2.2.3 Renewable energy technologies driving air gap membrane distillation.....	25
3 AGMD model using Minitab.....	26
4 Analysis with TRNSYS.....	27
4.1 TRNSYS model.....	28
4.1.1 AGMD module specification.....	28
4.1.2 Tank commercial specifications.....	29
4.1.3 Solar case.....	29
4.1.4 Biogas case.....	32
4.1.5 Hybrid case.....	35
4.2 TRNSYS results.....	37
4.2.1 Solar case.....	37
4.2.2 Biogas case.....	42
4.2.3 Hybrid case.....	43
5 Economic analysis.....	45
5.1 Economic Results.....	47

6	Techno-economic discussion.....	51
7	Conclusion and Outlook.....	53
8	Bibliography.....	55
9	Appendices.....	63

## LIST OF FIGURES

Figure 1 – Fluoride occurrence in groundwater in Africa [10] .....	9
Figure 2 – Methodology .....	12
Figure 3 – Regions of Ethiopia (Own elaboration. Based on [39]).....	13
Figure 4 – Fluoride content in Ethiopia [11] .....	14
Figure 5 – Drinking water service levels in 2015 (Own elaboration based on [44]).....	14
Figure 6 – Temperature and radiation hourly averages (Information obtained from Climate consultant software. On the left Awassa station: 7°N 38°E Elevation 1652m. On the right Addis Ababa station: 9°N 38°E Elevation 2355m [46]) .....	15
Figure 7 – Fluoride concentration in different water sources (Own elaboration. Based on [49]).....	16
Figure 8 - Optimal electrification mix in Ethiopia – GIS-based analysis [54]: Figure on the left shows electricity access targets: 150 and 300 kWh/capita/year for the rural and urban areas respectively; Figure on the right shows electricity access targets of 50 and 300 kWh/capita/year for the rural and urban areas respectively. ....	18
Figure 9 – Global horizontal irradiation (left) and direct normal irradiation (right) [56] .....	18
Figure 10 – Geothermal prospect areas in the Ethiopian Rift [67, 65].....	20
Figure 11 – Different types of MD configuration [79] .....	22
Figure 12 – Air Gap membrane distillation scheme (own elaboration) .....	22
Figure 14 – AGMD Module [76].....	24
Figure 15 – AGMD cassette [75].....	24
Figure 16 – Temperature from the well.....	28
Figure 17 – Stratified tank scheme (left) [95]. TRNSYS tank specifications (right). ....	29
Figure 18 – Scheme solar installation.....	30
Figure 19 – Scheme TRNSYS FPC model.....	32
Figure 20 – Scheme TRNSYS ETC model.....	32
Figure 21 – Biogas scheme .....	33
Figure 22 – Electricity demand 1 household in Watts (Own elaboration: based on [21]) .....	34
Figure 23 – Biogas TRNSYS diagram.....	35
Figure 24 – Hybrid scheme (ETC+CHP unit using biogas).....	36
Figure 25 – Hybrid TRNSYS diagram.....	37
Figure 26 – Simulation results for different solar field, with 2,3 and 4 AGMD units (in parallel) driven by FPC.....	38
Figure 27 – FPC Results for different dates a) April ,b) August and, c) December.....	39
Figure 28 – ETC for different sizes.....	40
Figure 29 – ETC Results for different dates a) April ,b) August and, c) December.....	41
Figure 30 – Biogas case .....	42
Figure 31 – Hybrid results.....	43
Figure 32 – Results hybrid case seasonally a) April ,b) August and, c) December .....	44
Figure 33 – Payback period (years) with a constant water cost (0.062 €/L),.....	48
Figure 34 – NPV sensitivity analysis (water cost constant = 0.062 €/L) for the Hybrid case.....	49
Figure 35 – PB sensitivity analysis (water cost constant = 0.062 €/L) for the Hybrid case. ....	49
Figure 36 – Water cost sensitivity analysis (PB constant = 10 years) for the Hybrid case.....	50

Figure 37 – Mean monthly rainfall variability [39] .....	63
Figure 38 – Temperature variation at the Awassa weather station (7°N 38E, Elevation 1652m [46]).....	63
Figure 13 – Heat transfer in AGMD (own elaboration based on [33, 36, 75]) .....	67
Figure 39 – cross-section of a basic flat-plate solar collector [113].....	69
Figure 40 – cross section of a evacuated tube solar collector [115] .....	69
Figure 41 – Schematic of a fixed-dome biogas plant [62].....	71

## LIST OF TABLES

Table 1 – Energy potential in Ethiopia [51, 40] .....	17
Table 2 – Existing Power Plants Installed Capacity [40].....	17
Table 3 – Livestock biomass potential in Ethiopia [63].....	19
Table 4 – Livestock holding types [21]. Percent among Livestock owning households by livestock type, region and place of residence. Ethiopia 2015/2016 .....	19
Table 5 – Advantages, disadvantages and applications of different technologies [36, 76, 33].....	23
Table 6 – AGMD characteristics (Provided from HVR and Scarab Development AB) .....	24
Table 7 - Permeate fluxes from different feed and cooling water temperatures at different flow rates [33] .....	25
Table 8 – Range of data.....	26
Table 9 – Minitab results summary .....	26
Table 10 – Modules by working hours .....	28
Table 11 – Equation block called “Membrane” .....	28
Table 13 – IAM coefficients for Apricus ETC.....	30
Table 12 – Data inputs to TRNSYS.....	31
Table 14 –Solar Pump characteristics .....	31
Table 15 –AGMD Pump characteristics .....	31
Table 16 – Biogas Specifications [97].....	33
Table 17 – CHP catalog Data Specifications Vitobloc 200 EM-9kW/20kW <sub>th</sub> [98] .....	33
Table 18 – Equation block called “Hybrid” .....	34
Table 19 – Digester specifications .....	34
Table 20 –AGMD Pump characteristics .....	35
Table 21 – CHP catalog Data Specifications Vitobloc 200 EM 6/15 [101] .....	35
Table 22 – Equation block called “Hybrid” .....	36
Table 23 – Solar results.....	37
Table 24 – Biogas summary.....	42
Table 25 – Hybrid optimize result.....	43
Table 26 – Capital costs FPC case.....	45
Table 27 – Capital costs ETC case .....	45
Table 28 – Capital costs CHP Biogas case .....	45
Table 29 – Capital costs hybrid case.....	46
Table 30 – Economic results for different cases .....	47
Table 31 - Summary results .....	52
Table 32 – Guideline values for naturally occurring chemicals that are of health significance in drinking-water [48] .....	64
Table 33 – JMP Definitions of water supply and sanitation [110] .....	65
Table 34 – Fluoride consequences [9, 10] .....	65
Table 35 – Defluoridation technologies review [10, 32, 31].....	66

## ABBREVIATIONS

AGMD	Air Gap Membrane Distillation
CHP unit	Combined Heat and Power unit
CPI	Consumer's Price Index
DF	Dental Fluorosis
DR	Discounted Rate
ETC	Evacuated Tube Collectors
FPC	Flat Plate Collectors
IRR	Internal Rate of Return
MD	Membrane distillation
MERV	Main Ethiopian Rift Valley
PB	Payback period
WHO	World Health Organisation

## NOMENCLATURE

$c_p$	[kJ/kgK]	Specific heat capacity
$\dot{m}_h$	[kg/s]	Mass flow on the hot side of MD
$\dot{m}_p$	[kg/s]	Mass flow of the permeate
$T_{hi}$	[°C]	Hot feed inlet temperature
$T_{ho}$	[°C]	Hot feed outlet temperature
$\dot{m}_{MD}$	[kg/s]	Mass flow on the MD (hot and cold side)
$\dot{m}_{col}$	[kg/s]	Mass flow on the collector
$T_{col,out}$	[°C]	Collector hot outlet temperature
$T_{col,in}$	[°C]	Collector cold inlet temperature

# 1 INTRODUCTION

## 1.1 Context

Water is fundamental to sustainable development, being the core of socio-economic development, healthy ecosystems and human survival [1, 2]. Among the Sustainable Development Goals (SDGs) there is one dedicated to water and sanitation (SDG 6), which intends to “achieve universal and equitable access to safe and affordable drinking water for all” by 2030 [3]. Currently, 2.1 billion people drink from contaminated water all over the world, and more than a third of the global population is affected by water scarcity [4]. Furthermore, water availability is becoming less predictable in many places due to droughts, rainfall variability, higher temperatures and extreme weather conditions, and ensuring that everyone has access to safe and clean water is critical [5].

Water from deep wells is usually assumed to be clean and healthy, with no bacteria. However, due to the variation of geology and water/rock interactions, many chemical elements can be found in such water resources [6]. Fluoride, for instance, can be found in water wells in the East African Rift Valley, which starts from the Jordan Valley and continues down through Sudan, Ethiopia, Uganda, Kenya and Tanzania (See Figure 1). In some areas, uranium (U) and arsenic (As) can also be found [7, 8]. These elements, in long-term intakes are harmful for humans. The intakes beyond 1.5 mg/L fluoride levels can result in dental fluorosis (DF) or problems in the skeleton [9].

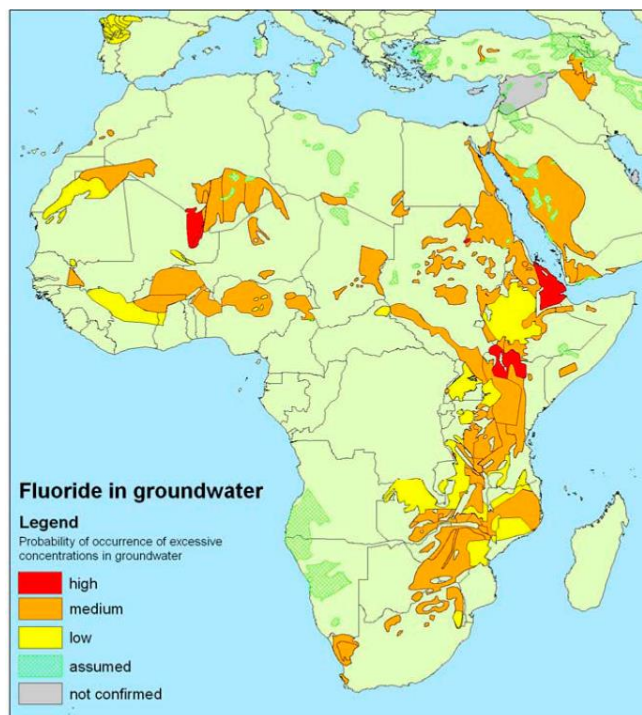


Figure 1 – Fluoride occurrence in groundwater in Africa [10]

Ethiopia has many groundwater resources, and the access to these resources is important for local population and for their economic development (e.g. agriculture, livestock, industry, tourism) [11]. However, donors, NGOs and governments have built water points without thinking about the cost associated to keep them clean and functioning over time [12, 13, 14]. It has been found that over 40% of the Ethiopian wells are contaminated of fluoride (See Figure 4). Levels up to 26 mg/L have been found in the Main Ethiopian Rift Valley (MERV) [15]. It is estimated that more than 14 million people in the Ethiopian Rift Valley still rely on fluoride-contaminated drinking water [15]. Additionally, several studies have observed health problems among Ethiopians associated to the consumption of fluoridated water, such as DF and skeletal fluorosis [16, 17, 18, 19].

According to WHO, the way to mitigate fluoridated water is: *first to identify alternative sources of potable water with low fluoride content, secondly to dilute high fluoride water with low fluoride water to attain a mass balance of within 1.5 mg/L, thirdly to use high calcium, magnesium and vitamin C diets and finally, when all these may not be feasible; to remove fluoride from water to meet the required level of 1.5 mg/L* [10]. Surface water in Ethiopia is polluted due to the lack of sanitation [20]. On the other hand, Ethiopian diet is mainly based in cereals [21], and can lack vitamin C [7]. This puts Ethiopian health at risk for cases where fluoride levels slightly exceed WHO recommendations (No diet can compensate excessively high fluoride intake) [10].

Defluoridating water for drinking and cooking purposes can be done by using methods such as bone charcoal adsorption [22], electrodialysis [23], ion exchange [24], nanofiltration [25], contact precipitation [26], sedimentation using aluminium sulfate (Nalgonda process) [27], activated alumina adsorption [28], reverse osmosis(RO) [29] or membrane distillation(MD) [30]. Bone charcoal is not universally accepted and its fluoride removal efficiency is unknown [10], whereas the fluoride-removal efficiencies for the rest of the processes are: between 70-90% for Nalgonda process, up to 90% for adsorption processes, 85-95% in electrodialysis, from 60 to 90% in ion exchange, and up to 99.5% in MD process [31]. RO powered by PV is seen as an interesting solution for large-scale systems, especially for desalination. However, the separation efficiency of fluoride is only 90-95%, can be more expensive and can have more leakages [10, 32, 31]. MD has gained importance, as it is the most efficient technology and can remove other metals like arsenic [33]. Moreover, MD can be solar-thermal driven and applied it to small/medium scale systems [34]. Besides that, by combining MD with renewable energy technologies in stand-alone systems can provide access to clean water and energy access in remote areas. Consequently, integrated systems such as membrane processes that use waste heat or renewable energies have attracted much interest lately [35].

Solar thermal collectors, geothermal or waste heat from a biogas engine can be used to power the membrane distillation process, since this method requires feed temperatures ranging from 60 to 90°C [36]. The system also needs electricity for circulation pumps and control systems, which can be provided by the power grid, PV or biomass. The integrated production of electricity can additionally improve rural access to this service. Polygeneration systems with biomass can provide biogas for cooking as well [36, 37]. Therefore, systems integrating renewable energies and membrane distillation can be more energy-efficient, since almost all the flows and products in the systems can be used, help to decrease global greenhouse gas emissions and improve living standards of rural communities by providing several services [36]. Studying the techno-economic viability of these systems benefits and informs both investors and policy makers.

## 1.2 Objectives

The main objective of this project is to analyze the technical and economic feasibility of renewable driven MD systems to remove the fluoride from well water in the MERV. This objective can contribute to achieving the United Nations Agenda 2030 for Sustainable Development and the Sustainable Development Goals (SDG). By enhancing water quality in the MERV, this project directly addresses SDG 6, i.e. *ensure availability and sustainable management of water and sanitation for all* [3]. Additionally, the present study indirectly addresses other issues contained in the SDGs such as ensuring a better health (SDG3), and consequently improving the possibility to receive a better education (SDG 4), among others. To that end, a membrane distillation (MD) unit coupled with different renewable technologies are assessed. For the purpose, the MD experimental data is provided by the Swedish Company Scarab Development AB. The specific objectives of this master thesis are:

- Compare techno-economically different energy technologies
- Design a renewable energy system integrating MD
- Estimate the capital and operation and maintenance (O&M) costs for the entire plant
- Perform a sensitivity analysis of the economic variables, evaluation the effects on drinking water costs, the benefits at the end of the installations' lifetime and the time to recover the investment.

By fulfilling these objectives, a framework for the future development of rural purification plants using MD in Ethiopia can be developed.

## 1.3 Methodology

First, a literature study of the situation in Ethiopia and MD-polygeneration systems are investigated. The background information provides a picture of Ethiopia regarding fluoride levels in well waters, rural situation, renewable energy potential, etc., and explores the different alternatives of water purification and polygeneration systems integrating MD.

Further, a preliminary demand analysis is performed assuming the following demands for 30 households in the MERV: water demand, electricity demand of the system and households, and cooking demand. Assuming an initial size of the main components of the system (e.g. solar collector area, size of pumps, pipes, storage tank and biogas combined heat and power), equipment-performance data is obtained from different commercial catalogs. To create a membrane distillation model inside TRNSYS, experimental data is introduced in Minitab and a regression statistical model is performed using the software in order to estimate the relationships between dependent variables (yield production and outlet temperatures in the MD) and indirect variables (inlet temperature and inlet feed flows). Thereafter, the following systems are evaluated in TRNSYS: evacuated tube collectors (ETC), flat plate collectors (FPC) and a biogas combined heat and power (CHP). The following data is introduced inside TRNSYS: the MD model from Minitab; commercial catalog data from the ETC, FPC and CHP; and weather data from Addis Ababa station. With the variability of the main variables (temperatures, flows, yield production, sun radiation, etc) from TRNSYS are used to optimize the components size. After knowing which systems are more suitable to be integrated with the membrane distillation unit, a detailed technical and economic analysis is done with the optimized solutions. With the best techno-economic option, a sensitivity analysis is performed. Finally, a techno-economic comparison of the results is discussed.

This master thesis is primarily concerned with the technical and economic analysis of the above mentioned technologies. The methodology that has been followed aims to estimate the size of the installations and calculate technical (efficiency, specific thermal demand and operation during a day) and economic indicators (net present value, payback, internal rate of return) to compare the technologies. Neither an environmental impact nor other approaches explicitly mentioned (e.g. policy or institutional aspects) are analyzed due to time constraints. Furthermore, brine disposal is not considered in the analysis due to time constraints and lack of data.

The methodology can be summarized in the following diagram:

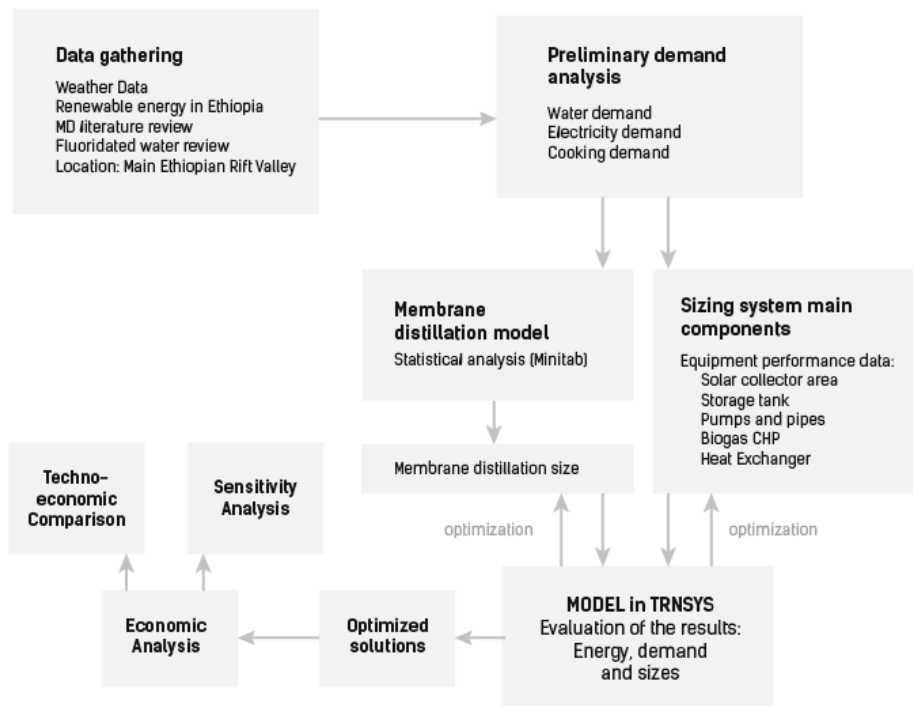


Figure 2 – Methodology

## 2 BACKGROUND

### 2.1 Ethiopia

In this section general data focused on Ethiopia is gathered. Socio-economic context and water problem are firstly discussed. In order to know which energy technologies are suitable for the membrane distillation unit, the current Ethiopian energy context and the potential of different renewable energy technologies (i.e. solar, biomass and geothermal potential) are evaluated. Climate is also examined, as plays an important role for solar energy.

#### 2.1.1 Introduction to Ethiopia

Ethiopia, with a surface area of 1.1 million km<sup>2</sup> [38], is located in the horn of Africa with a population of more than 102 million people (2016). As can be seen in Figure 3, Ethiopia is surrounded by Sudan, South Sudan, Kenya, Somalia, Djibouti and Eritrea. Ethiopia is divided into 9 federal states named as: Tigray, Afar, Amhara, Benishangul Gumaz, Gambela, Harari, Somali, Southern Nations Nationalities and Peoples' (SNNP) and Oromia<sup>1</sup> and two administration cities: Addis Ababa and Dire Dawa. SNNP and Oromia are the most populated regions: SNNP with 20% and Oromia with 40% of the population share [21], especially in the Main Ethiopian Rift Valley (MERV) area [39].

Ethiopia is characterized by a very young population that is growing fast (2.3% every year) and a high annual Gross Domestic Product (GDP) growth rate of 10%, with a GDP per capita of \$691 in 2014/2015 [40]. 46.6% of the GDP is associated to agriculture, which accounts for 85% of total employment [41] and is practiced by 98% of rural households, being cattle the most common livestock type. Cereals (rice, sorghum, barley and wheat) are widely cultivated, and Teff is the most commonly consumed food item. Urban areas usually consume a more diverse diet. Food availability is seasonal, where the major slack months are planting seasons (April to October) [21].

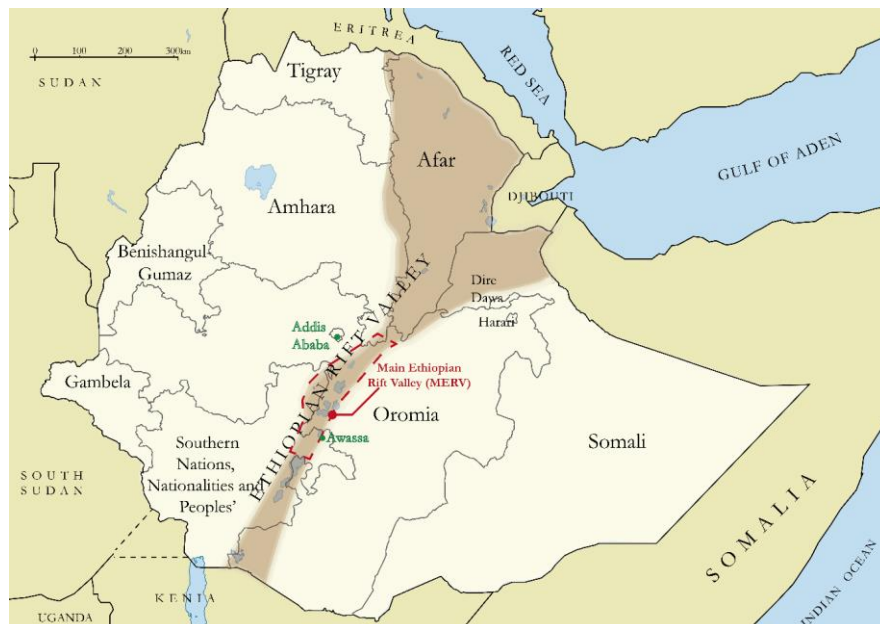


Figure 3 – Regions of Ethiopia (Own elaboration. Based on [39])

The Rift Valley is a fault between the Arabian and African plates. It is the longest rift on Earth, with 6300 km, from the Jordan Valley down through Sudan, Ethiopia, Uganda, Kenya and Tanzania. The Ethiopian Rift Valley runs in a south-westerly direction through the whole country (See Figure 3). The rift is

---

<sup>1</sup> Depending on the literature this region is called “Oromiya” or “Oromia”. In this document will be referred as Oromia.

characterized by its volcanic and geothermal activity, which makes lakes alkaline and causes high contents of metals in groundwater. Water with high metal contents are not suitable for human consumption [17, 10] yet the population relies on potentially contaminated well water because wells were considered a clean and safe option [12, 13, 14]. Figure 5 shows that most people in Oromia and SNNP regions drink from an unimproved facilities and surface water is often unavailable [17]. Only the region of Addis Ababa and Dire Dawa have made improvements in safe water access.

The most densely populated area in the Ethiopian Rift Valley can be found in the Main Ethiopian Rift Valley (MERV), which is part of SNNP (Southern Nations, Nationalities and People’s region) and Oromia regions [42], with densities of 150 to 300 people/km<sup>2</sup> [39]. Figure 4 shows that in the MERV, located in the middle of the country (where the red spots in the map are indicated), fluoride levels beyond 7.1 mg/L have been found, and most of the water sources have contents beyond the WHO guidelines [11]. Usually, people who lack in access to clean water, also lack access to electricity. In Ethiopia, only 27% of the population has access to electricity, being 12% in rural areas [43].

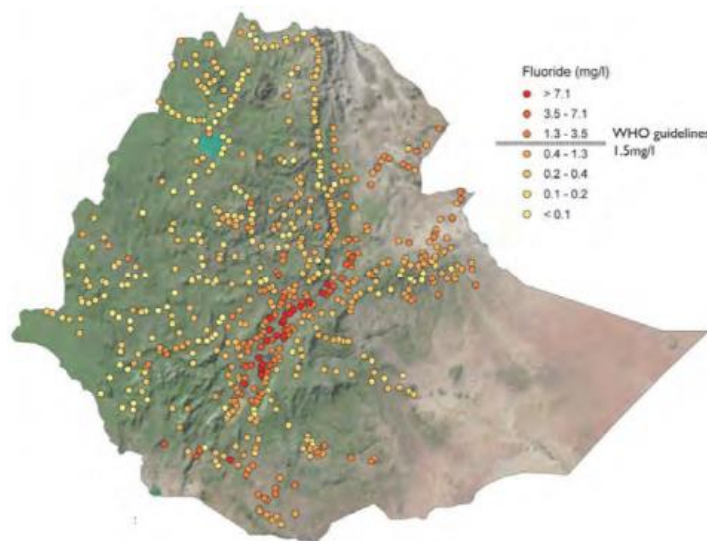


Figure 4 – Fluoride content in Ethiopia [11]

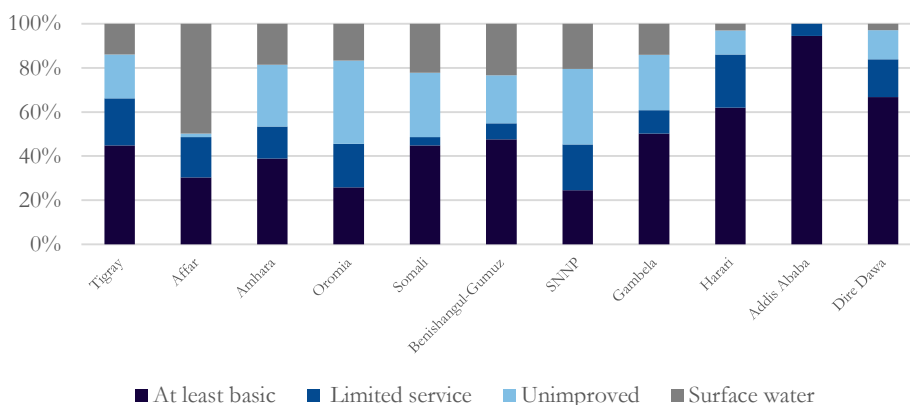


Figure 5 – Drinking water service levels in 2015 (Own elaboration based on [44])

(At least basic): Drinking water from an improved source, provided collection time is not more than 30 minutes for a roundtrip including queuing; (Limited service): Drinking water from an improved source for which collection time exceeds 30 minutes for a roundtrip including queuing; (Unimproved): Drinking water from an unprotected dug well or unprotected spring. (Surface water): Drinking water directly from a river, dam, lake, pond, stream, canal or irrigation canal.

## 2.1.2 Climate in Ethiopia

The climate in Ethiopia varies from region to region. There are three major climatic zones: desert areas with low or no rainfall in the east, north and south of the country; the west zone with one rainfall period; and the east and lowlands of south and southeast with two rainy seasons [45]. Cities of Addis Ababa and Awassa have weather data stations with similar latitudes and both have one rainy season (from March to October) [45]. These locations close to the MERV are used to analyze how is the weather in the MERV (Figure 6) as there is not an exact weather data station in there. Both locations have similar temperature and radiation variability as can be seen in Figure 6. Temperature vary from 5°C to 27°C, but minimum and maximum temperatures of 2.8°C and 32.2°C have been recorded [46]. There is little season variability, but nights are colder and days are hotter (especially in the afternoon). The direct normal radiation is higher from November to January, ranging between 600 Wh/m<sup>2</sup> and 700 Wh/m<sup>2</sup>, whereas from April to October is lower (i.e. 400-500 Wh/m<sup>2</sup>), due to rainfall and the higher sky coverage during that period [46]. According to a GIS-base climate analysis [47], in the MERV area (zones of Borena, Gedio, Sidama, Arsi, and East Shewa) the average number of rainy days per year is almost 100 days (i.e. rainfall >10 mm/day). Rainfall is mainly concentrated in the rainy season (July-September) but also some precipitation has been recorded during other times of year.

More information can be found in Appendix 1.

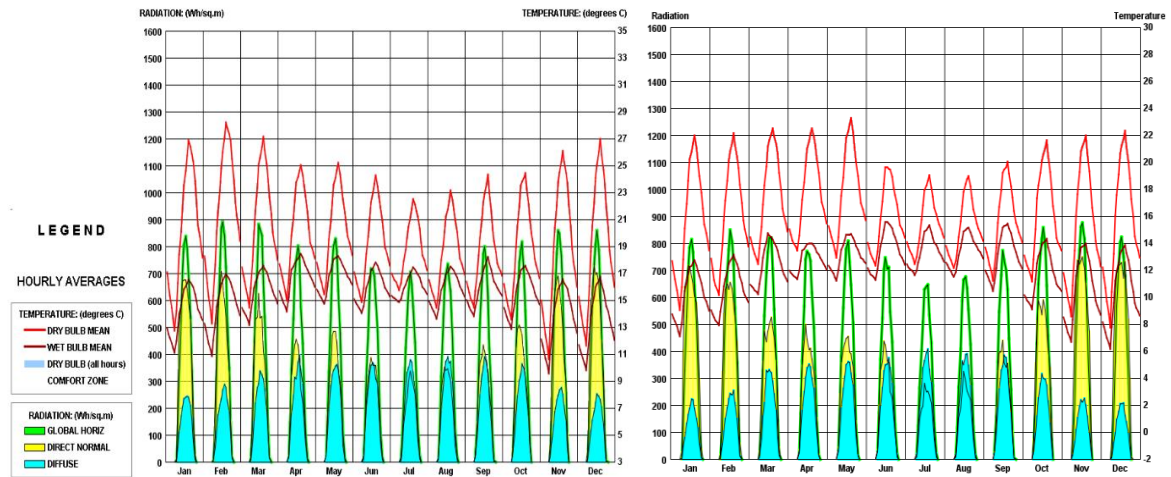


Figure 6 – Temperature and radiation hourly averages (Information obtained from Climate consultant software. On the left Awassa station: 7°N 38°E Elevation 1652m. On the right Addis Ababa station: 9°N 38°E Elevation 2355m [46])

## 2.1.3 Fluoride problem in Ethiopia

Fluoride is abundant in the environment and present in all the natural water sources. For instance, surface water generally contains from 0.01 to 0.03 mg/L of fluoride, whereas seawater contains from 1.2 to 1.5 mg/L [48]. The value in drinking water should not exceed 1.5 mg/L (See Appendix 2), but for artificial fluoridation of water supplies, the value is usually 0.5-1.0 mg/L [48]. In regions where there is geothermal or volcanic activity, fluoride concentrations can reach values of 25-50 mg/L [9]. In the Rift Valley there are thermal springs and volcanic activity, resulting in emanations of elements such as arsenic (As), boron (B), fluoride (F) and lithium (Li) [17]. This scenario results in groundwater with different concentrations of chemicals. In the MERV, fluoride concentrations are linked to the geological characteristics and values up to 25 mg/L have been observed [19]. Figure 7 shows a study of fluoride concentration in different water sources [49], which show that most of the contaminated spots, with concentrations above 20.0 mg/L, are located in the MERV.

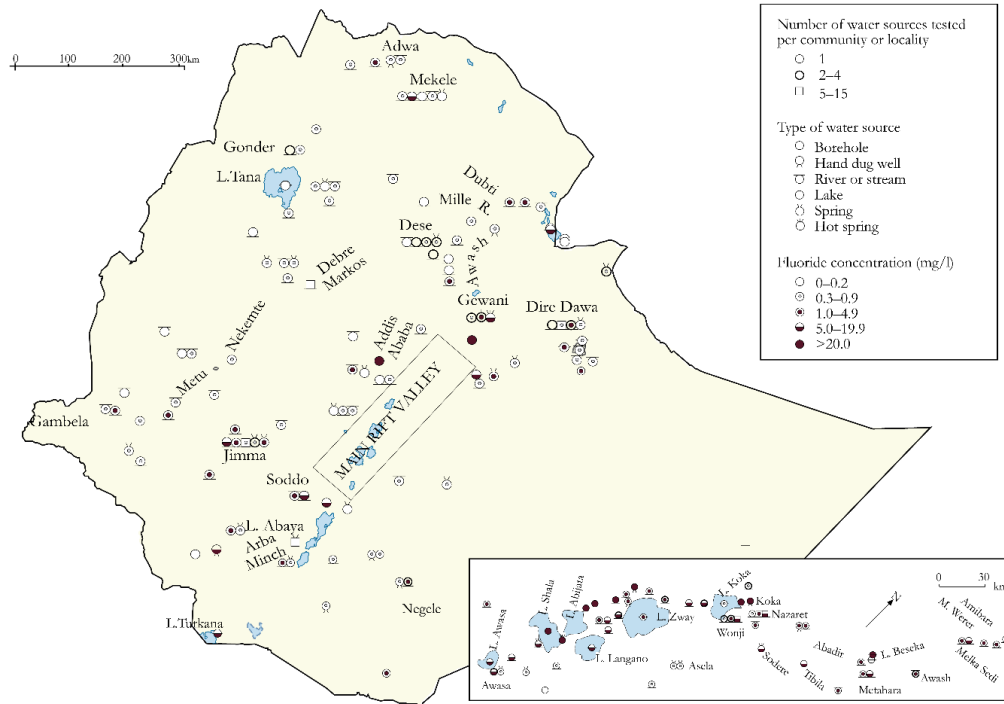


Figure 7 – Fluoride concentration in different water sources (Own elaboration. Based on [49])

Low concentrations of fluoride provide protection against dental caries, especially in children. That is why in regions such as USA, Canada or Europe, water is fluoridated on purpose (but not exceeding 0.5-1.0 mg/L and considering the diets). When fluoride is consumed, it is rapidly distributed by the systemic circulation to the intracellular and extracellular water of tissues; however, the ion normally accumulates in calcified tissues only, such as bone and teeth [9]. Depending on the intakes, fluoride consumption can lead to different problems (See Table 34 in Appendixes). Amounts between 1.5 and 3.0 mg/L in potable water can cause dental fluorosis, making teeth very hard and brittle. Up to 8 mg/L, fluoride results in skeletal fluorosis, bone malformation, weakening of the bones and even immobility. Excessive levels can also cause nausea, abdominal pains, headache, and reduce immunity, among other symptoms [13]. Children are especially at high risk, as the fluoride ingestion during the growth phase can result in depositions of fluoride in the skeleton (leading to mobility problems, stiffness of joints, etc.). However, fluoride is not irreversibly bound to bones. It has been proved that if people stop consuming fluoridated water, the body eliminates this substance [9].

#### 2.1.4 Renewable energy potential in Ethiopia

Ethiopia belongs to the Eastern Africa Power Pool (EAPP), a regional organization established in 2005 that aims to serve as an interconnector of electricity transmission between the member countries. Ethiopia is interconnected with the countries around: Djibouti (180 MW), Sudan (200 MW), Kenya (2000 MW are planned), Eritrea and Somalia. The federal institute responsible of developing energy policy programs and strategies is called The Ministry of Water, Irrigation and Energy (MoWIE). The Ethiopian Electric Utility (EEU), the Ethiopian Electric Power (EEP) and the Ethiopian Energy Authority (EEA) work under the MoWIE, and they are responsible of the different energy streams [45].

Ethiopia has a large renewable energy potential. Table 1 shows the potential of hydropower, solar, geothermal, wind and biomass in the country. The current installed electricity-producing capacity consists of 13 hydropower plants, one geothermal power plant, three wind farms, one biomass power plant and some diesel power plants (See Table 2). The use of diesel constitutes an enormous problem in Ethiopia, because emits greenhouse gases and its importation is expensive. Nevertheless, the Ethiopian energy policy enhances the use of carbon-neutral technologies, i.e. renewable energy technologies. Almost 96% of the

electricity is provided by hydropower. The rest is produced by renewables (i.e. solar, wind and geothermal) and a small percentage (0.1%) from diesel power plants. A majority of the population use biomass energy for cooking, such as wood, crop waste and animal dung [50].

Table 1 – Energy potential in Ethiopia [51, 40]

Resource	Unit	Potential	Resource	Unit	Potential
Hydropower	MW	45,000	Wood	Million tons	1120
Solar/day	kWh/m <sup>2</sup>	4 – 6	Agricultural waste	Million tons	15-20
Wind Power	GW	100	Natural Gas	Billion m <sup>3</sup>	113
Speed	m/s	>7	Coal	Million tons	300
Geothermal	MW	<10,000	Oil shale	Million tons	253

Table 2 – Existing Power Plants Installed Capacity [40]

Power plant	Capacity (MW)	In-service date	Type	Power plant	Capacity (MW)	In-service date	Type
1. Koka	43.2	1960	Hydropower	11. Dire Dawa	38	2004	Diesel
2. Awash II	32	1966	Hydropower	12. Awash 7 killo	35	2004	Diesel
3. Awash III	32	1971	Hydropower	13. Tekeze	300	2009	Hydropower
4. Finchaa	134	1973/2003	Hydropower	14. Gilgel Gibe II	420	2010	Hydropower
5. Meleka Wakena	153	1998	Hydropower	15. Beles	460	2010	Hydropower
6. Tis Aby I	11.4	1964	Hydropower	16. Fincha Amerti Neshi	97	2011	Hydropower
7. Tis Aby II	73	2001	Hydropower	17. Ashegoda	120	2012	Wind
8. Gilgel Gibe	184	2004	Hydropower	18. Adama I	51	2010	Wind
9. Alutto Langano	7.3	1999	Geothermal	19. Adama II	153	2015	Wind
10. Kaliti	14	2004	Diesel	20. Gibe III	1870	2015	Hydropower

Currently, 27% of the Ethiopian population has access to electricity, but in rural areas the percentage is reduced to 12% [52]. In general, electricity demand for households is low, with an average electricity demand per capita of 52 kWh [53], due to the low development level in the country. There are two rural electrification programs: The Universal Access Program (UEAP) and the Rural Electrification Fund (REF). The former one aims to provide electricity to rural areas, and the objective of the latter one is to develop an off-grid program focusing on renewable energy technologies. A GIS-based tool for rural electrification resulted in the optimal electrification mix in Ethiopia shown in Figure 8 [54]. The study did not consider the geospatial characteristics of electricity demand and supply, but helps to understand that an electricity generation mix supply (i.e. combining grid, micro-grid and stand-alone systems) is needed. As the Figure 8 suggests the MERV area might have already electricity access, but there is not much more information about the current situation (access to electricity or not, demand, etc.) in there and according to Ethiopian Central Statistical Agency, the former electricity grid might not be very reliable as 54.5% of the people living in rural areas (at national level) reported that 4 or more grid interruptions are usually observed per week [21]. Based on this setting, standalone systems or micro-grids could be more reliable and cheaper for neighborhoods and remote areas. Nevertheless, the cost-optimal electricity-supply option to serve rural households depends on each specific location, as well as many additional parameters (e.g. electricity demand, population density, distance to the grid, etc.) [54].

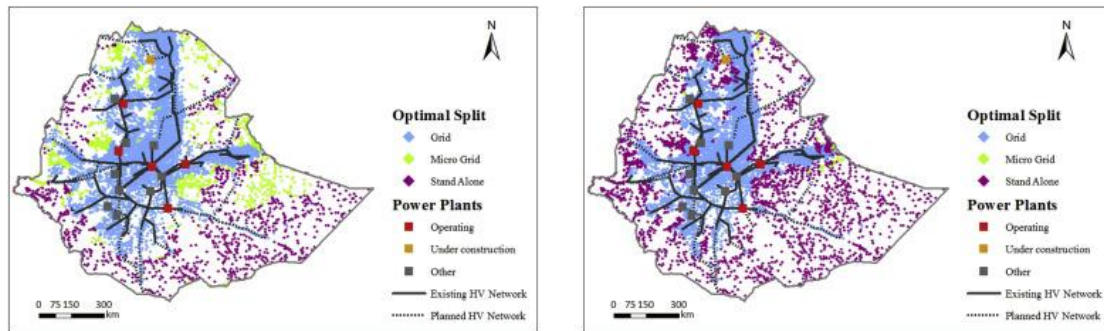


Figure 8 - Optimal electrification mix in Ethiopia – GIS-based analysis [54]: Figure on the left shows electricity access targets: 150 and 300 kWh/capita/year for the rural and urban areas respectively; Figure on the right shows electricity access targets of 50 and 300 kWh/capita/year for the rural and urban areas respectively.

### Solar:

Regarding solar, Ethiopia has an average annual solar radiation energy density per unit area of 1992.2 kWh/m<sup>2</sup>. The yearly mean average in the country of daily global horizontal radiation is 5.2kWh/m<sup>2</sup>, varying between a minimum of 4.55 kWh/m<sup>2</sup> in July and a maximum of 5.55 kWh/m<sup>2</sup> from February to March [55] as can be seen in Figure 9. The average direct normal radiation in the MERV is around 5-5.6 kWh/m<sup>2</sup>/day, and the average global horizontal irradiation is almost 6.4 kWh/m<sup>2</sup> /day. Therefore, Ethiopia has a high potential for solar PV (both off-grid and on-grid) but also for running any solar thermal system [34]. However, during the rainy season the availability of solar heat is lower, and the system cannot exploit its full potential. An optimized solution to cover the demands in these days needs to be found.

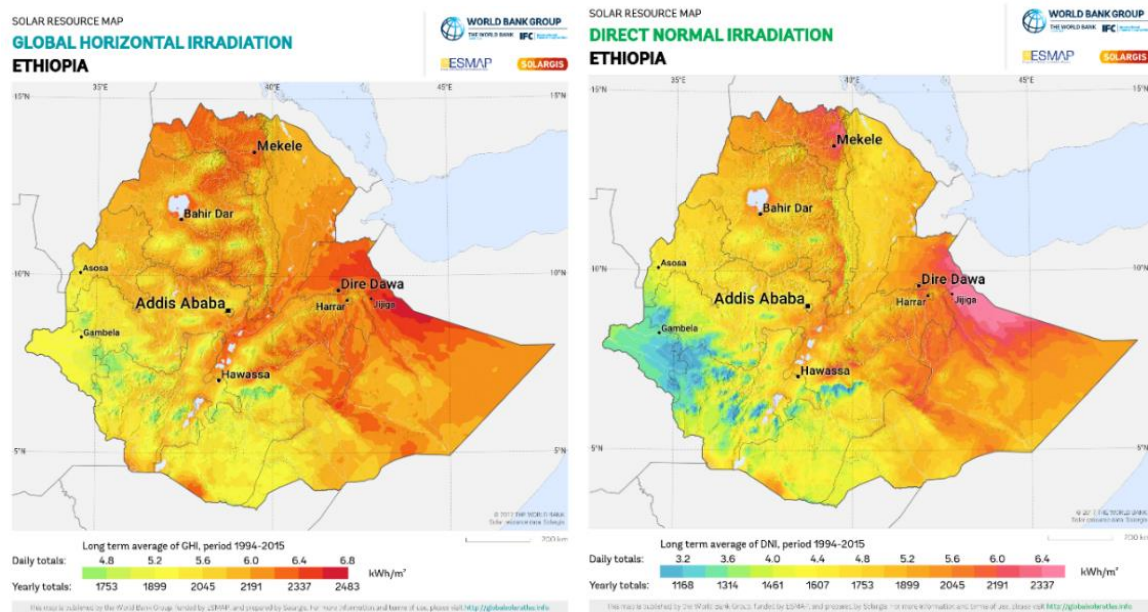


Figure 9 – Global horizontal irradiation (left) and direct normal irradiation (right) [56]

### Biomass:

Ethiopian is dependent on biomass energy resources such as fuel wood, dung and crop residues. Wood is becoming scarce due to the continued escalation of Ethiopian population [57]. The utilization of biomass in cooking stoves, especially in rural areas, is causing health-related problems [57]. Generally, the dung is directly combusted, wasting the nitrogen contents in the process. The biomass and animal manure removal are causing problems in agriculture, and a nutrient depletion of nitrogen, phosphorus and potassium has been observed in soil [58]. Thus, during a direct combustion of biomass, nitrogen reacts with oxygen, producing nitrous oxides. If, instead, biomass is used to produce biogas, the nitrogen remains in the

digestate (a nutrient-rich substance produced by anaerobic digestion that can be used as a fertilizer subsequently), resulting in a rich gas with a high carbon and energy content

Biogas production by anaerobic digestion can solve the lack of nutrients in the soil as the digestate that is produced can be used as an organic fertilizer [59]. The Ethiopian government has made efforts to expand small-scale biogas technology. In 2009, the National Biogas Programme of Ethiopia (NBPE) was implemented to develop a commercial biogas sector [57]. The objective was to construct 14,000 biogas plants in 18 districts in 4 years, but this expansion was hampered by a cement crisis in 2010 [60]. In 2013, 8,063 small-scale biogas plants were reported [60]. There is a second phase of the program (2014-2017), which aims to construct 20,000 additional biogas plants. In 2017, Ethiopia built the highest biomass power plant in Africa from combustion of household waste [61]. However, despite the significant national and international efforts, the potential is still hindered by the lack of good technical components such as valves, biogas lamps, etc. that are not locally available [62]. Thus, there is still a lot of potential to invest: almost 40% of GDP comes from agriculture [38] and 90% of households that own livestock have cattle, resulting in a population of 56.7 million of cattle (See Table 3). Cattle have an estimated biomass potential of 217.92 PJ/year [63], which can be used to solve both access to electricity and cooking health-related problems. Furthermore, integrating these systems with MD can provide communities with safe water.

Table 3 – Livestock biomass potential in Ethiopia [63]

Livestock	Population (million)	Dry dung (kg/day)	Collection Efficiency (%)	LHV(GJ/t)	Potential harvestable bioenergy PJ/y
<b>Cattle</b>	56.7	1.8	45	13	217.92
<b>Sheep</b>	29.3	0.4	35	14	20.96
<b>Goats</b>	29.1	0.4	40	14	23.79
<b>Horses</b>	2.03	3.0	50	11	12.23
<b>Chickens</b>	0.057	0.1	70	11	0.10
<b>Pigs</b>	0.034	0.8	80	11	0.87

The MERV is located between the regions of Oromia and SNNP. Both regions have cattle, sheep and poultry in most of their households, as can be seen in Table 4.

Table 4 – Livestock holding types [21]. Percent among Livestock owning households by livestock type, region and place of residence. Ethiopia 2015/2016

Resource	Cattle	Sheep	Goats	Horses	Donkeys	Mules	Camels	Poultry	Beehives
<b>Tigray</b>	82.8	27.3	35.4	0.2	45.1	0.4	3.7	77.5	18.3
<b>Amhara</b>	88.7	38.4	24.0	7.5	36.7	4.1	2.0	61.5	10.6
<b>Oromia</b>	<b>87.8</b>	41.7	31.0	10.6	48.1	1.6	2.0	<b>60.0</b>	8.9
<b>SNNP</b>	<b>85.9</b>	36.2	27.2	9.4	15.1	2.9	0.7	<b>58.8</b>	6.3
<b>Other regions</b>	61.9	47.6	65.5	1.2	43.8	0.8	19.8	31.7	2.7

### Geothermal:

The East African Rift has a large geothermal potential for power production, but has not been completely assessed to date [64]. The geology in the Ethiopian Rift is characterized for basal sheets from the Quaternary age, ignimbrites and non-consolidated pyroclastics [65]. There was a geothermal exploration in Aluto Langano, and 4 wells, drilled to a maximum depth of 2,500 m, were found to be productive with temperatures of about 350°C. Tendaho also showed geothermal potential of 270°C in three deep wells (2,100 m) and three shallow wells of 500 m. In these areas, there are two geothermal power plants projects ongoing in Ethiopia: The Aluto Langano project (estimated capacity at 75 MW) and Tendaho project (estimated capacity at 100 MW) [50]. Other hot springs and wells have been found to have geothermal

potential of low temperature (40-90°C), like in Abaya study [66, 64]. Geothermal can also be used as a heat source for the MD to produce water, but requires previous exploration to know the temperatures of the possible hot wells and hot springs (e.g. through in-situ tests). In the case of the current geothermal power plants at elevated temperatures, it could be interesting to use part of that heat for MD production to purify water in a larger scale. MD has been proven to be techno-economically viable using waste energy [33]. Figure 10 shows the prospect areas in the Ethiopian Rift to install geothermal.

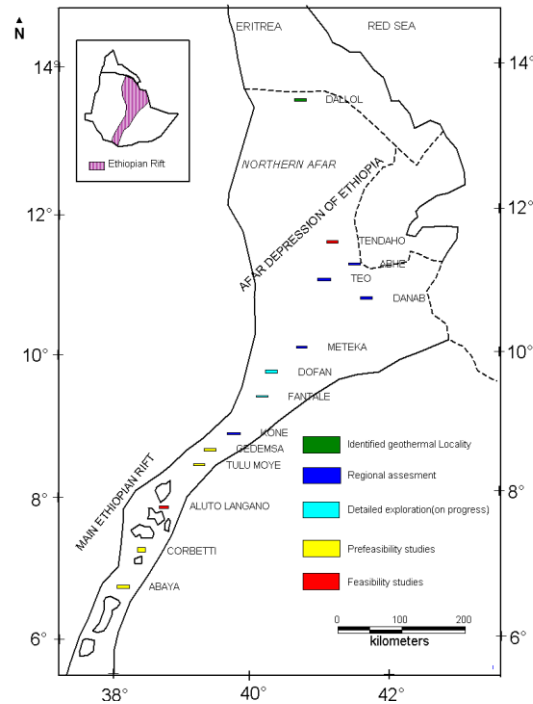


Figure 10 – Geothermal prospect areas in the Ethiopian Rift [67, 65]

Ethiopia has a large potential to invest in renewable energies, but the electrification of remote communities remains a challenge. Combination of the national grid, off-grid household systems and mini grids are the key to create energy access [50, 40, 54]. The current energy-policy framework wants to achieve the following objectives: ensure a reliable supply of energy at the right time and at affordable prices, particularly to support the country’s agricultural and industrial development; carbon neutral development, renewable energy based, and increase energy access and efficiency with the support and implication of public and private sectors [40]. To that end, Ethiopia needs to invest in such systems to ensure a low-carbon economy and at the same time, improve energy access and security, and alleviate poverty. However, this efforts are hampered due to the high capital costs of the alternative energy resources. Policy measures such as subsidies and incentives need to be introduced to support the change, but additionally Ethiopia should contribute to creating a secure environment for private investors [68].

## 2.2 Membrane distillation

Membrane Distillation (MD) process is discussed in this section. A review of different renewable energy technologies driving MD is done. The water purification company Scarab Development AB is also described as it provides experimental data from the MD unit used in this thesis.

### 2.2.1 Membrane distillation review

Membrane Distillation (MD) is a separation process driven by an imposed vapor pressure gradient across a hydrophobic microporous membrane. The temperature difference through the membrane results in a vapor pressure difference that causes water vapor transport through the pores from the hot feed to the cold side of the membrane. The ultrapure water vapor is condensed in contact with the condensing plate in the cold side of the MD, obtaining distilled water [33, 69]. In summary, the process involves the following steps [70]:

1. Evaporation of water and volatile compounds contained in the hot feed at the feed/membrane interface
2. Transfer of vapor through the membrane pores
3. Condensation of the permeate at the membrane/cold distillate interface

For this process, heating, cooling and electricity is needed. The MD can utilize low-grade heat source (<100°C), hence can use solar [71, 72], biomass [37], geothermal [73], or waste heat from district heating or from any industrial stream [33, 36, 74]. The advantages of MD technology include:

- Scalable to several applications varying the size
- 100% theoretical rejection of ions macromolecules, colloids, cells and other non-volatiles. Experimental rejections of 99.5% in most of the metals.
- Lower operating temperatures than conventional distillation and pressures (works at atmospheric pressure) than Reverse Osmosis
- Low sensitivity to variations of properties in the feed side (e.g. pH and salts)
- Few mechanical parts (Thus, safer than other technologies).
- Reduce vapor spaces compared to conventional distillation processes
- Lower flow leakages compared to reverse osmosis(RO).

Despite the heat source is usually a low-temperature heat source, MD has a high energy intensity. Other disadvantages are sensitivity to surfactants, or the requirement of separated treatments for undesirable volatiles such as ammonia and carbonates (i.e. degassing, pH control, or other methods are required) [75, 36, 33, 73]. Compared to other technologies (Table 35 in Appendix), MD has the highest separation efficiency of all technologies. More than 99% of separation efficiency has been observed in several MD applications [36, 76, 37, 33, 77, 78]. Compared to RO, the very low operating pressures of the MD result in thinner piping and fewer working problems. Consequently, the capital and maintenance expenses can be lower when compared to RO, if it is implemented commercially [79]. Activated alumina and Nalgonda techniques are more practical in rural areas when contrasted with other techniques, but cannot accomplish passable furthest reaches of fluoride and needs high dosages of chemicals (up to 700-1200 mg/L of  $Al(OH)_3$ ) [32].

In MD, hydrophobic membranes are used, which are typically fabricated out of polytetrafluoroethylene (PTFE), polypropylene (PP), and polyvinylidenedifluoride (PVDF) [75]. Common membranes properties required in MD are: a hydrophobic layer (a contact angle greater than 90°C and liquid entry-pressure greater than 2.5 bar), a pore size from 0.1 to 0.3  $\mu m$ , high porosity (80%), optimum thickness (30–60  $\mu m$ ), minimum thermal conductivity, thermal stability, chemical resistance to acids and bases during membrane cleaning, and durability. However, there are not commercial options that fulfills all these requirements [33].

There are four basic system designs: Direct Contact Membrane Distillation (DCMD), Air Gap Membrane Distillation (AGMD), Sweeping Gas Membrane Distillation (SGMD) and Vacuum Membrane Distillation (VMD) (See Figure 11). The choice of the configuration depends on the feed water, performance and heat source available.

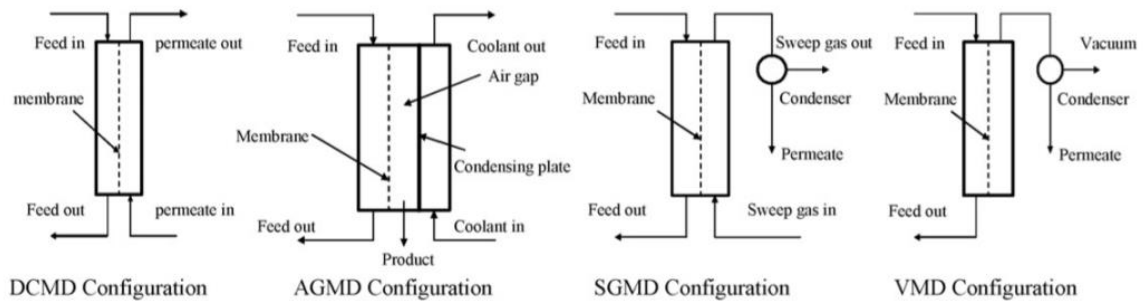


Figure 11 – Different types of MD configuration [79]

Figure 12 shows the AGMD configuration. The main difference between DCMD and AGMD is the thin layer of air placed between the membrane and the condensing plate. This air gap reduces heat losses and increases the thermal efficiency, as prevents a direct contact between the permeated vapor and the cooling water surface. Therefore, AGMD configuration reduces the temperature polarization but provides a lower permeate flux. However, thanks to the absence of direct contact between fluids, AGMD can remove traces of volatile components [79]. Table 5 shows advantages, disadvantages and applications of the different configurations.

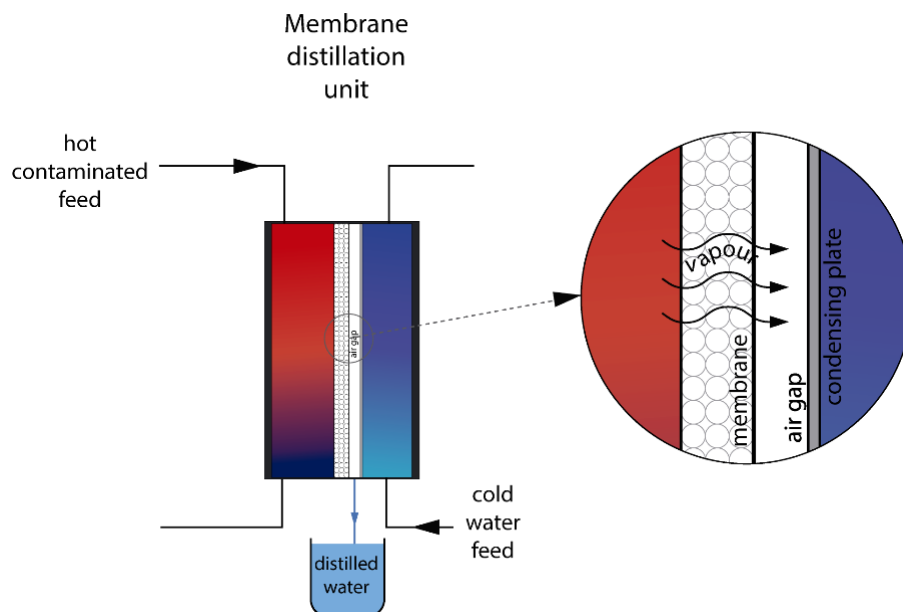


Figure 12 – Air Gap membrane distillation scheme (own elaboration)

Table 5 – Advantages, disadvantages and applications of different technologies [36, 76, 33]

MD configuration	Advantages	Disadvantages	Application area
DCMD	High permeate flux Possible internal heat recovery	High conductive heat losses High temperature polarization effect Risk of mass contamination of the permeate	Desalination and water treatment Nuclear industry Food industry Textile industry Chemical and Pharmaceutical industries
AGMD	Low conductive heat losses Low temperature polarization effect Possible internal heat recovery	Low permeate flux due to resistance to mass transfer	Desalination and water treatment Food industry Chemical industry
SGMD	Low conductive heat losses High permeate flux	Complicated to handle the sweeping gas Difficult heat recovery	Desalination and water treatment Chemical industry
VMD	Low conductive heat losses High permeate flux	higher risk of pore wetting Difficult heat recovery	Desalination and water treatment Food industry Textile industry Chemical industry

Ultra-pure water has none or very little salt content. A continuous consumption of this water can have severe consequences for the human body, like osmotic shock [80]. During post-treatment, the water must be remineralized prior to distribution. In the economic analysis, costs of salts are considered (like addition of  $\text{CaCl}_2 + \text{NaHCO}_3$ ) [81].

### 2.2.2 HVR and Scarab Development AB

Scarab Development AB is a Swedish company located in Stockholm and its main aim is to establish commercial solutions to environmental issues [82]. Their most successful solution is the development of an AGMD module that can use low-heat sources and purify water with high removal efficiencies. HVR Water Purification AB is a technology promoter for the company Scarab Development AB. It offers the patented technology WaterApp, consisting of a stand-alone water purification unit that can be easily fitted to any power plant using its low-temperature waste heat to produce pure water. WaterApp is scalable, and can be used with different heat sources: solar, geothermal, heat pumps and waste heat from biomass or from large to small sized power generation units, among others.

In KTH Royal Institute of Technology, different MD research concepts have been investigated involving performance evaluations, energy analysis and optimization of various water purification systems. HVR is involved in the research by supplying test materials (purification modules and membranes) and data.

There are ongoing MD projects from HVR with a school in Balasore (Odisha, India) and with two major manufacturers of small and medium power plants, i.e. Caterpillar and Wärtsila. When these projects are operational, performance studies and feedback from the customer will be used to make improvements in the commercialization of the equipment. Additionally, there are some more upcoming projects planned in Ethiopia and Bangladesh for drinking water supply. This thesis can create a framework for further studies.

WaterApp has several AGMD units and has been validated for different feed-water types, industrial environments and scales. Below, the configuration that has been used in this thesis for the simulations is presented, with experimental data being provided by HVR.

***Semi-commercial air gap membrane distillation***

The Air Gap Membrane Distillation (AGMD) module used in this thesis consists of 10 cassettes (2 parallel membranes in each cassette) with a total active area of 2.3 m<sup>2</sup> (and a total membrane area of 2.6 m<sup>2</sup>). The membrane material used is Polytetrafluoroethylene (PTFE) with polypropylene (PP) support. The size of the module is 63 cm wide and 73 cm high. The membrane characteristics are shown in Table 6.

Table 6 – AGMD characteristics (Provided from HVR and Scarab Development AB)

Active membrane area		<b>2.3 m<sup>2</sup></b>	
Total membrane area	2.6 m <sup>2</sup>	Air gap Length	1mm
Porosity	80%	Height of the module	730 mm
Average pore size	0.2 μm	Width of the module	630 mm
Membrane Thickness	0.2 mm	Thickness of the module	175 mm

Each cassette consists of two membranes and two coolant plates<sup>2</sup> as shown in Figure 14. The cooling channel serves as a mechanical support for the membranes. The module is constituted by 10 cassettes in parallel (Figure 13), and the hot and cold flows are separated from each other as shown in Figure 14.



Figure 13 – AGMD Module [76]

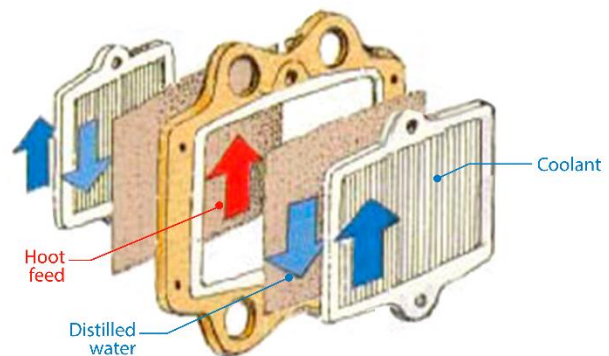


Figure 14 – AGMD cassette [75]

Experimental analysis carried out in [33] with this AGMD module showed that, the greater the temperature difference ( $dT$ , between the feed inlet and the coolant inlet), the greater the obtained permeate flux, at constant module feed and cooling flow rates (1200 L/h). Similarly, it has been found in [33] that the greater the feed and coolant flow rate, the more permeate flux is obtained, as it increases the heat transfer in the permeate side of the membrane module [79]. This behavior can be seen in Table 7.

<sup>2</sup> The specific details of the channel are not shown due to intellectual property rights

Table 7 - Permeate fluxes from different feed and cooling water temperatures at different flow rates [33]

$F_h$ (L/h)	$F_c$ (L/h)	$T_{ci}$ (°C)	$T_{hi}$ (°C)	$T_{co}$ (°C)	$T_{ho}$ (°C)	dT (K)	Yield (L/h)
780.0	600.0	21.7	65.7	28.0	58.2	44.0	6.5
900.0	780.0	21.7	65.0	28.4	57.7	43.2	6.7
900.0	780.0	21.8	65.3	28.4	57.9	43.5	7.6
1110.0	1020.0	28.1	64.1	33.1	58.5	35.9	8.9
1110.0	1020.0	26.2	66.8	32.7	60.8	40.5	10.8
1140.0	1020.0	35.7	75.5	40.2	69.2	39.7	14.0
1140.0	1020.0	30.1	76.2	36.1	68.8	46.1	15.4
1140.0	1020.0	25.1	75.5	31.4	67.7	50.5	16.0
1140.0	1020.0	17.2	75.1	25.3	66.0	57.8	17.5
1200.0	1140.0	25.6	80.4	34.1	71.2	54.9	18.9
1200.0	1140.0	15.7	80.7	25.9	70.0	65.0	20.3
1200.0	1200.0	30.6	65.0	33.7	61.0	34.5	8.2
1200.0	1200.0	30.8	62.2	34.3	57.7	31.4	9.0
1200.0	1200.0	26.6	61.8	30.6	57.3	35.2	9.4
1200.0	1200.0	35.2	71.3	39.4	66.2	36.1	10.2
1200.0	1200.0	49.8	80.2	53.9	75.5	30.4	10.3
1200.0	1200.0	15.5	65.3	19.9	59.7	49.8	11.3
1200.0	1200.0	19.7	71.7	26.0	64.3	52.0	15.3

### 2.2.3 Renewable energy technologies driving air gap membrane distillation

MD was first patented in 1963 by Bodell [83] but the real interest appeared at the early 1980s and 1990s. During the time period between 1999 and 2005, the number of MD studies that were published increased. Nonetheless, MD has not been completely commercially developed yet [79].

The MD unit can use low-grade heat sources ( $<100^{\circ}\text{C}$ ) and has been applied with different energy technologies and configurations. In case of the AGMD configuration, Mohan et. al studied the performance of a waste heat driven polygeneration system for electricity production, cooling and desalination [71]. Also, many research projects have focused on the MD coupled with solar energy for seawater desalination, highlighting the importance of this stand-alone systems for remote communities [84, 85, 86, 87]. Geothermal driving MD for desalination has also been applied by Bouguechaand Dhahbi [88].

In case of water purification, AGMD has been successfully applied with waste heat from district heating [33], cogeneration [76], and heat recovery from chillers and gas engines to supply water and pure water for the semiconductor industry [74]. Besides that, AGMD has been studied and applied with different renewable energy technologies such as solar thermal for standalone systems [72], in polygeneration systems for production of purified water, domestic hot water and cooling [71, 34], and in a biogas-based polygeneration system for villages in Bangladesh [37, 89].

The thermal energy demand of the AGMD is the main reason which limits its commercial development. Nevertheless, AGMD is a promising technology for treatment of any water, especially with the utilization of waste heat or its integration in renewable energy polygeneration systems.

### 3 AGMD MODEL USING MINITAB

An AGMD model is performed using Minitab and experimental data. The results from Minitab are used later to create a component in TRNSYS that behaves as an AGMD in a simplified and approximate way.

#### *Procedure*

Experimental data shown in Table 7 was provided by Scarab Development, using the module explained in Section 2.2.3. The experimental tests were performed by Woldemariam in [33]. This data was analyzed with Minitab 18 and a multiple regression model was obtained. Four variables were considered as independent variables: hot inlet temperature  $T_{hi}$ , cold inlet temperature  $T_{ci}$ , hot feed flowrate  $F_h$  (L/h) and cold feed flowrate  $F_c$  (L/h). The dependent variables are the permeate yield  $Y$  in liters per hour, hot outlet temperature  $T_{ho}$  and cold inlet temperature  $T_{co}$ . The minimum and maximum values of the model are:

Table 8 – Range of data

Data	Fh (L/h)	Fc (L/h)	Tci (°C)	Thi (°C)
Min	1020	900	13	55
Max	1200	1200	50	80

The relationship between yield  $Y$  and  $T_{hi}$  is usually exponential, but as can be seen in literature [33, 90], in the range of 50-80°C of  $T_{hi}$  it is mainly linear. The model created in Minitab fitted the data into a quadratic equation with the general form of:

$$Y = \alpha_0 + \alpha_1 T_{hi} + \alpha_2 T_{ci} + \alpha_3 F_c + \alpha_4 F_h + \alpha_{12} T_{hi} T_{ci} + \alpha_{13} T_{hi} F_c + \alpha_{14} T_{hi} F_h + \alpha_{23} T_{ci} F_c + \alpha_{24} T_{ci} F_h + \alpha_{34} F_h F_c + \alpha_{11} T_{hi}^2 + \alpha_{22} T_{ci}^2 + \alpha_{33} F_c^2 + \alpha_{44} F_h^2$$

Minitab optimized the equation to the best fit, removing terms that do not help to explain additional variation in  $Y$ .

#### *Model*

The results are as follows:

Table 9 – Minitab results summary

Equations	R <sup>2</sup>	p-value	Independent variable that contributes the most
$T_{co}(^{\circ}C) = 124.6 - 2.209 \cdot T_{hi} + 0.673 \cdot T_{ci} + 0.0611 \cdot F_c - 0.1339 \cdot F_h - 0.00397 \cdot T_{hi} T_{ci} + 0.002116 T_{hi} F_c + 0.000420 \cdot T_{ci} F_c + 0.000036 \cdot F_c^2$	99.91%	0.018	$T_{ci}$
$T_{ho}(^{\circ}C) = -24.9 + 1.504 \cdot T_{hi} - 0.2507 \cdot T_{ci} + 0.00914 \cdot F_h - 0.005262 \cdot T_{hi} T_{ci} - 0.00618 \cdot T_{hi}^2$	99.80%	0.002	$T_{hi}$
$Yield(l/h) = -78.2 + 0.0581 \cdot F_c + 0.179 \cdot T_{ci} + 1.246 \cdot T_{hi} - 0.000372 \cdot F_c \cdot T_{ci} - 0.000701 \cdot F_c \cdot T_{hi}$	98.19%	0.022	$T_{hi}$ and $T_{ci}$

These relationships work for the data range shown in Table 8. The R-squared is high and close to one in each case, and the p-value of each variable in the model is statistically significant (lower than 0.05). Furthermore, residuals of each equation are randomly distributed (i.e. there are not clusters or unusual values) although there is one data value that has a large residual and is not well fit by the equation. However, as the sample size is not large enough (n=22) any data in  $T_{co}$  and  $T_{ho}$  model is removed from the analysis. In the Yield model, a large residual is removed to improve R-squared and p-value (See page 72 for more details). This regression model has limitations but allows to perform an estimated design. In a more detailed analysis of the AGMD model, larger samples (typically 45 or more) should be used to obtain a better regression model. Other option can be to measure all the temperatures shown in Figure 38 to do a heat transfer model, as the one performed by Alsaadi et. al [91].

## 4 ANALYSIS WITH TRNSYS

The temporal and seasonal variability of the driving variables, such as ambient temperature, solar irradiance, hot inlet temperature and cold inlet temperature in the membrane, requires dynamic simulation of the systems. For that purpose, TRNSYS simulation tool is used, which allows designing an estimating a hypothetical and functional system, and optimizing it.

### **Procedure**

This study presents a techno-economic analysis of different energy technologies applied to a membrane distillation system in the Main Ethiopian Rift Valley. Yield production, thermal efficiency of the system, investment, benefits at the end of the installation's lifetime and payback period are indicators to be compared and decide which technology suits the best this application. Flat plate solar collectors (FPC), evacuated tube solar collectors (ETC) and a combined heat and power (CHP) unit using biogas from manure are considered as energy technologies.

Several cases of different complexity are analyzed: ETC case, FPC case, CHP Biogas case and Hybrid case. On the first two cases, only solar thermal (ETC and FPC) and the MD are considered (electricity is supplies by the grid). The area of study has access to electricity, but according to the Ethiopian Socio-economic Survey is not a continuous and reliable service [21]. Since the solar system only needs electricity for pumping purposes, electricity from the grid is assumed to be enough to run the installation. Otherwise, batteries and PV could be used to power it. On the CHP Biogas case, electricity production and heat to drive the MD are studied. Later, a hybrid case combining CHP and ETC are compared to the standalone systems.

The investigation aims to meet the thermal demand for the membrane distillation water purification process and produce safe drinking water. The electricity produced in the CHP and hybrid case aims to cover the energy needs in the installation (i.e. thermal and electricity demand), and any surplus could be sold to households around the system. Besides that, the need of production of biogas also generated other sub-products like fertilizers and gas for cooking, that can also be sold later.

The study estimates the sizes, cost of all the energies and the necessary inputs to meet the water production. The net present value (NPV), payback period (PB) and internal rate of return (IRR) are determined in order to examine the financial feasibility of every system.

### **Demand of water**

The demand of water and the distribution of neighborhoods are not specified. The considered size for the simulation is 30 houses (5 people/household [21], 150 people). For all cases the demand of drinking water needed is around 2.5 to 3 liters per person per day [92].

## 4.1 TRNSYS model

### 4.1.1 AGMD module specification

For an active area of 2.3 m<sup>2</sup> (one AGMD) with a hot feed of 80 °C, a cooling temperature of 20°C, and coolant and feed flow rates of 1200 L/h, the obtained distilled water yield is 18 L/h [33]. Table 10 shows the amount of modules that are required to supply 30 houses depending on the working hours (12 or 24 hours).

Table 10 – Modules by working hours

Case study	Total demand	Production by one module	Working hours	Modules needed	Production of the system by hour
30 houses	450 L/day	18 L/h/module	12	2 to 3	36 - 42 L/h
			24	1	18 L/h

Coolant and feed flow rates are kept to the optimal value ( $\dot{m}_{MD} = 1200 \text{ l/h}$ ). When the feed temperature ( $T_{hi}$ ) is lower than 45°C the AGMD is not working. When the feed temperature is greater than (GT) 45°C the AGMD model in TRNSYS is simplified by using the equations shown in Table 9. These equations are modelled in TRNSYS by using an equation block:

Inputs:  $T_{hi}$ ,  $T_{ci}$ , Coolant flow rate ( $F_c$ ) and hot feed flow rate ( $\dot{m}_{MD}$ ).

Outputs:

$$T_{ho}(^{\circ}\text{C}) = GT(T_{hi},45)*(-13.932-0.2507*T_{ci}+1.504*T_{hi}-0.00618*T_{hi}^2+0.005262*T_{ci}*T_{hi}) + (1-GT(T_{hi},45))*T_{hi}$$

$$T_{co}(^{\circ}\text{C}) = GT(T_{hi},45)*(-14.6+1.177*T_{ci}+0.3302*T_{hi}-0.00397*T_{ci}*T_{hi}) + (1-GT(T_{hi},45))*T_{ci}$$

$$\text{Yield(L/h)} = GT(T_{hi},45)*(-8.48-0.2674*T_{ci}+0.4048*T_{hi}) + (1-GT(T_{hi},45))*0$$

$$\dot{m}_{MD,out}(\text{L/h}) = \dot{m}_{MD} - \text{yield}$$

Table 11 – Equation block called “Membrane”

The well water is assumed to contain fluorides<sup>3</sup> and its temperature is assumed to vary from 15°C at night to 25°C during the day, following the same pattern of temperatures as the ambient temperature, as it is shown in Figure 15.

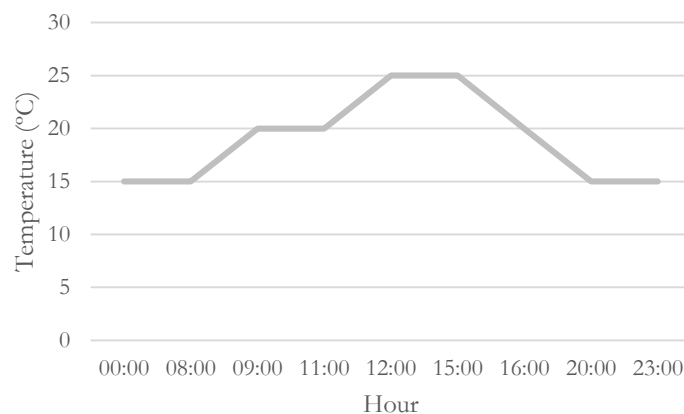


Figure 15 – Temperature from the well

<sup>3</sup> It is assumed that no matter what concentration the water point has (depending on the specific location it will vary), the AGMD will remove the fluoride as AGMD can remove fluoride with concentrations up to 500 mg/L.

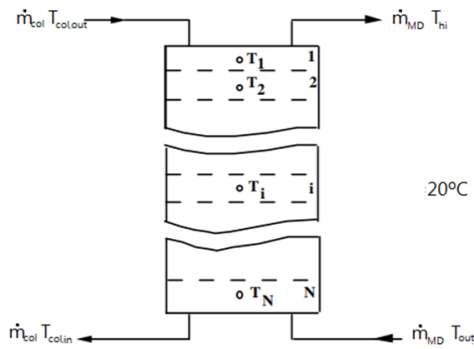
#### 4.1.2 Tank commercial specifications

The tank is used to store the water coming from the well, it is not used as thermal storage tank. For the simulations, the storage tank volume is always 2 m<sup>3</sup> for simplicity. The thermal behavior of the storage tank is modelled using a finite volume method. Type 4 from TRNSYS library is used. The tank is assumed to have three nodes of well-mixed fluid volume of equal sizes. Each layer (node) is at different temperature. The energy balance of the n<sup>th</sup> node model is given below [93]:

$$TC_n \frac{dT_n}{dt} = \dot{m}_{w,in} C_p (T_{n-1} - T_n) + \dot{m}_{w,out} C_p (T_{n+1} - T_n) - UA_n (T_n - T_a) + \frac{S_n \mu}{\delta} (T_{n-1} - T_n) - \frac{S_n \mu}{\delta} (T_n - T_{n+1}) \quad (1)$$

where T is the water temperature,  $\dot{m}_{w,in}$  is the inlet mass flow rate of water,  $\dot{m}_{w,out}$  is the outlet mass flow rate of water and TC is the thermal capacitance.  $C_p$  is the specific heat capacity of water, U is the thermal loss coefficient of the layer (a value of 0.56 W/mK is assumed),  $A_n$  is the envelope surface area of one node, S is the surface area of the tank,  $\mu$  is the conductivity and  $\delta$  is the thickness of the tank.

Part of the coolant (flow=yield) is used to refill the tank, at  $T_{co}$ . In the membrane distillation block, the hot flow  $\dot{m}_{MD,out} = \dot{m}_{MD} - Yield$  and the refilling flow is mixed resulting in:  $\dot{m}_{MD} \cdot T_{out} = T_{ho}(\dot{m}_{MD} - Yield) + T_{co} \cdot Yield$ .



Tank Specifications	
Tank volume	2 m <sup>3</sup>
Fluid specific heat	4.19 kJ/kgK
Tank loss coefficient	0.55 W/m <sup>2</sup> K
Height of node (1,2 and 3)	0.76 m
Control signal (auxiliary elements)	0 (always OFF)

Figure 16 – Stratified tank scheme (left) [93]. TRNSYS tank specifications (right).

#### 4.1.3 Solar case

The solar case is designed only to supply the demand of water. The electricity of the pumps is supplied by the grid. Figure 17 shows the general solar scheme. The solar collector field (either ETC or FPC) absorbs the irradiation coming from the sun and heats up water up to  $T_{col,out}$ . Afterwards, it exchanges heat with the contaminated water going to the AGMD in a plate heat exchanger. The warm water at  $T_{hi}$  temperature goes to the AGMD unit and cold water coming from the well, at  $T_{ci}$  temperature, goes to the coolant side of the AGMD. The temperature difference evaporates part of the water (1.6%) and distilled water is obtained. The water containing fluoride comes back to the thermal tank. As part of the water is distilled, the tank is refill with the water from the coolant side of the AGMD at  $T_{co}$ , recovering part of the heat.

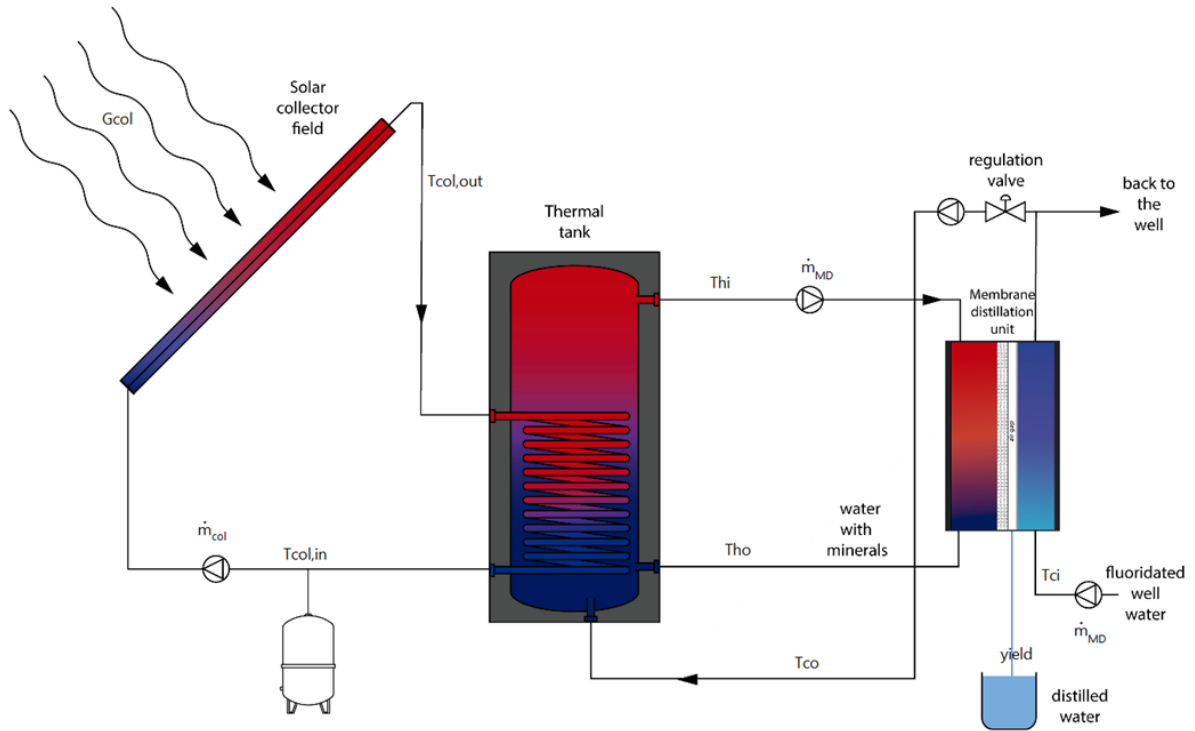


Figure 17 – Scheme solar installation

#### 4.1.3.1 Weather data

Weather data is obtained from TRNSYS type 109<sup>4</sup>, and the data file is obtained from Addis Ababa (Ethiopia) [46]. The solar radiation, solar angle of incidence, and ambient temperatures are obtained from the component type 109. The component type 109 uses a weather data file TMY2 (Typical Meteorological Year) which includes the Typical Meteorological Year derived from data sets from 1961 to 1990 produced by the National Renewable Energy Laboratory (NREL's). [93].

#### 4.1.3.2 Solar collectors

FPC and ETC are simulated using type 1b and type 71 available in TRNSYS library. Type 1b uses equation 21 and 23 (See Appendix 7) to simulate the FPC. Type 71 uses equation 21, 22 and 24 to simulate the ETC. Manufacture data are obtained from the commercial catalogs of the company Apricus. The inputs to TRNSYS are shown in Table 13.

In case of the ETC, an external data file containing the incidence angle modifier (IAM – see Appendix 7) coefficients from Apricus catalog is considered for the TRNSYS simulation.

Table 12 – IAM coefficients for Apricus ETC

	0°	10°	20°	30°	40°	50°	60°	70°
$K(\theta_t, \mathbf{0})$	1	1	1	0.99	0.98	0.97	0.94	0.88
$K(\mathbf{0}, \theta_l)$	1	1.03	1.07	1.16	1.31	1.4	1.44	1.3

In order to optimize the model, several total collector's areas are simulated to meet the demand. The solar field is constituted with maximum 7 ETC or 10 FPC in a row but all of them connected in parallel.

<sup>4</sup> Along this document all "Type" mentioned are referred to the component model inside the library of TRSNYS 16. Each component is defined by mathematical equations to model the behavior of a specific system.

Table 13 – Data inputs to TRNSYS

		ETC	FPC
Collector aperture area		2.84	2.8
Fluid specific heat	kJ/kg°C	4.18	4.18
Efficiency mode (1, 2 or 3)	(equation 21 – see Appendix 7)	2	2
Flow rate	$G_{test}$ (kg/h m <sup>2</sup> )	50	40
Intercept efficiency	$\eta_0$	0.714	0.755
Efficiency slope	$a_1$	1.243	3.738
Efficiency curvature	$a_2$	0.009	0.007
Model		Apricus ETC-30	Apricus FPC A32

Flow rate is recommended by manufacturers in case of ETC 1, ETC 2 and FPC 1. 50L/hm<sup>2</sup> flow rate is assumed in case of FPC 2. The fluid specific heat is from water (no glycol mixture is considered).

#### 4.1.3.3 Other components

The required power for the pumps is calculated assuming a hydraulic total head loss using the following equation [93]:

$$P(kW) = \frac{Q \cdot \rho \cdot g \cdot H}{3.6 \cdot 10^6}$$

Where Q is the flow capacity (m<sup>3</sup>/h),  $\rho$  is the density of the fluid (kg/m<sup>3</sup>), g is the gravity (9.8 m/s<sup>2</sup>) and H is the differential head in meters. Depending on the size of the system, the flows and the hydraulic head loss will change. Pumps are later dimensioned according to the simulation results. The circulation pumps are modeled using Type 3. Pump power demand is simply set to the rated value whenever the control signal indicates that the pump is in operation. 5% of the pump power is assumed to be converted to fluid thermal energy.

Table 14 –Solar Pump characteristics

Pump type 3d (Pump model Wilo-Yonos Maxo)		
Maximum flow rate	$\dot{m}_{col}$ (L/h)	Flow rate in the collectors
Fluid specific heat	$C_p$ (kJ/kg)	4.185
Maximum power	W	70
Conversion coefficient		0.05

Table 15 –AGMD Pump characteristics

Pump type 3d (Pump model Wilo-Stratos Pico)		
Maximum flow rate	$\dot{m}_{MD}$ (L/h)	1200 L/h/AGMD
Fluid specific heat	$C_p$ (kJ/kg)	4.185 kJ/kg
Maximum power	W	10
Conversion coefficient		0.05

In the solar case, the pumps are turned off when there is not sun. That is simulated using an equation block. When there is not radiation, the pumps are turned off. In reality, some hysteresis should be included.

#### 4.1.3.4 TRNSYS diagram

Finally, the TRNSYS diagram that connects all the components are shown in Figure 18 and Figure 19. Two plotters are used to control the simulation: Plotter 1 containing the information from the collectors ( $T_{col,out}$ ,  $T_{col,in}$ ,  $\dot{m}_{col}$  and  $G_{col}$ ) and Plotter 2 containing the temperatures from the tank, membrane and well water and the yield. All the outputs are integrated by hour and exported to a text file. All the results are further analyzed in excel.

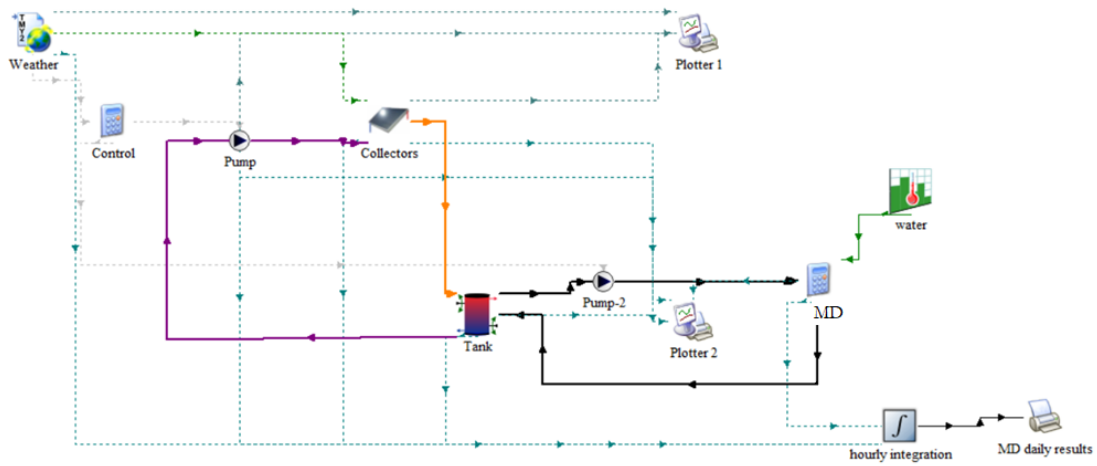


Figure 18 – Scheme TRNSYS FPC model

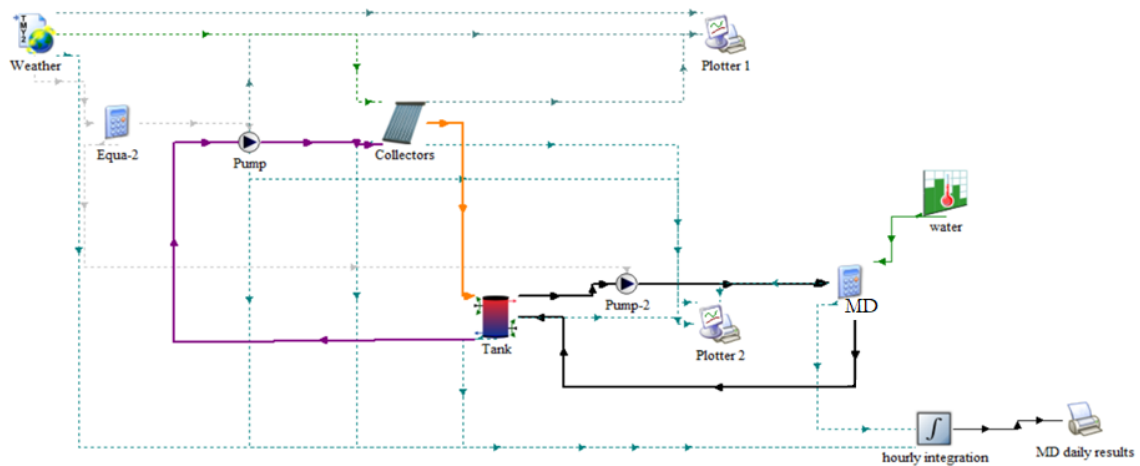


Figure 19 – Scheme TRNSYS ETC model

#### 4.1.4 Biogas case

The Biogas case is designed to supply the thermal demand of the AGMD, thus the demand of water. But, the electricity produced from the CHP unit supplies to the pumps in the installation and for the household's demand. Part of the biogas from the digester can also be used for cooking. The effluent from the digester, after a disinfection, can be used for agriculture as fertilizer.

Figure 20 shows the general biogas scheme. Manure from cattle is introduced to the plug flow digester. At mesophilic temperature of 35°C and a retention time of 30 days [89], the digester can start producing biogas. This biogas can be stored in a gas holder after cleaning it with a gas scrubber. The obtained gas is assumed to have the average biogas characteristics shown in Table 16. This gas can be used for cooking or in the CHP unit. The CHP unit is a compact engine that includes a heat exchanger (to provide heat to the heat source), a 3-cylinder gas engine and a synchronous generator. The electricity is produced by the combustion process within the gas engine. The rotational movement is converted into electricity (by the generator) [94]. The CHP unit produces low-temperature heat (70-80 °C) from the cooling system and high temperature heat (150-200 °C) by the flue gases. The former heat can be used to maintain the digester under mesophilic conditions. The heat from the exhaust gases exchanges heat with the AGMD unit using

shell and tube heat exchanger. The warm water at  $T_{hi}$  temperature goes to the AGMD unit and resultantly, distilled water is obtained. The water containing fluoride comes back to the thermal tank, as in the solar case. As part of the water is distilled, the tank is refill with the water from the coolant side of the AGMD at  $T_{co}$ , recovering part of the heat. Also, this coolant at  $T_{co}$  can help to maintain the digester at mesophilic temperatures.

Table 16 – Biogas Specifications [95]

<b>Methane content</b>	65%
<b>Carbon dioxide</b>	33%
<b>Energy Content (65% of pure methane)</b>	7 kWh/m <sup>3</sup>
<b>Density</b>	1000 kg/m <sup>3</sup>

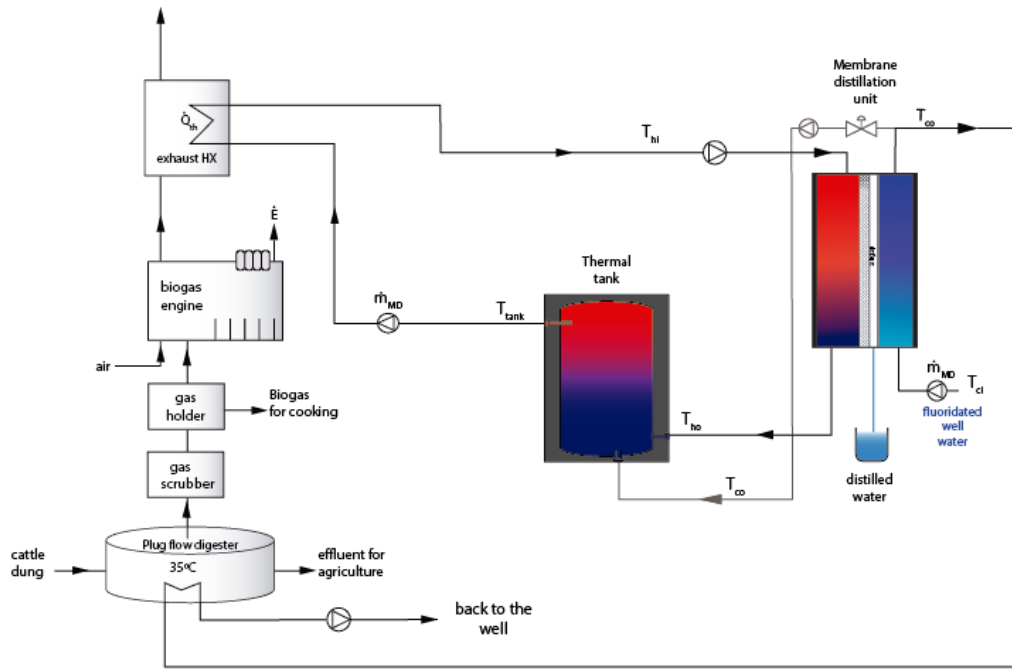


Figure 20 – Biogas scheme

The biogas produced in the digester is assumed to have a methane content of 65%, which contains an energy of 7 kWh/m<sup>3</sup> [95]. The catalog specifications of the chosen CHP unit are shown in Table 17.

Table 17 – CHP catalog Data Specifications Vitobloc 200 EM-9kW/20kW<sub>th</sub> [96]

<b>Power rate</b>	50%	75%	100%
<b>Electricity Output (kW)</b>	4.3	6.4	8.5
<b>Thermal Output (kW)</b>	11.4	14.6	18.0
<b>Fuel input (kW)</b>	17.0	22.7	28.6

In the TRNSYS model, only the thermal output from the CHP unit and the AGMD, tank and well water are considered. The CHP unit in steady-state conditions is assumed to supply the necessary heat power (kW) to have  $T_{hi}$  at 70 to 80°C (and produce the corresponding electricity output). For that, equation 10 is implemented and the necessary heat from the CHP unit is calculated:

$$Q_{CHP} = \frac{4.18 \cdot \dot{m}_{MD} (l/h) \cdot (T_{out} - T_{in})}{3600} \quad (2)$$

When the temperature coming from the tank is below 70°C, the CHP unit switches ON and provides heat to that stream, providing 80°C to the AGMD. This is programmed in TRNSYS inside of an equation block called “CHP”. When the temperature coming from the tank ( $T_{in}$ ) is greater than 70°C ( $GT(T_{in},70)$ )

the CHP is not working, when is not greater than 70°C it provides heat (provides 12°C to have 80°C constantly which is a heat output of around 15 kW). The heat output is calculated in each time step (1h).

Table 18 – Equation block called “Hybrid”

Inputs:
Temperature coming from the tank ( $T_{in}$ ), hot feed flow rate ( $\dot{m}_{MD}$ )
Middle equation:
Necessary
Output:
$T_{out} (°C) = (T_{in} + 12) * (1 - GT(T_{in}, 70)) + T_{in} * GT(T_{in}, 70)$
$Q_{CHP} (kW) = (1 - GT(T_{in}, 70)) * \dot{m}_{MD} * 4.18 * (T_{out} - T_{in}) / 3600$
*GT=Greater than (it works like an “IF” in code language)

#### 4.1.4.1 Biogas digester specifications

For simplicity, electricity and cooking demand and digester specifications are estimated. The digester specifications are shown in Table 19. The digester is assumed to store the manure from the cattle with a time retention from 30 days and produce all the necessary biogas to meet cooking and electricity demands (a manure volume of 120 m<sup>3</sup> is anticipated for economic calculations). The gas holder after the digester is assumed to have enough volume to store all the unused product gas for a while during the day. A daily load profile for each case has been assumed for simplicity. The digester is assumed to be under mesophilic conditions at the optimized pressure and temperature (1 bar 35 °C).

Table 19 – Digester specifications

<b>Digester type</b>	<b>Plug flow</b>
<b>Feedstock</b>	Cattle (1.8 kg/day/head) [63]
<b>Total solid</b>	5-12% [97]
<b>Volatile Solids</b>	75-85% [97]
<b>Biogas Yield</b>	0.20-0.30 m <sup>3</sup> /kg VS /head [97]
<b>Retention days</b>	30 [97]
<b>Temperature and pressure inside digester</b>	35°C and 1 bar [89]

In the case of electricity, the following loads per household were chosen according a socio-economic household survey data from Ethiopia: lighting incandescent bulbs (60 W x 2 in total during 6 h), one radio (2.5 W during 7 h), one TV (84 W during 4 h and 3.5 W in standby) and one mobile phone charger (4 W during 2 h) [21]. It results in a demand of 1.15 kWh/day/household. The cooking demand is assumed to be 1.2 m<sup>3</sup> of biogas (4 h of cooking [98]) per household. The demand of one household (5 people/household) along a day is shown in the following graph:

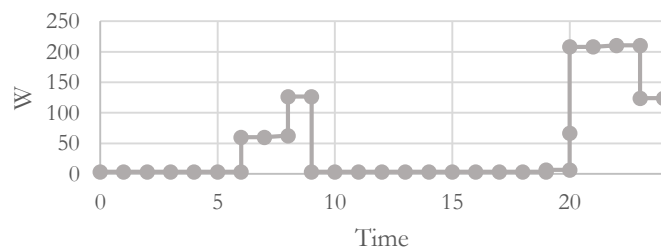


Figure 21 – Electricity demand 1 household in Watts (Own elaboration: based on [21])

#### 4.1.4.2 Other components

The circulation pumps are modeled using Type 3. Pump power demand is simply set to the rated value whenever the control signal indicates that the pump is in operation. 5% of the pump power is assumed to be converted to fluid thermal energy.

Table 20 –AGMD Pump characteristics

<b>Pump type 3d</b> (Pump model Yonos PICO 40/1-8)		
Maximum flow rate	Flow (L/h)	1200 L/h/AGMD x 1 AGMD
Fluid specific heat	C <sub>p</sub>	4.185 kJ/kg
Maximum power		5 W
Conversion coefficient		0.05

#### 4.1.4.3 TRNSYS biogas diagram

Finally, the TRNSYS diagram that connects all the components is shown in Figure 22. One plotter is used to control the simulation containing the temperatures from the tank, membrane and well water; the yield and the heat power that the biogas needs to supply to the system. All the outputs are integrated by hour and exported to a text file. All the results are further analyzed in excel.

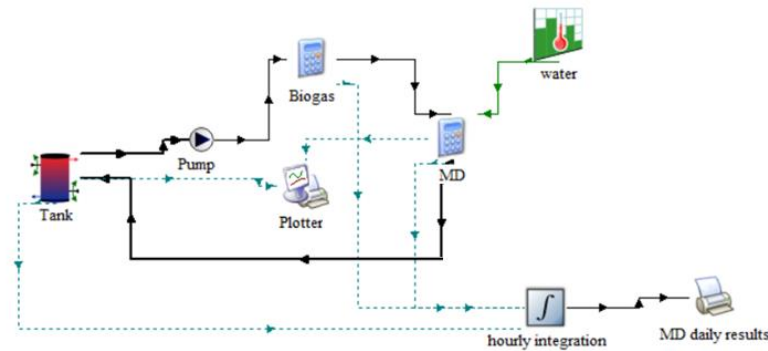


Figure 22 – Biogas TRNSYS diagram

#### 4.1.5 Hybrid case

A combined system using biogas and evacuated tube collector is proposed in order to reduce the number of necessary AGMD units, the size of the CHP unit, the size of the solar field, and have a supply of electricity and biogas for cooking (Compared to the solar case). In this case, the biogas works during the night and/or when the temperature coming from the tank drops below 70 °C. Therefore, the membrane works always in the range of 70-80 °C, maximizing the yield production. Equation 18 is used to implement that. The size of the CHP unit is reduced to 6 kW of electricity. Table 21 shows the catalog data from Viessmann:

Table 21 – CHP catalog Data Specifications Vitobloc 200 EM 6/15 [99]

<b>Power rate</b>	50%	75%	100%
<b>Electricity Output (kW)</b>	3.0	4.5	6.0
<b>Thermal Output (kW)</b>	9.5	11.5	14.0
<b>Fuel input (kW)</b>	13.9	17.7	22.0

Figure 23 shows the general hybrid scheme. It works similarly to the previous schemes. The AGMD is always running. When the temperature coming from the tank is lower than 70°C (with a hysteresis to avoid switching on and switching off the CHP), the CHP unit supplies the necessary heat to the flow. The solar field exchanges heat in the tank when the sun is shining.

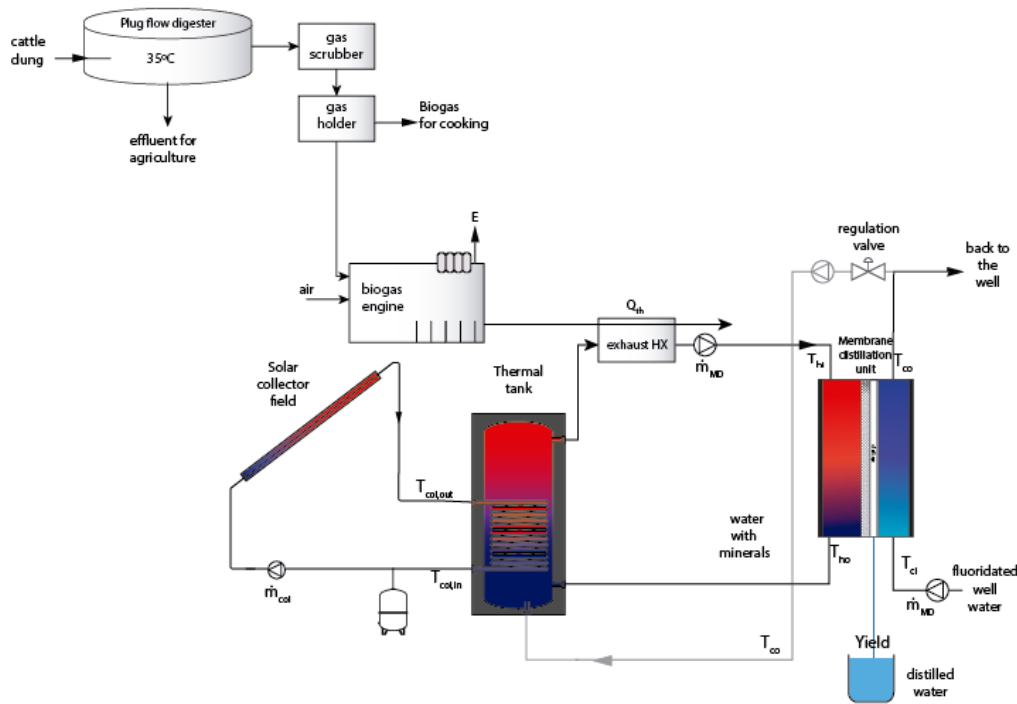


Figure 23 – Hybrid scheme (ETC+CHP unit using biogas)

#### 4.1.5.1 TRNSYS biogas diagram

The TRNSYS diagram is shown in Figure 24. The control type runs the solar pump during the day and during the night turns on the CHP unit (using Type 14) and if the temperature coming from the tank ( $T_{in}$ ) is below 70 °C, the CHP unit supplies a temperature of  $T_{in}+10^{\circ}\text{C}$  to the membrane (corresponding to the maximum heat output 14kW) and produces electricity. As it will work during the night, part of the electricity is stored in a battery to be used during the day by the installation and the households. The necessary heat provided by the CHP unit is calculated with equation 10 (as in the Biogas case). The following equations are in the CHP block called “Hybrid”:

Table 22 – Equation block called “Hybrid”

<p>Inputs:</p> <p>Temperature coming from the tank (<math>T_{in}</math>), hot feed flow rate (<math>F_h</math>),</p> $T_{out}(^{\circ}\text{C})=(T_{in}+10)*(1-GT(T_{in},70))+T_{in}*GT(T_{in},70)$ $Q_{\text{CHP}}(\text{kW})=(1-GT(T_{in},70))*m*4.18*(T_{out}-T_{in})/3600+GT(T_{in},70)*0$ <p>*GT=Greater than (it works like an “IF” in code language)</p>
---

The simulation is done for a whole year and hourly yield, temperatures, solar irradiation and heat provided by the CHP unit ( $Q_{\text{CHP}}$ ) are outputs obtained and exported to a text file. All the results are further analyzed in excel.

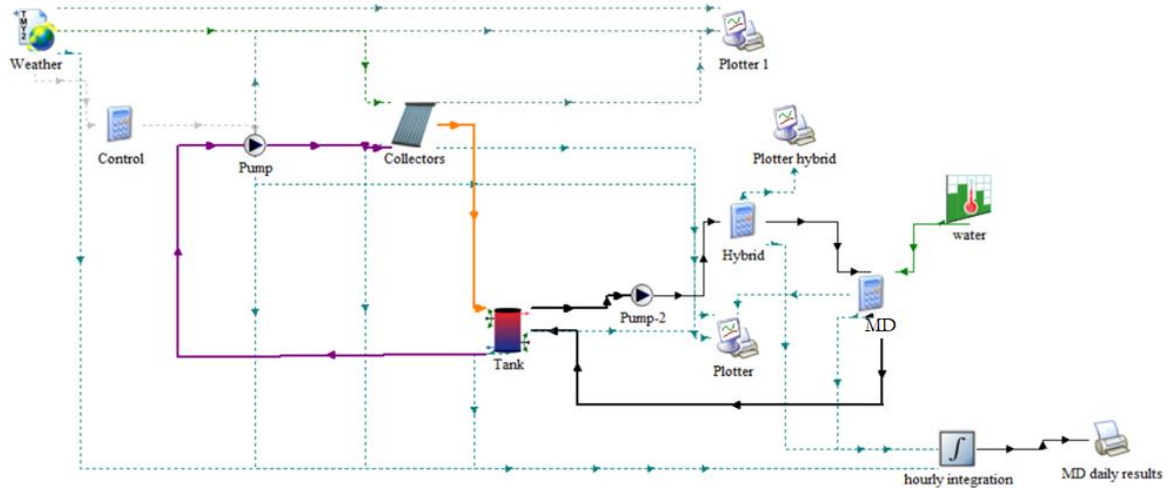


Figure 24 – Hybrid TRNSYS diagram

## 4.2 TRNSYS results

### 4.2.1 Solar case

Several solar fields have been simulated in order to optimize the hypothetical plant.

In both cases, ETC and FPC, with one AGMD unit is not possible to cover the demand. The temperature in the tank goes down during the night and the AGMD cannot produce as much yield as during the day. But, with 3 AGMD working during daylight it covers the yearly demand of 169 m<sup>3</sup>/year in the ETC integration case and 4 AGMD units covers 162 m<sup>3</sup>/year in the FPC integration case. In the case of ETC, less solar field is needed to meet the water demand as it reaches higher temperatures and higher efficiencies. The optimized sizes to cover this demand are: 85 m<sup>2</sup> with ETC and 212.8 m<sup>2</sup> with FPC.

Sometimes, the achieved simulation reaches temperatures of 90-95°C in the AGMD. As the AGMD model only works in the range of 55-80°C hot feed temperatures, the yield is probably higher than the one obtained as the AGMD shows that the permeate flux increases exponentially with feed solution temperature [100]. The system efficiency is calculated using equation 11, which considers the amount of solar irradiance that reaches the solar field and the thermal power delivered by the solar collectors, multiplied by the heat exchanger efficiency:

$$\text{Solar Efficiency (\%)} = \frac{\int_0^{8760h} \dot{Q}_{useful} \cdot 0.8}{\int_0^{8760h} I_{total} \cdot A_{field}} \cdot 100 \quad (3)$$

Table 23 – Solar results

Solar Field (m <sup>2</sup> )	m <sub>col</sub> (m <sup>3</sup> /h)	m <sub>AGMD</sub> (m <sup>3</sup> /h)	AGMD units	Yearly production (m <sup>3</sup> /y)	Average production (l/d)	Specific thermal Demand (kWh/m <sup>3</sup> )	Specific electric demand (kWh/m <sup>3</sup> )	I <sub>total</sub> (kWh/m <sup>2</sup> /y)	η
FPC 213	9.12	4.8	4	162	463	871	7.71	1,935	30%
ETC 85	4.50	3.6	3	169	464	796	3.91	1,935	76%

### FPC optimized case

Figure 25 shows the different yield production for different solar field and number of AGMD in parallel. The yearly demand of 30 households is 164 m<sup>3</sup>/year. To meet 167 m<sup>3</sup>/year it needs at least 4 AGMD in parallel and 212.8 m<sup>2</sup> of solar field (76 FPC) as it only works during the daylight and there is no thermal tank storing energy (to work during the night). As can be seen in Figure 25, the more yield production the more field is needed. But, when the field is big (>195 m<sup>2</sup> with 2 AGMD and >195 m<sup>2</sup> with 3 AGMD), it leads to temperatures higher than 100°C at the tank and the membrane which can cause a degradation of the materials. To solve that, a bigger storage tank can be used to store energy and produce also during the night. But for time restrictions this has not been studied in this thesis.

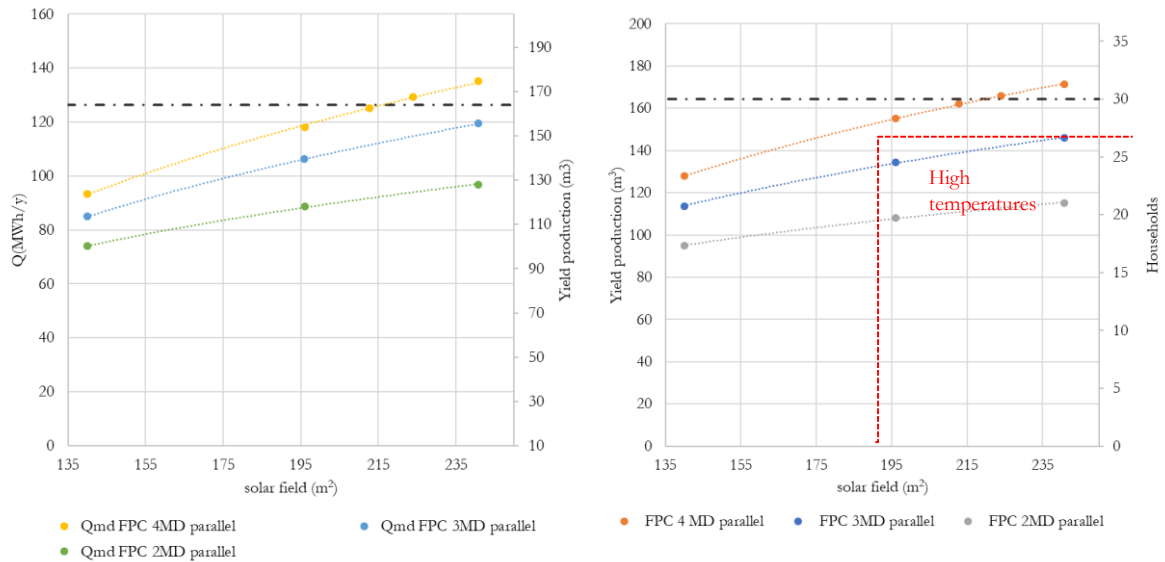
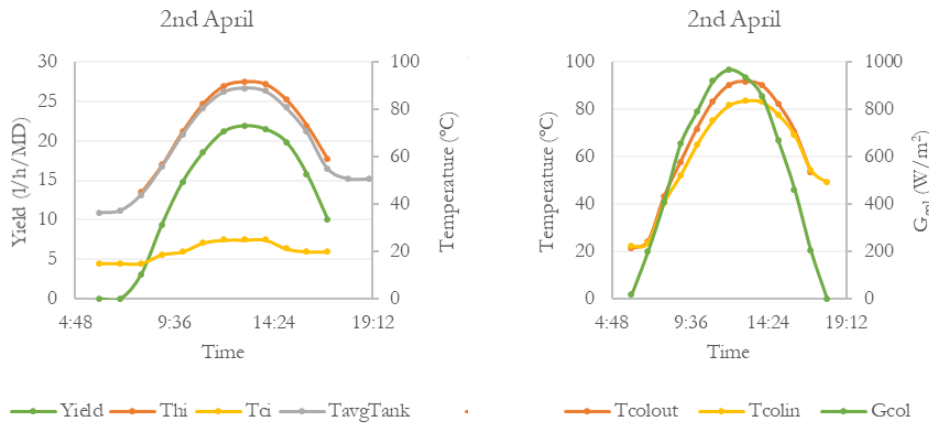


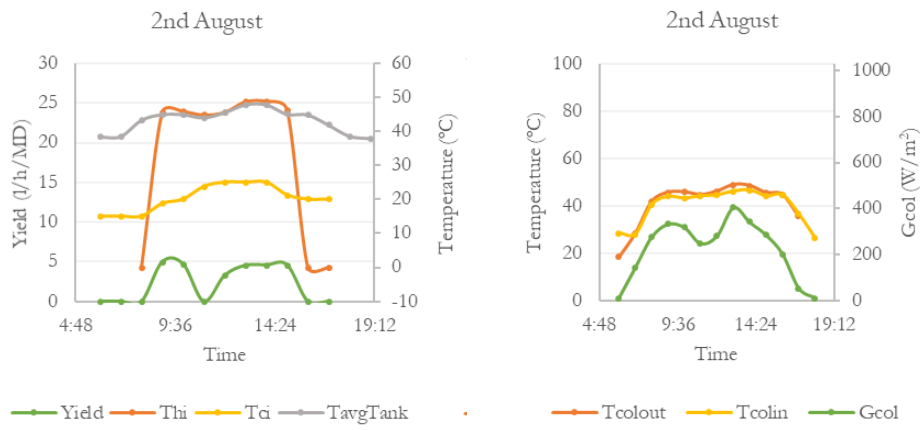
Figure 25 – Simulation results for different solar field, with 2,3 and 4 AGMD units (in parallel) driven by FPC.

The optimized size results in 212.8 m<sup>2</sup> of solar field, which consists of 76 FPC in parallel and 4 AGMD units in parallel. The mean water production is 463 L/day, but the daily permeate yield varies seasonally from 120-780 L/day. But as the demand is 450 L/day, the rest could be stored for the seasons with lower productivities. The following figures shows the daily variation for different seasons of the hot feed inlet temperature ( $T_{hi}$ ), cold feed inlet temperature ( $T_{ci}$ ), yield per module (Yield in L/h), average tank temperature ( $T_{avgtank}$ ), collector hot outlet temperature ( $T_{col,out}$ ), collector cold inlet temperature ( $T_{col,in}$ ) and solar irradiance ( $I_{col}$  in W/m<sup>2</sup>h).

#### a) 2<sup>nd</sup> April (FPC)



b) 2<sup>nd</sup> August (FPC)



c) 16<sup>th</sup> December (FPC)

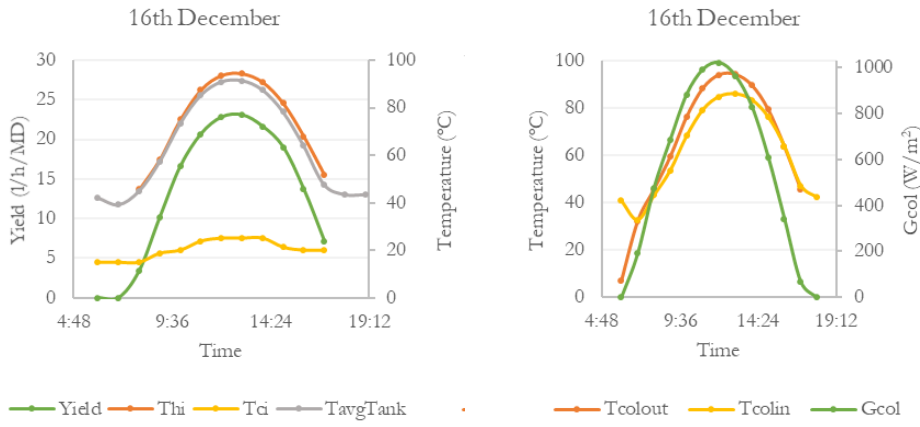


Figure 26 – FPC Results for different dates a) April ,b) August and, c) December

### ETC optimized case

ETC also works during sun hours, but as the efficiency is higher, it can heat up the membrane with less solar field. The solar field and the AGMD units in parallel are varied. With two AGMD units in parallel, it cannot meet the demand, even though the solar field is increased. When the solar field reaches 119 m<sup>2</sup> it would meet the demand but temperatures above 100°C in the tank and the AGMD appear (degradation of materials). The optimized size results in 85.2 m<sup>2</sup> of solar field, which consists of 30 ETC in parallel and 3 AGMD units in parallel. The average permeate yield is 464 m<sup>3</sup>/day, but depending on the season, the daily permeate yield varies from 280-700 L/day. But as the demand is 450 L/day, the rest could be stored for the seasons with lower productivities.

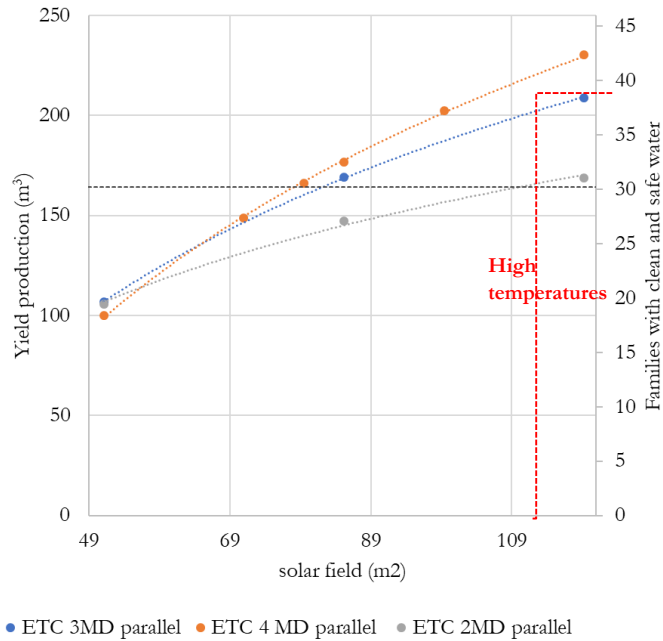
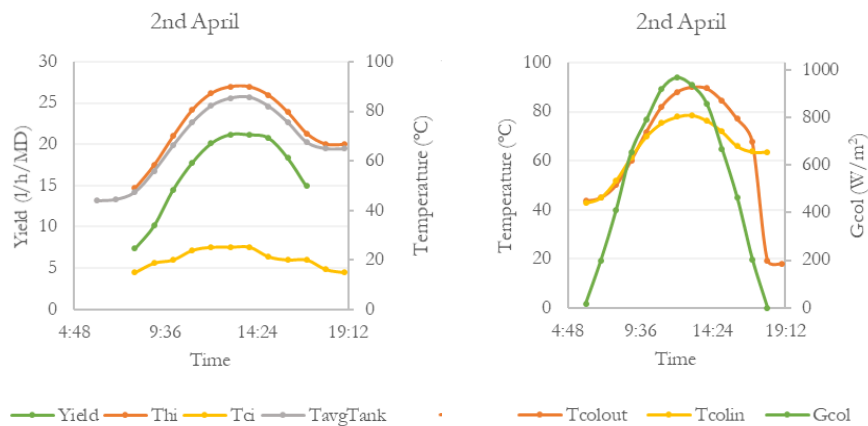


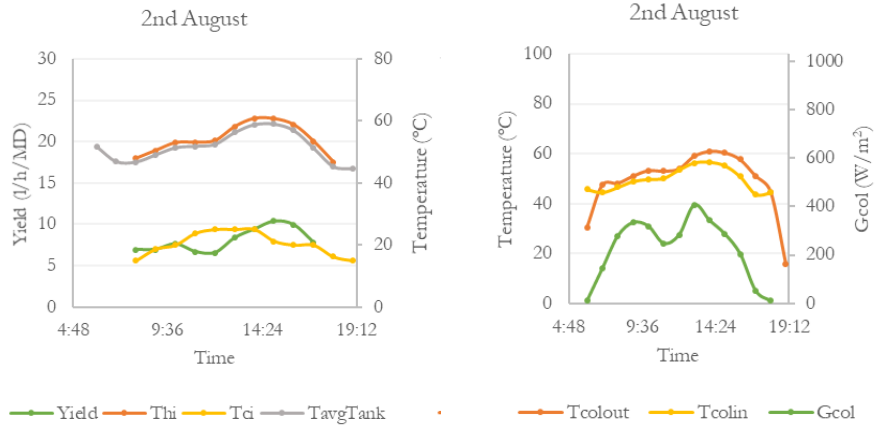
Figure 27 – ETC for different sizes

The following figures show the daily variation for different seasons of the hot feed inlet temperature ( $T_{hi}$ ), cold feed inlet temperature ( $T_{ci}$ ), yield per module (Yield in L/h), average tank temperature ( $T_{avg,tank}$ ), collector hot outlet temperature ( $T_{col,out}$ ), collector cold inlet temperature ( $T_{col,in}$ ) and solar irradiance ( $I_{col}$  in W/m<sup>2</sup>h). In all the figures can be seen that  $T_{hi}$  increases gradually with the increase of solar radiation, reaching a maximum at midday. In April the maximum is 27 l/h/module at midday, whereas in seasons with lower radiation (June-August) it only produces a maximum of 23 l/h/module, varying from 18 to 23 l/h/module. Therefore, the overproduction in the dry seasons needs to be stored to meet the demand in the rainy season.

a) 2<sup>nd</sup> April (ETC)



b) 2<sup>nd</sup> August (ETC)



c) 16<sup>th</sup> December (ETC)

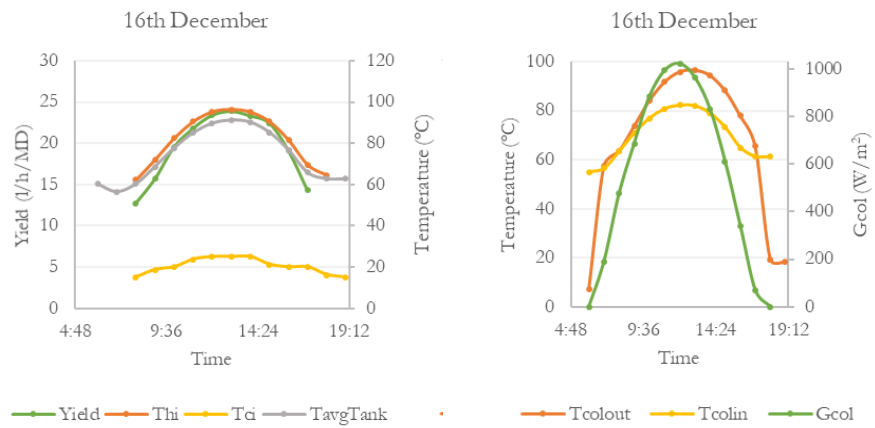


Figure 28 – ETC Results for different dates a) April ,b) August and, c) December

## 4.2.2 Biogas case

The optimal size to cover the thermal demand of the AGMD is a CHP unit of 9 kWe / 20 kW<sub>th</sub>, as the average maximum instantaneous thermal demand is 15 kW. For that model EM-9/20 from Viessman company is used [96]. As can be seen in Figure 29, the temperature of the AGMD is maintained above 70°C the entire day resulting in a yearly production of 165 m<sup>3</sup>. This system has the advantage that it can meet the demand with only one membrane unit. The average electricity production is 46 MWh/year, which can be used to cover the demand of the installation itself (electricity demand of 1.2 MWh/year) and the electricity demand 110 houses.

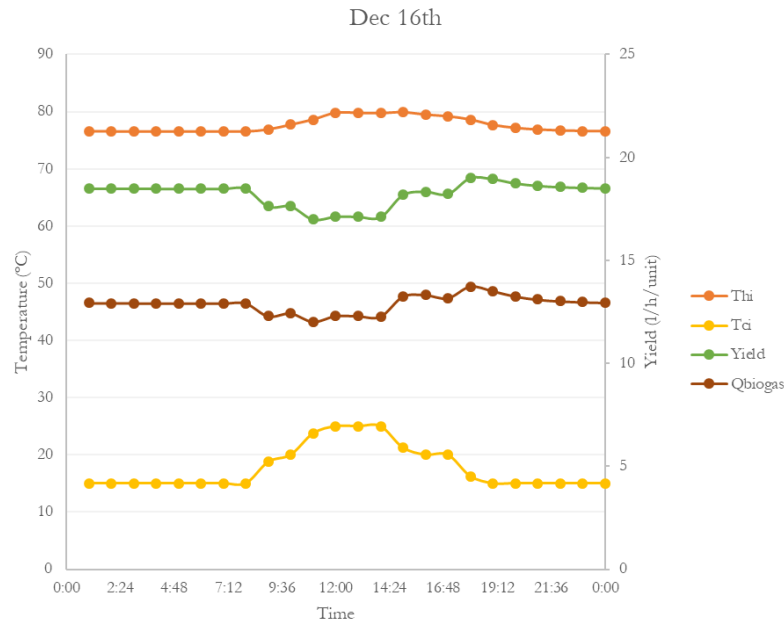


Figure 29 – Biogas case

The yearly biogas demand in the engine is 28,000 m<sup>3</sup>, which is a daily average demand of 77 m<sup>3</sup>/day. At least a digester of 120 m<sup>3</sup> is assumed to cover the demand of the biogas, cooking demands and store the rest of it. To meet that, at least 600 cattle will be needed (1080 kg/day of manure).

Table 24 – Biogas summary

Size	m <sub>AGMD</sub> (m <sup>3</sup> /h)	AGMD units	Yearly production (m <sup>3</sup> /y)	Average production (l/d)	Specific thermal demand (kWh/m <sup>3</sup> )	Specific electric demand (kWh/m <sup>3</sup> )	Electricity production (MWh/y)	η
9 kWe / 20 kW <sub>th</sub>	1.2	1	165	450	740	7.04	46	56%

### 4.2.3 Hybrid case

The combination of biogas and solar might be useful for places that have limited resources. For instance, when a lot of manure is available but limited and solar potential is intermediate. Different solar collector field sizes have been developed with the combination of a CHP unit. Biogas helps the solar to supply 80°C to the AGMD when the temperature is not hot enough (usually when the radiation is lower than 200 W/m<sup>2</sup>). Figure 30 shows the summarized hybrid results: The more solar field (heat from the sun is higher- Q<sub>sol</sub>), the less biogas is needed( less heat from the biogas engine is needed Q<sub>bio</sub>). There is a reduction of 30% in the biogas demand between the case with 14.2 m<sup>2</sup> and 34m<sup>2</sup>; the next case, with a solar field of 42.6 m<sup>2</sup> have a biogas demand of 74 MWh/year almost the same as in the hybrid case of 34m<sup>2</sup> with a biogas demand of 70 MWh/year; which means that even than the solar field is increased, biogas is providing most of the heat. Therefore, the optimal size for this case (1,935 W/m<sup>2</sup>/year) is 34 m<sup>2</sup> of solar field and a biogas CHP unit of 6 kW<sub>e</sub> / 14 kW<sub>th</sub> as it can meet the demand minimizing the costs (moderate demand of biogas with an optimal solar field size).

Table 25 summarizes the results for the optimal size.

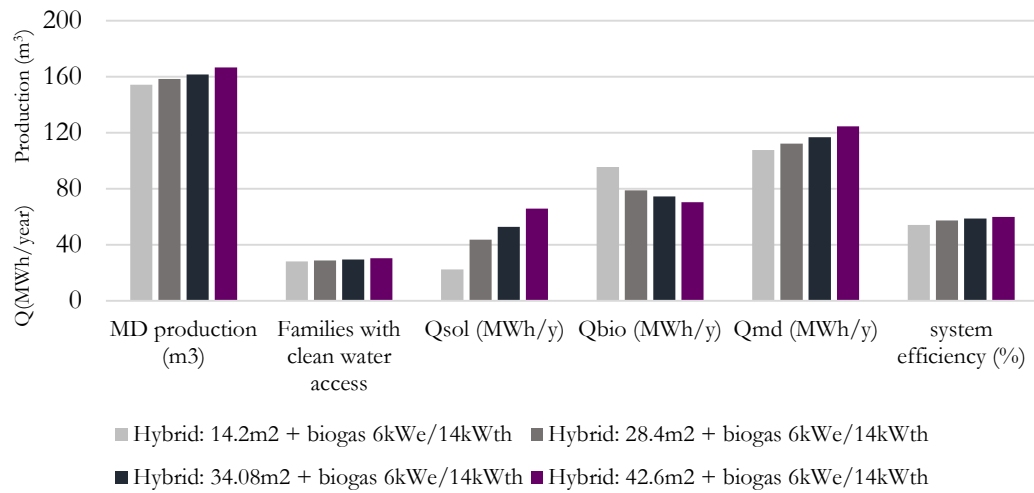


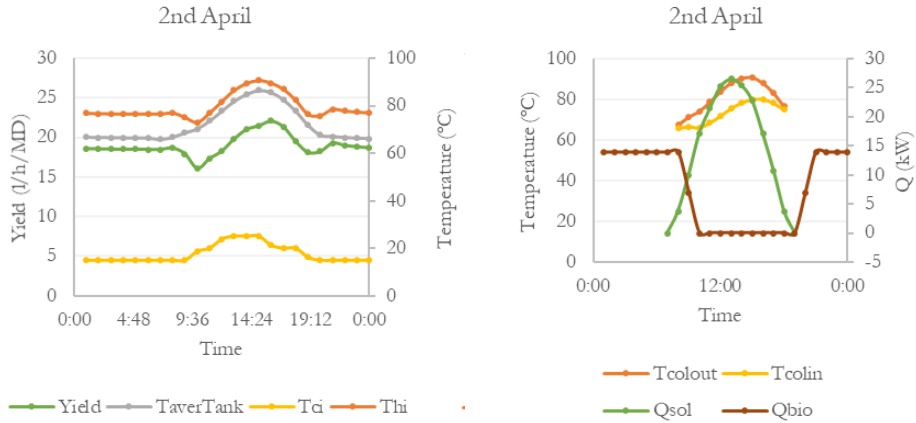
Figure 30 – Hybrid results

Table 25 – Hybrid optimize result

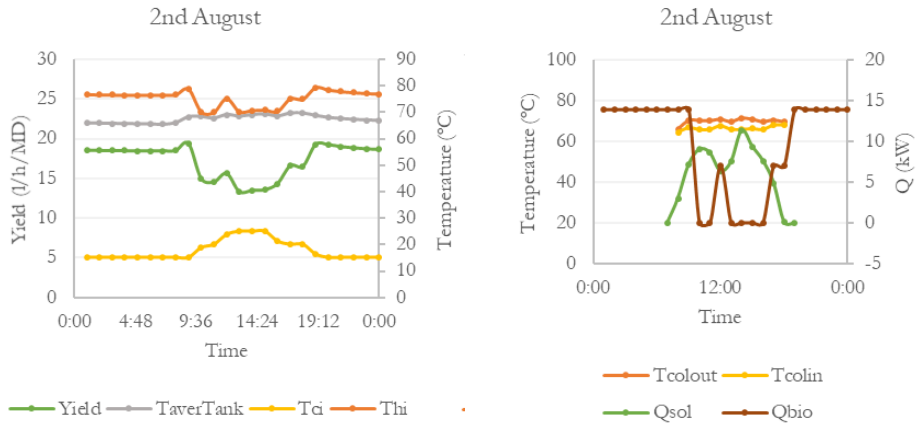
Collector Area	N collectors	AGMD	AGMD production (m <sup>3</sup> )	Average daily production (L/day)	Q <sub>sol</sub> (MWh)	Q <sub>bio</sub> (MWh)	Q <sub>AGMD</sub> (MWh/y)	kWh/m <sup>3</sup>	system efficiency
34.08	12	1	162	443	53	74	117	788	59%

As the figures show, at the beginning of the day the CHP is ON. Once the sun starts shining, the CHP turns off and the solar field provides the heat to the AGMD. when the radiation decreases when the sun sets (around 20:00) the CHP is turned on providing heat during the night. As Figure 31 shows, depending on the season, biogas will cover more(in case of rainy season: figure 32b) or less heat demand (figure 32 a and c), but it will always produce yield from 15 up to 25 L/h (covering the yearly demand of 30 houses). In this case is not necessary to store water for the rainy season: the installation can meet the minimum average daily demand of 450 l/day every day in one year. The temperatures vary depending on the hour of the day, but are maintained above 70°C hot AGMD feed which means that the AGMD production is maximized.

a) 2<sup>nd</sup> April (Hybrid)



b) 2<sup>nd</sup> August (Hybrid)



c) 16<sup>th</sup> December (Hybrid)

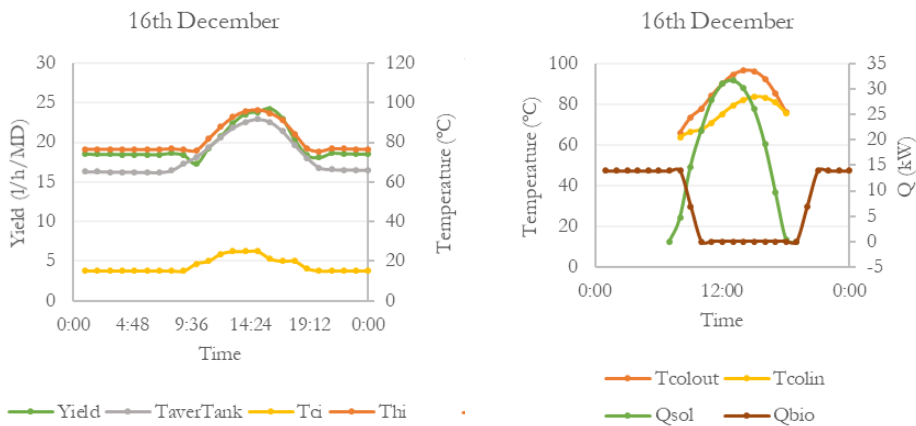


Figure 31 – Results hybrid case seasonally a) April, b) August and, c) December

## 5 ECONOMIC ANALYSIS

Depending on the case the cost of water and its price will vary. The target water cost is 0.3€/liter or lower in order to obtain an affordable price for Ethiopians<sup>5</sup>. The maximum allowable payback period is up to 10 years. A sensitivity analysis is done later varying the discounted rate (DR); the Consumer Price Index (CPI), the electricity cost (to sell), the biogas cost (to sell) and the investment cost of the AGMD unit.

**Investment Cost ( $C_0$ ):** The capital costs show in the following tables for each components of the systems are used to calculate the investment costs ( $C_{0,case i}$ ) of each case:

Table 26 – Capital costs FPC case

Investment costs	Unitary cost	Units	Costs(€)
Collector FPC cost ( $C_{col}$ )	194.6 €/m <sup>2</sup> [101]	212.8 m <sup>2</sup>	<b>41,410.9 €</b>
Pump ( $C_{pumps}$ )	881Wp <sup>0.4</sup> [34]	300 W, 2 x 7 W	786.4 €
AGMD units ( $C_{AGMD}$ )	5400 €/unit [37, 71, 90, 84]	4 AGMD units	21,600.0 €
Hydraulics/piping/filters ( $C_{hydraulics}$ )	30%·C <sub>col</sub> [84, 34]		18,903.3€
Storage tank ( $C_{tank}$ )	6,257 €/unit <sup>a</sup>	1 unit, 2 m <sup>3</sup>	6,267.0 €
Distillated water tank ( $C_{water}$ )	2,984 €/unit <sup>a</sup>	1 unit, 1 m <sup>3</sup>	2,984.0 €
Installation costs	5% of total component cost [34]		4,597.6 €
<b>Total</b>			<b>96,549.1 €</b>

<sup>a</sup> Manufacturer provided costs (Salvador Escoda)

Table 27 – Capital costs ETC case

Investment costs	Unitary cost	Units	Costs(€)
Collector ETC cost ( $C_{col}$ )	220.8 €/m <sup>2</sup> [101]	85.2 m <sup>2</sup>	<b>18,812.2 €</b>
Pump ( $C_{pumps}$ )	881Wp <sup>0.4</sup> [34]	150W, 2x4W W	606.1 €
AGMD units ( $C_{AGMD}$ )	5400 €/unit [37, 71, 90, 84]	3 AGMD units	16,200.0 €
Hydraulics/piping ( $C_{hydraulics}$ )	30%·C <sub>col</sub> [84, 34]		10,503.7 €
Storage tank ( $C_{tank}$ )	6,257 €/unit <sup>a</sup>	1 unit, 2 m <sup>3</sup>	6,267.0 €
Distillated water tank ( $C_{water}$ )	2,984 €/unit <sup>a</sup>	1 unit, 1 m <sup>3</sup>	2,984.0 €
Installation costs	5% of total component cost [34]		2,768.6 €
<b>Total</b>			<b>58,141.5 €</b>

<sup>a</sup> Manufacturer provided costs (Salvador Escoda)

Table 28 – Capital costs CHP Biogas case

Investment costs	Unitary cost	Units	€
CHP system (169.7 €/kW --> 9 kW)	169.7 €/kW [102]	9 kW	1,528.2
Digester (170€/m3)	170 €/m <sup>3</sup> [102]	140 m <sup>3</sup>	23,800.0
Cost of manure (1 year)	0.04 €/kg [103]	1044 kg/day of manure	15,242.4
Pump ( $C_{pumps}$ )	881Wp <sup>0.4</sup> [34]	2 x 4 W	193.6
AGMD units ( $C_{AGMD}$ )	5,400 €/unit [37, 71, 90, 84]	1 AGMD units	5,400.0
Hydraulics/piping ( $C_{hydraulics}$ )	30%·C <sub>col</sub> [84, 34]		1,620.0
Storage tank ( $C_{tank}$ )	6,257 €/unit <sup>a</sup>	1 unit, 2 m <sup>3</sup>	6,267.0
Distillated water tank ( $C_{water}$ )	2,984 €/unit <sup>a</sup>	1 unit, 1 m <sup>3</sup>	2,984.0
Piping and fittings	15%·Digester [104]		3,570.0
Installation costs	5% of total component cost [34]		1,714.9
<b>Total</b>			<b>62,320.1</b>

<sup>a</sup> Manufacturer provided costs (Salvador Escoda)

<sup>5</sup> From a semi-structured interview with a local resident, the water price of bottle water is 30cts€/liter.

Table 29 – Capital costs hybrid case

Investment costs	Unitary cost	Unit	€
Collector ETC cost ( $C_{col}$ )	220.8 €/m <sup>2</sup> [101]	34 m <sup>2</sup>	<b>7,507.2 €</b>
CHP system (169.7 €/kW --> 9 kW)	169.7 €/kW [102]	6 kW	1,018.8 €
Digester (170€/m <sup>3</sup> )	170 €/m <sup>3</sup> [102]	100 m <sup>3</sup>	17,000.0 €
Cost of manure (1 year)	0.04 €/kg [103]	891 kg/day of manure	13,008.6 €
Pump ( $C_{pumps}$ )	$881W_p^{0.4}$ [34]	70 W, 2 x 4 W	957.4 €
AGMD units ( $C_{AGMD}$ )	5,400 €/unit [37, 71, 90, 84]	1 AGMD units	5,400.0 €
Hydraulics/piping ( $C_{hydraulics}$ )	$30\% \cdot C_{col}$ [84, 34]		3,872.2 €
Storage tank ( $C_{tank}$ )	6,257 €/unit <sup>a</sup>	1 unit, 2 m <sup>3</sup>	6,267.0 €
Distilled water tank ( $C_{water}$ )	2,984 €/unit <sup>a</sup>	1 unit, 1 m <sup>3</sup>	2,984.0 €
Piping and fittings	$15\% \cdot \text{Digester}$ [104]		2,550.0 €
Installation costs	5% of total component cost [34]		1,298.4 €
<b>Total</b>			<b>54,356.4 €</b>

<sup>a</sup> Manufacturer provided costs (Salvador Escoda)

### The Net Present Value (NPV)

A discounted cash flow model is considered. The economic benefits (returns,  $r_i$ ) are obtained through selling clean and safe water. Also, in the biogas and hybrid case, electricity and biogas for cooking are considered as earnings. The projection costs ( $c_i$ ) are operation and maintenance costs (O&M 2% of the total investment costs [84]) and costs of salts (0.015 €/m<sup>3</sup>) for all cases. In case of solar, the electricity cost is also added (with an annual increase of 5%). In the biogas and hybrid case, the cost of the manure is considered in O&M.

With a given discounted rate (DR = 8%) and consumer price index (CPI = 2.5%), the current value of the future returns is calculated with the following equation [105]:

$$NPV = -C_0 + \sum_{i=0}^{N=20} \frac{r_i}{(1+DR)^i} - \sum_{i=0}^{N=20} \frac{c_i}{(1+DR)^i} \quad (4)$$

Where the returns and costs in all cases are as follows:

$$r_i = \text{Yield} \left( \frac{L}{\text{year}} \right) \cdot W_{price} \left( \frac{\text{€}}{L} \right) \cdot (1+CPI)^{i-1} \quad (5)$$

$$c_i = O\&M \left( \frac{\text{€}}{\text{year}} \right) (1+CPI)^{i-1} + \text{salts} \left( \frac{\text{€}}{\text{m}^3} \right) \cdot \text{Yield} \left( \frac{\text{m}^3}{\text{year}} \right) (1+CPI)^{i-1} \quad (6)$$

In case of hybrid and CHP case, the earnings from selling electricity and biogas for cooking are added to that:

$$r_{i, \text{hybrid and CHP}} = \text{Yield} \left( \frac{L}{\text{year}} \right) \cdot W_{price} \left( \frac{\text{€}}{L} \right) \cdot (1+CPI)^{i-1} + E \left( \frac{kWh}{\text{year}} \right) \cdot C_e \left( \frac{\text{€}}{kWh} \right) \cdot (1+CPI)^{i-1} \\ + B \left( \frac{\text{m}^3}{\text{year}} \right) \cdot C_B \left( \frac{\text{€}}{\text{m}^3} \right) (1+CPI)^{i-1} \quad (7)$$

In case of solar, the costs of consuming electricity from the grid with an annual increase of 5% are added:

$$c_{i, \text{solar}} = O\&M \left( \frac{\text{€}}{\text{year}} \right) + \text{salts} \left( \frac{\text{€}}{\text{m}^3} \right) \cdot \text{Yield} \left( \frac{\text{m}^3}{\text{year}} \right) + E \left( \frac{kWh}{\text{year}} \right) \cdot C_{ethiopia, \text{grid}} \left( \frac{\text{€}}{kWh} \right) \\ \cdot (1+0.05)^{i-1} \quad (8)$$

Plus, every five years the membranes are changed and the added cost to that is:

$$C_{\text{membrane, replacement (every 5 years)}} = 15\% \cdot C_{MD} \quad [84] \quad (9)$$

The NPV reflects the future revenues converted into the equivalent earnings at the beginning time of the project. If it is greater than zero, the investment cost is recovered and there are benefits.

### The Pay Back period (PB)

It is the amount of time to recover the initial investment, i.e., value of  $i$  that  $NPV=0$  for a given discounted rate ( $DR=8\%$ ) [105]:

$$0 = -C_0 + \sum_{i=0}^{N=PB} \frac{r_i}{(1+DR)^i} - \sum_{i=0}^{N=PB} \frac{c_i}{(1+DR)^i} \quad (10)$$

### The Internal Rate of Return (IRR)

IRR is the value of the discounted rate that NPV is zero. It enables to compare different alternatives by forcing the NPV of each investment to zero. IRR must be greater than the interest rate to consider the case profitable; if it is less, then the case is non-profitable. Therefore, the calculating formula of IRR would be as following [105]:

$$NPV = 0 = -C_0 + \sum_{i=0}^{N=20} \frac{r_i}{(1+IRR)^i} - \sum_{i=0}^{N=20} \frac{c_i}{(1+IRR)^i} \quad (11)$$

## 5.1 Economic Results

Table 30 shows a summary of economic results. As it can be seen, the FPC case has the highest initial cost, as it needs a lot of solar thermal collectors and 4 AGMD units to meet the demand. Solar (FPC and ETC) has lower operating costs because it does not need to buy any fuel, it only needs to clean the solar panels, add salts to the water tank and maintain the installation in good conditions. The Biogas case has the highest operating costs because the manure purchase to the farmers is considered. Hybrid case is a compromised choice, with the lowest initial costs and medium operating costs. The FPC case results in the highest water cost to be able to recover the high initial costs in 10 years. Biogas has the second highest water cost due to the operating costs. Economically the ETC case results the best one, as it has high NPV at the end of 20 years (high benefits), the higher IRR and the water cost is low. Nevertheless, the hybrid case is also a good choice as it has a IRR greater than the DR, high NPV and the lowest water cost. Also, it offers more sub-products to the households: electricity and biogas at a low price. More details in Table 30.

Table 30 – Economic results for different cases

Parameter	FPC	ETC	Biogas	Hybrid
<b>Initial cost (€)</b>	96,549.1 €	58,141.5 €	62,320.1 €	54,356.4 €
<b>Operating costs (O&amp;M + salts +manure) (€/year)</b>	1,933.48 €	1,165.32 €	16,959.2€	14,154.0€
<b>Lifetime (years)</b>	20	20	20	20
<b>Discounted rate (%)</b>	8%	8%	8%	8%
<b>CPI (%)</b>	2.5%	2.5%	2.5%	2.5%
<b>Water cost (€/liter)</b>	0.1	0.063	0.083	0.062
<b>Biogas cost(€/m<sup>3</sup>)</b>	-	-	0.15	0.15
<b>Electricity cost – to sell (€/kWh)</b>	-	-	0.15	0.15
<b>Electricity cost – to buy (€/kWh)</b>	0.5 <sup>a</sup>	0.5 <sup>a</sup>	-	-
<b>Payback period (year)</b>	10.0	10.0	10.0	10.0
<b>Net present value (NPV)</b>	56,975.6 €	34,201.1 €	36,343.5 €	33,218€
<b>Internal rate of return (IRR)</b>	12.9%	14.7%	10.5%	10.0%

<sup>a</sup>Price from Socio-economic survey (500BIRR/month) [21] 1 EUR = 32.4254 ETB ↔ 1 ETB = 0.0308400 EUR

If the water cost is maintained constant as 0.062€/liter (the water cost for the hybrid case calculated with an allowable payback of 10 years), the time to recover the investment in each case will change. Figure 32 shows the payback period for that water cost (0.062€/L) for each technology. As it can be seen, the lower payback period is for the Hybrid case (10 years) but the ETC case is also competitive showing almost the same time recovery (10.4 years). With a water cost of 0.062 €/L, the resulting payback period is higher for the biogas and FPC case.

ETC case has a simpler operation, as it does not depend on the farmers or on the biogas production. But the Hybrid case can have more benefits to the community. Depending on the demands of each community (just water or water, electricity and biogas) one or other option would be more interesting. For further analysis, the hybrid case is chosen.

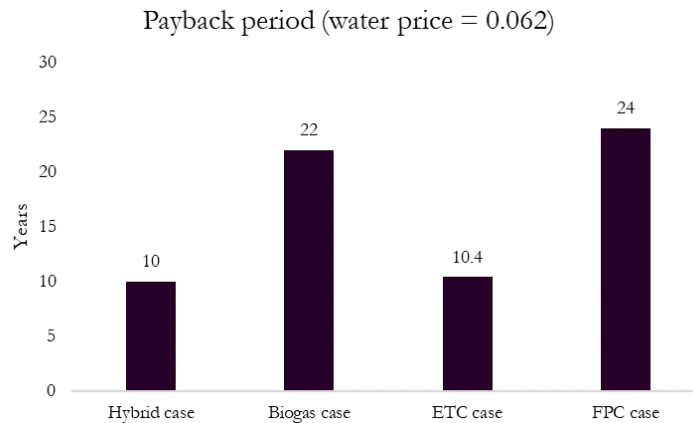


Figure 32 – Payback period (years) with a constant water cost (0.062 €/L), with constant economic variables (DR=8%, CPI=2.5%)

### Sensitivity analysis

For the hybrid case (details in Table 30), the NPV for these conditions (DR = 8%, CPI = 2.5%) is 33,218€ along 20 years. But the market can change, and a sensitivity analysis varying the DR, CPI, electricity cost (to sell), biogas cost (to sell) and AGMD investment costs is done. Figure 33 shows a sensitivity analysis on the NPV for the hybrid case for a constant water cost of 0.062 €/liter. NPV is mainly affected by the variation of the biogas cost (to sell), the electricity cost (to sell) and the interest rate. The higher the DR, the lower NPV at the end of 20 years, so the project will be influenced directly by changes in the market. The higher the biogas and electricity cost (to sell), the higher the NPV at then of 20 years, as it will increase the incomes especially the electricity. The AGMD cost is only 13% out of the total initial cost, so a variation in this price does not affect much the benefits. A variation in the CPI does not disturb the NPV as it will increase both the incomes and costs.

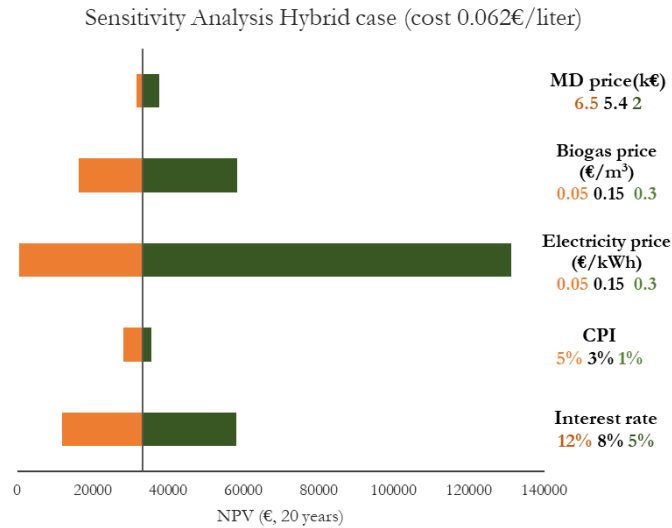


Figure 33 – NPV sensitivity analysis (water cost constant = 0.062 €/L) for the Hybrid case.

These variations also disturbed the PB. For a constant price of water of 0.062 €/L: the higher electricity and biogas cost (to sell), the PB is lower as there are more incomes and the investment is recovered sooner. Increasing the interest rate also increases the PB. Variation in CPI and AGMD price do not affect much to the PB.

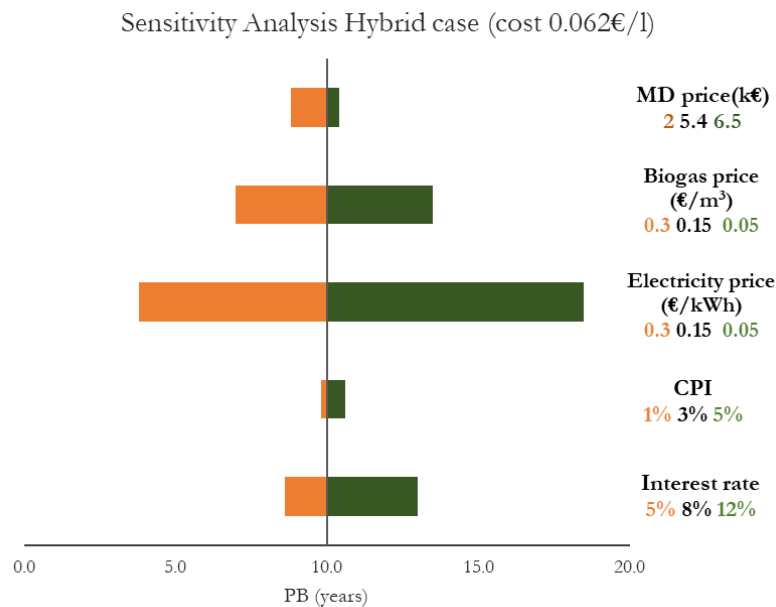


Figure 34 – PB sensitivity analysis (water cost constant = 0.062 €/L) for the Hybrid case.

For a constant payback period of 10 years, and varying the same variables the ideal water cost will to recover the investment in 10 years will vary as well. If the biogas and electricity cost is higher, the water cost can be lower. The water cost is not affected much by the market or the AGMD costs.

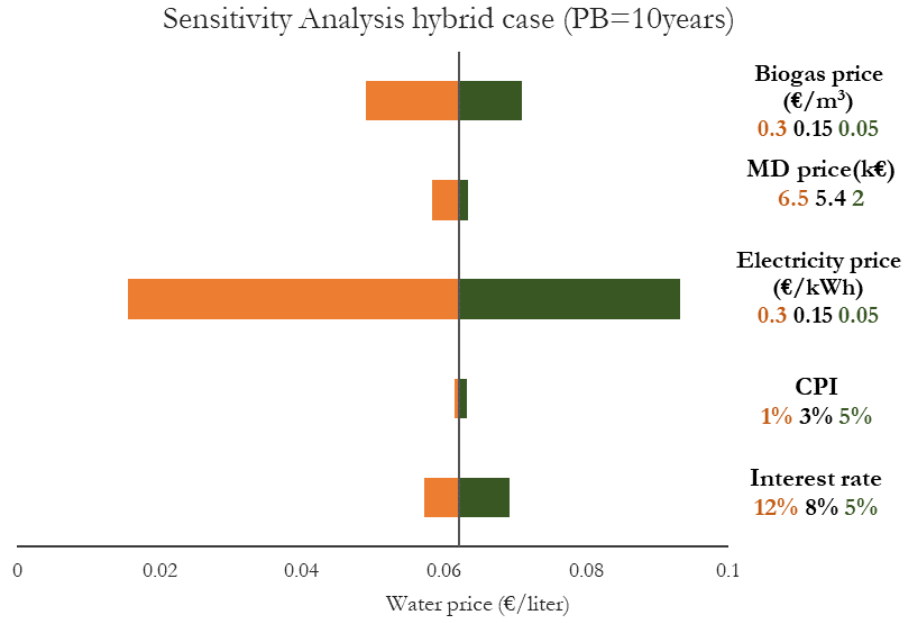


Figure 35 – Water cost sensitivity analysis (PB constant = 10 years) for the Hybrid case.

## 6 TECHNO-ECONOMIC DISCUSSION

Table 31 presents a summary of all the results. The different cases that have been studied are hardly comparable among them because each of the systems provide different services (just water, or water, biogas for cooking and electricity). As a general approach, clean water is considered as the main service to be provided due to the high priority of water security in the sustainable development of a community. Therefore, the biogas and electricity supply are seen as a positive but secondary outcome of some of the cases. Eventually, the specific requirements of each particular community should be considered to select the optimal option. According to the obtained results, all the cases produce the same amount of water per year as all of them are sized to meet the water demand. Furthermore, the specific demand of the system is similar in every case as the systems are meant to maximize the production on the membrane side. Nevertheless, it can be seen in the daily variation of the temperatures (Figure 26, Figure 28, Figure 31 and Figure 29) that in the Biogas case the temperatures are more steady than in the rest of the cases, meaning that the use of the AGMD is maximized (it has the highest temperature difference during 24h a day). In the Hybrid case temperature are not as steady as in the Biogas case due to the variation of the solar radiation during the day.

Regarding the efficiency of the system on the production side the ETC is the most efficient one. However, in a real system the global efficiency increases with the number of components in a system, because the individual inefficiencies are added up. Consequently, since the ETC case has three AGMD units in parallel and 30 ETC in parallel can be more inefficient compared to the Hybrid case with one AGMD, 1 CHP unit and 12 ETCs and also less efficient than the Biogas case with just one AGMD and 1 CHP unit. The FPC would be the most inefficient one, with 76 FPC in parallel and 4 AGMDs.

In terms of the costs, the lowest investment cost is obtained in the Hybrid case with a total of 54,356.4 €, followed by the ETC case with 58,141.5 €, the Biogas case with 62,320.1 € and finally the FPC case with 96,549.1 €. The highest investment cost in the FPC case is mainly due to the large amount of FPC that are required, which account for 43% of the total costs. In the ETC case, the solar field cost is reduced in half (from 41,410.9 € which is required in the FPC case, to 18,812.2 € in the ETC case) as ETC is more efficient and can provide the same amount of heat with less solar field. Besides that, a smaller solar field requires less pipes and hydraulics components, which also results in lower investment costs for the ETC case compared to the FPC case. In the Hybrid and Biogas cases, the biggest contribution to the investment cost is the digester, accounting for 30% and 40% over the total costs, respectively. In the Hybrid case there is a reduction on the necessary heat from the biogas because the rest is provided by solar, which results in a smaller digester volume. Moreover, as in the Hybrid case the solar field is smaller than in the ETC or FPC case, the costs associated to hydraulic equipment and solar collector are smaller. Regarding the operation and maintenance, the associated costs are higher for the Biogas and Hybrid cases because the purchase of the manure is considered as an operational cost. In terms of the maintenance of solar systems, ETC typically presents maintenance problems that can be solved easier than those in FPC, but the costs are usually higher. Thus, once there is a loss of vacuum in the pipes in ETC, only the affected pipes need to be replaced. In contrast, when a FPC is broken (e.g. loss of insulation, break of the glass cover, etc.), the whole solar collector needs to be replaced, which is less expensive than replacing a whole evacuated tube collector.

To conclude, the ETC and the Hybrid cases have shown the best economic results, where both have a low water cost for a payback period of 10 years, a high NPV and a good IRR. FPC case is too expensive for Ethiopia, a developing country where the majority of the population has low incomes<sup>6</sup>. Despite the economic results are not the best in a context with abundance of solar resources, Biogas case can be competitive for rural areas with low solar radiation. ETC can be a more suitable option for communities with low incomes in order to improve their access to clean water in a short-term. In long term they are

---

<sup>6</sup> The average annual income in 2011 was 4100 Birr (129.55€) in the country and 752 Birr (23.78€) in rural areas. [136]

going to need electricity and improve their cooking stoves, for that Hybrid case is a good investment. Nevertheless, a biogas engine requires higher maintenance and operation service such as the collection of manure, the disposal of the manure in the digester, maintenance of the digester at good operation variables, collection and disinfection of the effluent from the digester, etc. For that purpose, more educated workers are needed in the Hybrid case rather than the ETC case. But in both cases, a worker will be needed to maintain a good equilibrium of salts in the water that is going to be sold and to purchase the water to the community.

Table 31 - Summary results

Parameter	FPC	ETC	Biogas	Hybrid
Solar field (m <sup>2</sup> )	212.8	85.2	-	34.1
Biogas size	-	-	9kW <sub>e</sub> /20kW <sub>th</sub>	6kW <sub>e</sub> /14kW <sub>th</sub>
Water production (m <sup>3</sup> )	162	169	165	162
Specific energy Demand (kWh/m <sup>3</sup> )	778	781	740	788
Electricity Demand (MWh <sub>e</sub> /y)	1.2	0.7	1.2	1.5
Electricity production(MWh/y)	-	-	46	27
Thermal system's efficiency (%)	30	76	56	59
Initial cost (€)	96,549.1 €	58,141.5 €	62,320.1 €	54,356.4 €
Operating costs (O&M + salts +manure) (€/year)	1,933.48 €	1,165.32 €	16,959.2€	14,154.0€
Lifetime (years)	20	20	20	20
Discount rate (%)	8%	8%	8%	8%
CPI (%)	2.5%	2.5%	2.5%	2.5%
Water cost (€/liter)	0.1	0.063	0.083	0.062
Biogas cost(€/m <sup>3</sup> )	-	-	0.15	0.15
Electricity cost – to sell (€/kWh)	-	-	0.15	0.15
Electricity cost – to buy (€/kWh)	0.5	0.5	-	-
Payback period (year)	10	10	10	10
Net present value (NPV)	56,975.6 €	34,201.1 €	36,343.5 €	33,218€
Internal rate of return (IRR)	12.9%	14.7%	10.5%	10.0%

## 7 CONCLUSION AND OUTLOOK

In conclusion, it has been seen that fluoride-contaminated water is a crucial problem in the MERV. In Ethiopia, 14 million people still relies on contaminated water from water wells and AGMD could be an option to solve this. Besides that, 73% of the population lacks of energy access, there. Integrating the AGMD with renewable energy technologies could also help to provide access to electricity and other services in rural areas. But the main priority in the government should be to remove fluoride from water and to invest in having a reliable and clean access to water.

The TRNSYS and AGMD regression model from this thesis have its limitations but it allows to perform an estimated design. In a more detailed analysis of the AGMD model, larger samples (typically 45 or more) should be used to obtain a better regression model. Other option can be to measure all the temperatures shown in Figure 38 to do a heat transfer model, like the one performed in [91]. In the TRNSYS model thermal storage could be explored. This study has analyzed 4 renewable energy technologies (FPC, ETC, CHP using biogas or a hybrid system (ETC+CHP)) using TRNSYS to drive a membrane distillation based water purification system. It has shown that any of the technologies can provide clean water to the community in a whole year. The solar cases need water storage to be able to provide water in the rainy season (when there is less sun radiation). The CHP and hybrid case doesn't need this storage, and provides water just using one AGMD running 24h of the day. These last two cases can also provide electricity, biogas for cooking and fertilizer for agriculture which will help Ethiopia to improve the electricity access, the health cooking-related problems and the lack of nutrients in their soil. Hybrid case and ETC case are the most attractive options techno-economically. Depending on the necessities of the community and the availability of resources one or other case should be installed. In the MERV area there is sufficient solar radiation, therefore the hybrid case is recommended as it could benefit considerably the community where is installed. The sensitivity analysis for this case has shown that the price of electricity and biogas (To sell to the community) will affect directly the economic performance of the installation. In case the AGMD is developed in a commercial way with lower prices (economy of scale) will help to reduce the investment cost, but as it is shown in the sensitivity analysis, it will not affect considerably the water cost or the economy of the installation.

It is difficult to make a good comparison as the cases are very different and not all of them are supplying the same services. From the technical side only the water production and thermal efficiency are compared. In reality, the necessities of the community where these kind of installations are going to be installed should be explored. Besides that, materials available in the area, the Ethiopian policies and the lack of trained people should be considered. All the installations require a big investment that might not be possible to afford by the community. A private, institutional or governmental investor can solve this. Applying a subscription business model [106], where people are not paying for the installation itself but a monthly subscription (like "taxes") can also be considered. In this way, people are having a reliable service of clean and safe water by paying an affordable price. But there is still a necessity of training people, and to study the available materials and technologies in the area.

### **Outlook**

For further investigations, the end-user's issues such as the collection of manure, maintenance of the system, Ethiopian culture and social acceptance of the membrane needs to be considered in order to proceed for installing these kind of systems. Also, solar thermal storage is not studied in this thesis, but other studies have shown that with high thermal storage it can run for four hours after the sun is gone [107] which will lead to lower AGMD units and lower investment costs in the end. For instance, a 186 m<sup>2</sup> of solar field and 7.2 m<sup>3</sup> of heat storage can run 12 AGMD modules (120 m<sup>2</sup> membrane, 2 rows in parallel of 6 AGMD units in series), resulting in a production of 3.5 m<sup>3</sup>/day in Gran Canarias. Finally, the model in TRNSYS needs to be demonstrated via in-field trials to be able to explore these kind of projects in different areas and to improve the economic analysis.

Besides that, the application of AGMD in a major scale in current or future power plants in the country should be explored by the government. An integrated system combining the waste heat from the future geothermal and biomass power plants with AGMD can be a very interesting solution in the country. This integration will be in line with the Ethiopian energy policy objectives [40], as the heat energy source will be renewable, carbon neutral and the system will be more energy-efficient, while reducing system costs.

The brine disposal costs are not considered in this thesis, but it is important to mention that due to its great environmental impact, it should be considered in the future. The water is recirculating fluoride to the tank increasing the concentration of it inside the tank and the brine needs to be removed once in a while (there is not data for this) to ensure the good operation of the installation. Due to time constraints brine disposal wasn't considered during the thesis, but it won't affect the economic comparison as all the analyzed systems produce the same amount of water (therefore, the same amount of brine per year and consequently, the same associated costs). For brine disposal, brine evaporation ponds can be studied to be used to remove the minerals and fluoride from the water stored in the tank and sell the product (concentration of salts). Also, for Ethiopia in general (at the national level) a total management of the water can be used in order to increase the clean and safe water access: including rain water harvesting, desalination, and waste water treatment like the one in Singapore [80].

Finally, these type of projects that integrate renewable energy technologies with additional services are in principle attractive in terms of the associated socio-economic benefits. However, in reality, as mentioned before, operation and maintenance problems or the high investment costs are constraints to attract investors, and great policy efforts and a good business model would be required for the project to be successful.

## 8 BIBLIOGRAPHY

- [1] UNa, "Water and sustainable development," 2015. [Online]. Available: [http://www.un.org/waterforlifedecade/water\\_and\\_sustainable\\_development.shtml](http://www.un.org/waterforlifedecade/water_and_sustainable_development.shtml). [Accessed 26 02 2018].
- [2] UNb, "Water and sustainable development - Information brief," UNEW-DPAC, 2015.
- [3] UNc, "Sustainable Development Goals: 6 Clean Water and sanitation," 2017. [Online]. Available: <http://www.un.org/sustainabledevelopment/water-and-sanitation/>. [Accessed 02 March 2018].
- [4] M. A. Walton, "Energy has a role to play in achieving universal access to clean water and sanitation," IEA, 22 March 2018. [Online]. Available: [http://www.iea.org/newsroom/news/2018/march/commentary-energy-has-a-role-to-play-in-achieving-universal-access-to-clean-water.html?utm\\_content=buffer9a2b2&utm\\_medium=social&utm\\_source=twitter.com&utm\\_campaign=buffer](http://www.iea.org/newsroom/news/2018/march/commentary-energy-has-a-role-to-play-in-achieving-universal-access-to-clean-water.html?utm_content=buffer9a2b2&utm_medium=social&utm_source=twitter.com&utm_campaign=buffer). [Accessed 25 March 2018].
- [5] UN Water, "Water and Climate Change," 2017. [Online]. Available: <http://www.unwater.org/water-facts/climate-change/>. [Accessed 05 March 2018].
- [6] D. Banks, A. K. Midtgård, G. Morland, C. Reimann, T. Strand, K. Bjorvatn and U. Siewers, "104/© Blackwell Science Ltd, GEOLOGY TODAY, May–June 1998 Is pure groundwater safe to drink?: natural 'contamination' of groundwater in Norway," *Geology Today*, vol. 14, no. 3, pp. 104-113, 1998.
- [7] T. Rango, J. Kravchenko, B. Atlaw, P. G. McCornick, M. Jeuland, B. Merola and A. Vengosh, "Groundwater quality and its health impact: An assessment of dental fluorosis in rural inhabitants of the Main Ethiopian Rift," *Environment International*, 2012.
- [8] T. Rango, A. Vengosh, G. Dwyer and G. Bianchini, "Mobilization of arsenic and other naturally occurring contaminants in groundwater of the Main Ethiopian Rift aquifers," *Water Research*, vol. 37, no. 15, pp. 5801-5818, 2013.
- [9] WHO, "Fluorides," Inchem, Geneva, 2002.
- [10] B. Thole, "Ground Water Contamination with Fluoride and Potential Fluoride Removal Technologies for East and Southern Africa," Intech, 2013.
- [11] Ministry of Water Resources in Ethiopia, "Ethiopia: Strategic Framework for Managed Groundwater Development," 2011.
- [12] J. Skinner, "Where every drop counts: tackling rural Africa's water crisis," IIED, London, 2009.
- [13] T. Kiros, "UNICEF," 2011. [Online]. Available: [https://www.unicef.org/wash/ethiopia\\_59056.html](https://www.unicef.org/wash/ethiopia_59056.html). [Accessed 01 March 2018].
- [14] A. Menfistu, "Ethiopia: A UNICEF rural water and sanitation programme ensures a healthy life," 2016. [Online]. Available: [www.unicef.org/esaro/5440\\_eth2016\\_rural-wash-programme.html](http://www.unicef.org/esaro/5440_eth2016_rural-wash-programme.html). [Accessed 01 March 2018].
- [15] A. Johnson, L. Osterwalder, F. Zewge, R. Rohner, P. M. Mutheki and E. Samuel, "Bone char-based filters, developed by the Catholic Diocese of Nakuru, Kenya, are being tested in rural Ethiopia in a collaborative project between Eawag, Addis Ababa University and Kenyan, Ethiopian and Swiss NGOs," Sandec News, 2011.

- [16] R. F. A. B. B. & M. Y. Tekle-Haimanot, "Fluoride Levels in Water and Endemic Fluorosis in Ethiopian Rift Valley. In Tropical Geogaph and medical," vol. 39, no. 3, pp. 209-217, 1987.
- [17] C. Reimann, K. Bjorvatn, B. Frengstad, Z. Melaku, R. Tekle-Haimanot and U. Siewers, "Drinking water quality in the Ethiopian section of the East African Rift Valley I - Data and health aspects," *Science of the Total Environment*, 2003.
- [18] F. v. Steenbergen, R. T. Haimanot and A. Sidelil, "High Fluoride, Modest Fluorosis: Investigation in Drinking Water Supply in Halaba (SNNPR, Ethiopia)," *Jornal of Water Resource and Protection*, vol. 3, pp. 120-126, 2011.
- [19] S. Godfrey, "Drilling Deep to Keep Children's Teeth and Bones Protected," Ethiopia, 2015.
- [20] T. H. Debela, A. Beyene, E. Tesfahun, A. Getaneh, A. Gize and Z. Mekonnen, "Fecal contamination of soil and water in sub-Saharan Africa cities: The case of Addis Ababa, Ethiopia," *Ecobydrology & Hydrobiology*, vol. 18, no. 2, pp. 225-230, 2018.
- [21] Central Statistical Agency of Ethiopia; National Bank of Ethiopia; World Bank, "Integrated Surveys on Agriculture Ethiopia Socioeconomic Survey," 2017.
- [22] N. Castillo, R. Ramos, R. Perez, R. Garcia de la Cruz, A. Aragon-Pin, J. Martinez-Rosales, R. Guerrero-Coronado and L. Fuentes-Rubio, "Adsorption of Fluoride from Water Solution on Bone Char," *Industrial Engineering Chemistry Research*, vol. 46, pp. 9205-9212, 2007.
- [23] A. Sivasamy, K. P. Singh, D. Mohan and M. Maruthamuthu, "Studies on defluoridation of water by coal-based sorbents," *Chemical Technology and Biotechnology*, vol. 76, no. 7, pp. 717-722, 2001.
- [24] Meenakshi and R. Maheshwari, "Fluoride in drinking water and its removal," *Hazardous Materials*, vol. 137, pp. 456-463, 2006.
- [25] A. Lhassani, M. Rumeau, D. Benjelloun and M. Pontie, "Selective demineralization of water by nanofiltration Application to the defluorination of brackish water," *Water research*, vol. 35, no. 13, pp. 3260-3264, 2001.
- [26] E. Dahi, "Contact precipitation for defluoridation of water," in *Paper presented at 22nd WEDC Conference*, New Delhi, 1996.
- [27] N. Razbe, R. Kumar, Pratima and R. Kumar, "Various options for removal of fluoride from drinking water," *Applied Physics*, vol. 3, pp. 40-47, 2013.
- [28] S. George, P. Pandit and A. Gupta, "Residual aluminium in water defluoridated using activated alumina adsorption-modeling and simulation studies," *Water Research*, vol. 44, pp. 3055-3064, 2010.
- [29] P. I. Ndiaye, P. Moulln, L. Dominguez, J. C. Millet and F. Charbit, "Removal of fluoride from electronic industrial effluent by RO membrane separation," *Desalination*, vol. 173, pp. 25-32, 2005.
- [30] WHO, "Exposure to inadequate or excess fluoride: A major public health concern," 2010.
- [31] L. Feenstra, L. Vasak and J. Griffioen, "Fluoride in groundwater: Overview and evaluation of removal methods," Igrac, 2007.
- [32] S. S. Waghmare and T. Arfin, "Fluoride Removal from Water by various techniques: Review," *International Journal of Innovative Science, Engineering & Technology*, vol. 2, no. 9, 2015.
- [33] D. M. Woldemariam, "District Heating-Driven Membrane Distillation for Water Purification in Industrial Application," KTH, Stockholm, 2017.

- [34] N. Kumar and A. Martin, "Techno-economic optimization of solar thermal integrated membrane distillation for cogeneration of heat and pure water," *Desalination and Water Treatment*, vol. 98, pp. 16-30, 2017.
- [35] W. Lun Ang, A. W. Mohammad, N. Hilal and C. P. Leo, "A review on the applicability of integrated/hybrid membrane processes in water treatment and desalination plants," *Desalination*, vol. 363, pp. 2-18, 2015.
- [36] C. Ekqvist, "A feasibility study of running a small-scale water purification unit with base station waste heat," 2010.
- [37] E. U. Khan, "Feasibility analysis of biogas based polygeneration for rural development in bangladesh," 2014.
- [38] World Bank, "Data Bank - Country Profile: Ethiopia," 2016. [Online]. Available: [http://databank.worldbank.org/data/Views/Reports/ReportWidgetCustom.aspx?Report\\_Name=CountryProfile&Id=b450fd57&tbar=y&dd=y&inf=n&zm=n&country=ETH](http://databank.worldbank.org/data/Views/Reports/ReportWidgetCustom.aspx?Report_Name=CountryProfile&Id=b450fd57&tbar=y&dd=y&inf=n&zm=n&country=ETH). [Accessed 06 March 2018].
- [39] Central Statistical Agency; Ethiopian Development Research Institute; International Food Policy Research Institute, "Population and Housing census: Atlas of Ethiopia," 2007.
- [40] Ministry of Water Irrigation and Electricity, "The ethiopian power sector: a renewable future," Berlin Energy Transition Dialogue, Berlin, 2017.
- [41] M. Berhanu, S. A. Jabasingh and Z. Kifile, "Expanding sustenance in Ethiopia based on renewable energy resources – A comprehensive review," *Renewable and Sustainable Energy Reviews*, vol. 75, pp. 1035-1045, 2017.
- [42] S. Geissler, D. Hagauer, A. Horst, M. Krause and P. Sutcliffe, "Biomass Energy Strategy," Ethiopian Ministry of Water and Energy, 2013.
- [43] World Bank, "Access to electricity (% of population)," 2014. [Online]. Available: <https://data.worldbank.org/indicator/EG.ELC.ACCS.ZS?locations=ET>. [Accessed 03 April 2018].
- [44] WHO; UNICEF, "Joint Monitoring Programme for Water Supply, Sanitation and Hygiene: Ethiopia," 2017.
- [45] C. Sundin, "Exploring the water-energy nexus in the Omo river basin," KTH, Stockholm, 2017.
- [46] Energy Plus, "Weather Data Awassa station(EPW file)," Energy Plus, Awassa, 2014.
- [47] K. V. Suryabagavan, "GIS-based climate variability and drought characterization in Ethiopia over three decades," *Weather and Climate Extremes*, vol. 15, pp. 11-23, 2017.
- [48] WHO, Guidelines for drinking-water quality (Fourth edition), Fluoride, chapter 12.1, pp. 371-373, Fourth edition ed., WHO, 2011.
- [49] H. Kloos and R. T. Haimanot, "Distribution of fluoride and fluorosis in Ethiopia and prospects for control," *Tropical Medicine and International Health*, vol. 4, no. 5, pp. 355-364, 1999.
- [50] M. Issa, "Energy Report - Ethiopia," Embassy of Sweden, Addis Abeba, 2016.
- [51] United States Agency for International Development, "Ethiopia-Energy," 2014. [Online]. Available: <https://www.usaid.gov/powerafrica/ethiopia>. [Accessed 06 March 2018].

- [52] World Bank, "Access to electricity (% of population)," 2014. [Online]. Available: <https://data.worldbank.org/indicator/EG.ELC.ACCS.ZS?locations=ET>. [Accessed 06 March 2018].
- [53] World Bank; International Bank for Reconstruction and Development, "State of Electricity Access Report," WorldBank, 2017.
- [54] D. Mentis, M. Andersson, M. Howells, H. Rogner, S. Siyal, O. Broad, A. Korkovelos and M. Baziliana, "The benefits of geospatial planning in energy access – A case study on Ethiopia," *Applied Geography*, vol. 72, pp. 1-13, 2016.
- [55] U. Stutenbäumer, T. Negash and A. Abdi, "Permonce of a small-scale photovoltaic systems and their potential for rural electrification in Ethiopia," *Renewable energy*, vol. 18, pp. 35-48, 1999.
- [56] Solargis, "Solar resource maps and GIS data," 2017. [Online]. Available: <https://solargis.com/maps-and-gis-data/download/ethiopia>. [Accessed 06 March 2018].
- [57] N. Abadi, K. Gebrehiwot, A. Techane and H. Nerea, "Links between biogas technology adoption and health status of households in rural Tigray, Northern Ethiopia," *Energy Policy*, vol. 101, pp. 284-292, 2017.
- [58] C. L. v. Beek, E. Elias, G. S. Yihenew, H. Heesmans, A. Tsegaye, H. Feyisa, M. Tolla, M. Melmuye, Y. Gebremeskel and S. Mengist, "Soil nutrient balances under diverse agro-ecological settings in Ethiopia," *Nutrient Cycling in Agroecosystems*, vol. 106, pp. 257-274, 2016.
- [59] J. Lansche and J. Müller, "Life cycle assessment (LCA) of biogas versus dung combustion household cooking systems in developing countries – A case study in Ethiopia," *Journal of Cleaner Production*, vol. 165, pp. 828-835, 2017.
- [60] L. M. and E. B., "Bottlenecks and Drivers of Ethiopia/s Domestic Biogas Sector, International Association for Management of Technology," in *Proceedings of the LAMOT Conference*, 2015.
- [61] Embassy of Ethiopia, "Ethiopia leads with Africa's first waste-to-energy plant," Embassy of Ethiopia, 5 March 2018. [Online]. Available: <https://ethiopianembassy.be/en/2018/03/05/ethiopia-leads-with-africas-first-waste-to-energy-plant/>. [Accessed 6 June 2018].
- [62] L. M. Kampa and E. B. Forn, "Ethiopia's emerging domestic biogas sector: Current status, bottlenecks and drivers," *Renewable and Sustainable Energy reviews*, vol. 60, pp. 475-488, 2016.
- [63] E. W. Gabisa and S. H. Gheewala, "Potential of bio-energy production in Ethiopia based on available biomass residues," *Biomass and Bioenergy*, vol. 111, pp. 77-87, 2018.
- [64] A. Minissale, G. Corti, F. Tassi, T. Darrahc, O. Vaselli, D. Montanari, G. Montegrossi, G. Yirgud, E. Selmo and A. Tecluf, "Geothermal potential and origin of natural thermal fluids in the northern Lake Abaya area, Main Ethiopian Rift, East Africa," *Journal of Volcanology and Geothermal Research*, vol. 336, pp. 1-18, 2017.
- [65] P. A. Omenda, "THE GEOTHERMAL ACTIVITY OF THE EAST AFRICAN RIFT," KenGen, Kenya, 2007.
- [66] T. Chernet, "Geology and hydrothermal resources in the northern Lake Abaya area (Ethiopia)," *Journal of African Earth Sciences*, vol. 61, pp. 129-141, 2011.
- [67] World Bank, "Ethiopia: Geothermal sector development project," 2014.

- [68] D. D. Guta, "Policy Brief: ENERGY RESOURCE USE OPTIONS FOR IMPROVED ENERGY SECURITY IN ETHIOPIA," in *Dresden Nexus Conference*, Dresden, 2015.
- [69] L. Martínez-Díez and M. Vásquez-González, "Temperature and concentration polarization in membrane distillation of aqueous salt solutions," Universidad de Málaga, Málaga, 1998.
- [70] M. Tomaszewska, "Membrane Distillation - Examples of application in technology and environmental protection," *Polish Journal of Environmental Studies*, vol. 9, no. 1, pp. 27-36, 2000.
- [71] G. Mohan, U. Kumar, M. K. Pokhrel and A. Martin, "A novel solar thermal polygeneration system for sustainable production of cooling, clean water and domestic hot water in United Arab Emirates: Dynamic simulation and economic evaluation," *Applied Energy*, vol. 167, pp. 173-188, 2016.
- [72] Nutakki, "Co-Production Performance Evaluation of a Novel Solar Combi System for Simultaneous Pure Water and Hot Water Supply in Urban Households of UAE," *Energies*, vol. 10, 2016.
- [73] R. Sarbatly and C.-k. Chiam, "Evaluation of geothermal energy in desalination by vacuum membrane," *Applied Energy*, vol. 112, pp. 737-746, 2013.
- [74] C. Liu and V. R. Martin, "Applying Membrane Distillation in High-Purity Water Production for Semiconductor Industry," Xzero, 2005.
- [75] A. Kullab, "Desalination using Membrane Distillation - Experimental and Numerical study," KTH, Stockholm, 2011.
- [76] A. Kullab, "Desalination using membrane distillation," KTH, Stockholm, 2011.
- [77] A. Boubakri, R. Bouchrit, H. Amor and S. A.-T. Bouguecha, "Fluoride removal from aqueous solution by direct contact membrane distillation: Theoretical and experimental studies," 2014.
- [78] S. Tavakkoli, O. R. Lokare, R. D. Vidic and V. Khanna, "A techno-economic assessment of membrane distillation for treatment of Marcellus shale produced water," *Desalination*, vol. 416, pp. 24-34, 2017.
- [79] M. El-Bourawi, Z. Ding, R. Ma and M. Khayet, "A framework for better understanding membrane distillation separation process," *Membrane Science*, vol. 285, pp. 4-29, 2006.
- [80] P. J. Brown and C. L. Cox, "Filtration of drinking water," in *Fibrous Filter Media*, 2017 Elsevier Ltd., 2017, p. 245-274.
- [81] Lenntech, "Remineralisation," Lenntech, 2018. [Online]. Available: <https://www.lenntech.com/processes/remineralisation/remineralisation.htm#ixzz5HXkuguws>. [Accessed 2018 June 10].
- [82] Scarab Development AB, "Background," 2017. [Online]. Available: <http://www.scarab.se/background.html>. [Accessed 14 March 2018].
- [83] B. Bodell, "Silicone rubber vapor diffusion in saline water distillation," United States Patent Serial, (285,032), 1963.
- [84] J. Blanco and W. Gernjak, "Performance and cost estimations of final industrial size of MEDESOL-2 technology," University of La Laguna, Almería, 2010.
- [85] G. F. D. W. J. K. T. M. A. Hagedorn, "Methodical design and operation of membrane distillation plants for desalination," *Chemical Engineering Research and Design*, vol. 125, pp. 265-281, 2017.

- [86] A. Cipollina and G. Micale, "Coupling sustainable energy with membrane distillation processes for seawater desalination," *Amman*, 2010.
- [87] R. Saffarini, E. K. Summers, H. Arafat and J. Leinhard, "Technical evaluation of stand-alone solar powered membrane distillation systems," *Desalination*, p. 286, 2012.
- [88] M. D. S. Bouguecha, "Fluidised bed crystalliser and air gap membrane distillation as a solution to geothermal water desalination," *Desalination*, vol. 152, pp. 237-244, 2002.
- [89] E. U. Khan, "Renewables based polygeneration for rural development in Bangladesh," Stockholm, 2017.
- [90] N. U. Kumar and A. Martin, "Experimental modeling of an air-gap membrane distillation module and simulation of a solar thermal integrated system for water purification," *Desalination and Water Treatment*, vol. 84, p. 123–134, 2017.
- [91] A. Alsaadi, N. Ghaffour, J.-D. Li, S. Gray, L. Francis, H. Maab and G. Amy, "Modeling of air-gap membrane distillation process: A theoretical and experimental study," *Journal of Membrane Science*, vol. 445, pp. 53-65, 2013.
- [92] P. H. Gleick, "Basic Water Requirements for Human Activities: Meeting Basic Needs," *Water International*, vol. 21, no. 2, pp. 83-92, 2009.
- [93] TRNSYS, "Mathematical Reference Volume 5," TRNSYS 16.
- [94] VIESSMAN, "Technical description: Vitobloc 200 CHP Unit heat and power type EM-6/15," VIESSMAN, 2017.
- [95] P. J. Jorgensen, "Biogas - green energy," PlanEnergi, Aarhus, 2009.
- [96] Viessmann, "Vitobloc 200 EM-9/20," Viessman, [Online]. Available: <https://www.viessmann.it/it/riscaldamento-casa/cogenerazione/cogeneratori-metano-o-gpl/vitobloc-200-em-9-20.html>. [Accessed 1 March 2018].
- [97] R. Steffen, O. Szolar and R. Braun, "Anaerobic digestion: making energy and solving modern waste problem," AD-Nett report, Vienna, 2000.
- [98] (B)energy, "(B)energy Products," (B)energy, 2018. [Online]. Available: <http://www.be-nrg.com/bproductos/>. [Accessed 30 April 2018].
- [99] Viessmann, "Vitobloc 200 EM-6/15," Viessmann, [Online]. Available: <https://www.viessmann.it/it/riscaldamento-casa/cogenerazione/cogeneratori-metano-o-gpl/vitobloc-200.html>. [Accessed 1 March 2018].
- [100] A. Alkudhiri, N. Darwish and N. Hilala, "Treatment of saline solutions using Air Gap Membrane Distillation: Experimental study," *Desalination*, vol. 323, pp. 2-7, 2013.
- [101] EIA, "Renewable and alternative fuels," EIA, December 2010. [Online]. Available: [https://www.eia.gov/renewable/annual/solar\\_thermal/](https://www.eia.gov/renewable/annual/solar_thermal/). [Accessed 10 March 2018].
- [102] F. T. Hamzehkolaei and N. Amjady, "A techno-economic assessment for replacement of conventional fossil fuel based technologies in animal farms with biogas fueled CHP units," *Renewable Energy*, vol. 118, pp. 602-614, 2018.
- [103] G. Eshete, K. Sonder and F. t. Heegde, "Feasibility study of a national programme for domestic biogas in Ethiopia," SNV, Addis Ababa, 2006.

- [104] S. Gwavuya, S. Abele, I. Barfuss, M. Zeller and J. Müller, "Household energy economics in rural Ethiopia: A cost-benefit analysis of biogas energy," *Renewable Energy*, vol. 48, pp. 202-209, 2012.
- [105] W. B. Rouse, *The economics of human systems integration: Valuation of Investments in People's Training and Education, Safety and Health, and Work Productivity*, New Jersey: John Wiley & Sons, 2011.
- [106] D. J. Teece, "Business Models, Business Strategy and Innovation," *Long Range Planning*, vol. 43, pp. 172-194, 2010.
- [107] R. Schwantes, A. Cipollina, F. Gross, J. Koschikowski, D. Pfeifle, M. Rolletscheck and V. Subiela, "Membrane distillation: solar and waste heat driven demonstration plants for desalination," *Desalination*, vol. 323, pp. 93-106, 2013.
- [108] D. Tadesse, A. Desta, A. Geyid, W. Girma, S. Fisseha and O. Schmoll, "Rapid assessment of drinking-water quality in the federal democratic republic of ethiopia," 2010.
- [109] EFSA, "Dietary reference values for fluoride," European Food Safety Authority, 2013.
- [110] M. Dhahbi, S. Bouguech and R. Chouik, "Numerical study of the coupled heat and mass transfer in membrane distillation," *Desalination*, vol. 152, pp. 245-252, 2002.
- [111] S. Kubota, K. Ohta, I. Hayano, M. Hirai, K. Kikuchi and Y. Murayama, "Experiments on seawater desalination by membrane distillation," *Desalination*, vol. 69, pp. 19-26, 1988.
- [112] T. A. S. Tiwari G.N., "Flat-Plate Collectors," in *Handbook of Solar Energy. Energy Systems in Electrical Engineering*, Singapore, Springer, 2016, pp. 171-246.
- [113] J. A. Duffie and W. A. Beckman, *Solar Engineering of Thermal Processes*, Wisconsin: Wiley, 2010.
- [114] T. A. S. Tiwari G.N., "Evacuated Tubular Solar Collector (ETSC)," in *Handbook of Solar Energy*, Singapore, Springer, 2016, pp. 293-325.
- [115] A. Papadimitratos, S. Sobhansarbandi, V. Pozdin, A. Zakhidov and F. Hassanipour, "Evacuated tube solar collectors integrated with phase change materials," *Solar Energy*, vol. 129, pp. 10-10, 2016.
- [116] E. Zambolin and D. D. Col, "Experimental analysis of thermal performance of flat plate and evacuated tube solar collectors in stationary standard and daily conditions," *Solar Energy*, vol. 84, no. 8, pp. 1382-1396, 2010.
- [117] A. Buonomano, F. Calise and A. Palombo, "Solar heating and cooling systems by CPVT and ET solar collectors: A novel transient simulation model," *Applied energy*, vol. 103, pp. 588-606, 2013.
- [118] D. Mangal, D. Lamba, T. Gupta and K. Jhamb, "Acknowledgement Of Evacuated Tube Solar Water Heater Over Flat plate solar water heater," *Int J Eng*, vol. 4, p. 279, 2010.
- [119] M. A. Sabiha, R. Saidur, S. Mekhilef and O. Mahian, "Progress and latest developments of evacuated tube solar collectors," *Renewable and Sustainable Energy Reviews*, vol. 51, pp. 1038-1054, 2015.
- [120] J. A. Duffie and W. A. Beckman, *Solar Engineering of Thermal Processes*, Wisconsin: Wiley, 2013.
- [121] M. Lantz, "The economic performance of combined heat and power from biogas produced from manure in Sweden – A comparison of different CHP technologies," *Applied Energy*, vol. 98, pp. 502-511, 2012.

- [122] S. Esayas, M. J. Mattle and L. Feyisa, "Household water treatment: Defluoridation of drinking water by using bone char technology in Ethiopia," *34th WEDC International Conference, Addis Ababa*, 2009.
- [123] D. Y. Hou, J. Wang, B. Q. Wang, Z. K. Luan, X. C. Sun and X. J. Ren, "Fluoride removal from brackish groundwater by direct contact membrane distillation," *IWA*, vol. 61, 2010.
- [124] S. Yarlagadda, V. Gude, L. Camacho, S. Pinappu and S. Deng, "Potable water recovery from As, U, and F contaminated ground waters by direct contact membrane distillation process.," 2011.
- [125] T. Ayenew, "Water management problems in the Ethiopian rift: Challenges for development," *Journal of African Earth Sciences*, vol. 48, no. 2-3, pp. 222-236, 2007.
- [126] UNICEF, "In Ethiopia, UNICEF helps meet water supply challenges in drought-hit Raya Azebo district," 2011. [Online]. Available: [https://www.unicef.org/wash/ethiopia\\_59056.html](https://www.unicef.org/wash/ethiopia_59056.html). [Accessed 05 March 2018].
- [127] USAid, "Fluorosis mitigation with innovative technologies," 2013. [Online]. Available: <https://usaid-gov.secure.force.com/PublicProjectDetail?pid=a0cd0000006faBwAAI&cid=Ethiopia>. [Accessed 05 March 2018].
- [128] D. H. Mazengia, "Ethiopian Energy Systems - Potentials, Opportunities and Sustainable Utilization," Upsala University, 2010.
- [129] FLOWERED, "Developing innovative water defluoridation technologies," 2017. [Online]. Available: <http://www.floweredproject.org/en/index.php>. [Accessed 05 March 2018].
- [130] K. Y. Kebede, "Viability study of grid-connected solar PV system in Ethiopia," *Sustainable Energy Technologies and Assessments*, vol. 10, pp. 63-70, 2015.
- [131] FAO, "Land and Water: Water scarcity," 2017. [Online]. Available: <http://www.fao.org/land-water/water/water-scarcity/en/>. [Accessed 26 02 2018].
- [132] City Population of Ethiopia, "Ethiopia: Regions, Major Cities and Towns," Ethiopia, 14 11 2015. [Online]. Available: <http://www.citypopulation.de/Ethiopia.html>. [Accessed 28 March 2018].
- [133] World Bank, "Moldova Biogas Generation from animal manure pilot project," Environment Management plan, 2010.
- [134] Boletín Oficial del Estado, "Documento básico de ahorro de energía," BOE, Spain, 2013.
- [135] FAO, "Characterization of six cattle breeds in North Ethiopia," Animal Genetic Resources Information, 2007.
- [136] A. Belachew, "Disparities in Rural and Urban Incomes in Ethiopia: 1981-2011," 2014.

## 9 APPENDICES

### Appendix 1. Climate in Ethiopia

In the MERV (central Ethiopia) the rainfalls varies a lot: November, December, January and February rains up to 50mm; March to June and September to October rains from 101-200mm; and July and August are the rainy seasons with rainfalls up to 300mm.

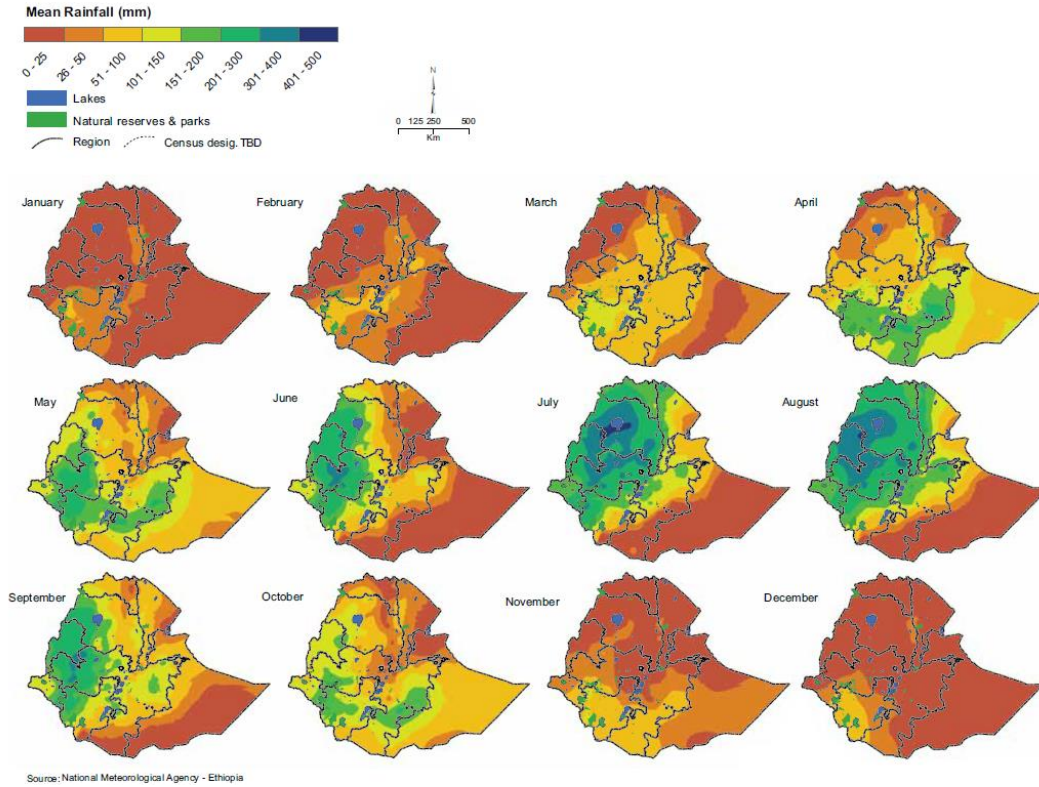


Figure 36 – Mean monthly rainfall variability [39]

The air temperature doesn't vary much: in the MERV the mean temperature is around 20°C the whole year, but temperatures of 30 and 4°C has been recorded (Climate consultant from weather data of Awassa [46]).

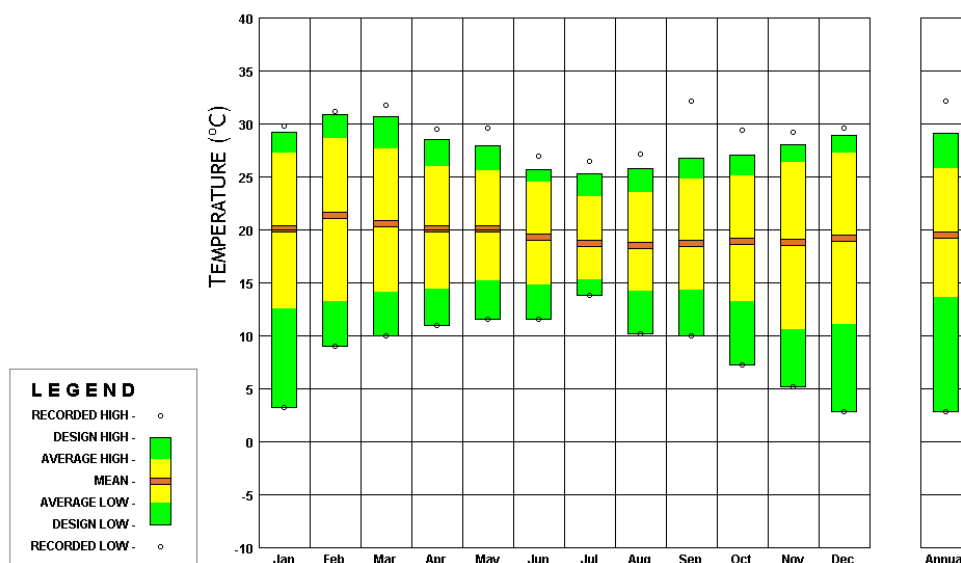


Figure 37 – Temperature variation at the Awassa weather station (7°N 38E, Elevation 1652m [46])

## Appendix 2. World Health Organization Drinking Water Guidelines

Table 32 – Guideline values for naturally occurring chemicals that are of health significance in drinking-water [48]

Chemical	Guideline Value (mg/L)	Remarks
<b>Inorganic</b>		
Arsenic	0.01 (A,T)	
Barium	0.7	
Boron	2.4	
Chromium	0.05 (P)	For total chromium
Fluoride	1.5	<b>Volume of water consumed and intake from other sources should be considered when setting national standards</b>
Selenium	0.04 (P)	
Uranium	0.03 (P)	Only chemical aspects of uranium addressed
<b>Organic</b>		
Microcystin LR	0.001 (P)	For total Microcystin-LR (free plus cell-bound)

A, provisional guideline value because calculated guideline value is below the achievable quantification level; P, provisional guideline value because of uncertainties in the health database; T, provisional guideline value because calculated guideline value is below the level that can be achieved through practical treatment methods, source protection, etc.

### Appendix 3. JMP definitions of water supply and sanitation

Table 33 – JMP Definitions of water supply and sanitation [108]

Category	Water supply	Sanitation
Improved	Household connection	Connection to a public sewer
	Public standpipe	Connection to septic system
	Borehole	Pour-flush latrine
	Protected dug well	Simple pit latrine
	Protected spring	Ventilated improve pit latrine
	Rainwater collection	
Unimproved	Unprotected well	Service or bucket latrines (where excreta are manually removed)
	Unprotected spring	
	Vendor-provided water	Public latrines
	Bottle water <sup>a</sup>	Latrines with an open pit
	Tanker truck-provided water	

<sup>a</sup> Normally considered to be “unimproved” because of concerns about the quantity of supplied water

<sup>b</sup> Considered to be “unimproved” because of concerns about access to adequate amount of water, about inadequate treatment, or about transportation of the water in inappropriate containers.

### Appendix 4. Fluoride

Dietary recommendations: The adequate intake of fluoride from all sources (including non-dietary sources) is 0.05mg/kg body weight per day for both children and adults, including pregnant and lactating women. [109]. Fluoride can be found in food products such as fish or tea. Depending on the area water has natural fluoride content from 0.01 to 0.3 mg/L and water that has been fluoridated (to prevent caries) depends on the fluoride food content, but the limit is up to 1mg/L [9].

Table 34 – Fluoride consequences [9, 10]

Fluoride concentration	Consequences
Fluoride deficiency: less intake than the recommended for EFSA	Dental caries, tooth decay and possibly osteoporosis
Adequate intake: 0.05 mg/kg body weight per day	Strengthen teeth and skeleton
Prolonged consumption of water with fluoride concentrations between 1.5 and 4.0 mg/L	Dental fluorosis: by browning and mottling of teeth
Prolonged consumption of water with fluoride concentrations between 4.0 and 10 mg/L	Skeletal fluorosis: by weakening of bones and malformation of the skeleton
Beyond 10 mg/L	Crippling fluorosis: immobility because of the growing together of bone junctions

## Appendix 5. Defluoridation technologies

Table 35 – Defluoridation technologies review [10, 32, 31]

Technology/ Material	Typical capacities (mg/g)	Removal efficiency (%)	The science	Strengths	Limitations
Activated alumina	3.5– 10.0	>90%	Precipitations involving $Al_2O_3$ and in $F^-$ ions water	High selectivity for fluoride	lowers pH of water, residual $Al^{3+}$
Nalgonda	0.7 – 3.7	70-90%	Reactions of Alum, $Al_2(SO_4)_3$ and lime( $CaO$ )	Same chemicals used for ordinary water treatment	High chemical dose, high sludge disposal required
Bone char	2.3 – 4.7	Low <sup>2</sup> -	Filtration and ion exchange in $Ca_5(PO_4)_3OH$ structure	Availability of raw materials	Not universally acceptable
Bauxite	3.0 – 8.9	-	Precipitations involving $Al_2O_3$ and $F^-$ and other oxides e.g. $Fe_2O_3$ ions water	Available locally in some areas. High capacity.	Residual colour and turbidity in treated water if used raw
Gypsum	1.1 – 6.8	-	Ion exchange involving $CaSO_4$ and $F^-$ and other compounds e.g. $Ca(OH)_2$	Locally available in some areas	High Residual Calcium sulphate
Magnesite	1.0 – 3.7	-	Ion exchange and precipitation involving $MgO$ and $F^-$ and other compounds e.g. $Mg(OH)_2$	Simple technique, locally available in some areas	High pH & residual Mg.
HAP	0.5 – 2.9	-	Ion exchange and precipitation involving $Ca_5(PO_4)_3OH$ and $F^-$ and other compounds e.g. $Ca_5H$ $(PO_4)_3(OH)_2$	Naturally available in some areas	Residual Phosphate
Bauxite, gypsum, magnesite composite	4.2– 11.3	-	ion exchange and precipitation in reactions of $Al_2O_3$ , $CaSO_4$ , $MgCO_3$ , $MgO$	Simple and versatile. Better than use of each of the materials	Energy intensive, fairly novel technique.
Zeolites	28 – 41	>90	ion exchange and surface complexation reactions	High capacity	Limited availability
Membrane distillation	High	>99%	Separation is enable due to phase change	Complete removal of all metals. High capacity at temperatures between 50-80°C	High cost. Need for a heat source and special training of people
Electrodialysis	High	85-95%	Ion exchange membranes under the driving force of an electric current	Separation of ionic components. Flexible. Low chemical request. High water recovery	High cost. Necessity of concentrate treatment. Need for electricity and special training of people
Reverse Osmosis	High	85-95%	Ion exchange membranes under the driving force of pressure	Very high capacities. Removal of other dissolved solids.	Expensive technique. It needs pH improvement after purification. Need for special training and electricity

## Appendix 6. Heat Transfer at the AGMD

### Heat Transfer at the AGMD

The heat transfer across the AGMD is the following: (1) heat flux from the feed solution to the liquid-vapor interface across the thermally boundary layer in the feed channel; (2) heat flux by conduction and latent heat of vaporization across the membrane; (3) heat transfer from the permeate side of the membrane to the condensation layer/film on the condensation plate; (4) heat transfer from the condensation film to the cooling liquid across the condensation plate and thermal boundary layer of the cooling liquid [75].

#### (1) Heat flux from the feed solution to the evaporation surface

The heat transfer at the boundary layer formed at each side of the membrane surface imposes a resistance to heat transfer and causes a temperature difference between the temperatures at the membrane surface and the bulk temperatures of the feed and distillate. This phenomenon is known as “temperature polarization” and is measured with the coefficient  $\tau$  [69]:

$$\tau = \frac{T_{m_1} - T_{m_2}}{T_{b_1} - T_{b_2}} \quad (12)$$

where  $T_{m_1}$  is the feed temperature on the membrane surface [°C],  $T_{m_2}$  is the temperature of the permeate at the air gap inlet [°C],  $T_{b_1}$  is the bulk feed temperature [°C], and  $T_{b_2}$  is the bulk permeate temperature [°C]. The coefficient  $\tau$  measures how much of the overall temperature difference (between the bulk feed temperatures) contributes to the driving force. Feed temperatures varies between 60 and 90°C but can be as low as 30°C. The temperature in the cooling stream is typically between 20 and 40°C [36]. Figure 38 shows a schematic diagram of the phenomenon. The bulk feed temperature  $T_{b_1}$  is gradually decreased across the thermal boundary layer. Similarly, at the permeate side the temperature at the membrane surface  $T_{m_2}$  is higher than that of the permeate bulk phase ( $T_{b_2}$ ), due to the thermal boundary layer on that side. Higher fluxes minimize this effect, but other methods like applying turbulence (mesh spacers) or the design of the flow passage are used. [79]

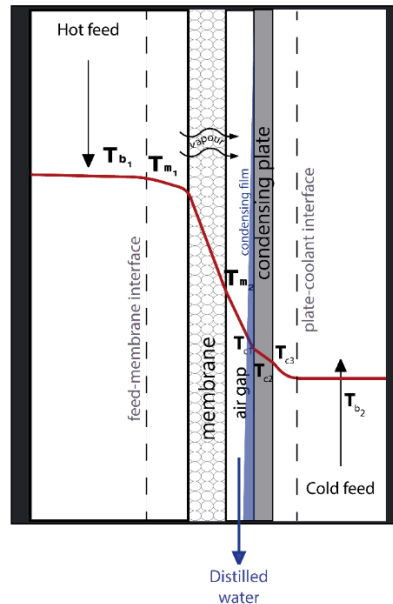


Figure 38 – Heat transfer in AGMD (own elaboration based on [33, 36, 75])

The heat flux  $Q$  from the feed bulk to the interface at the membrane side can be describe as [110, 111]

$$Q_1 = (h_m + NC_p)(T_{b_1} - T_{m_1}) \quad (13)$$

where  $h_m$  is the film heat-transfer coefficient,  $N$  is the mass flux, and  $C_p$  is the liquid specific heat capacity.

**(2) Heat flux by conduction and latent heat of vaporization across the membrane**

Across the membrane, conductive and latent heat transfer occurs. There is heat conduction between the membrane material and pores filled with air/gas (which acts as a stagnant film). The latent heat is due to the vaporization of the feed. This flux results in:

$$Q_2 = \frac{k_m}{d} (T_{m_1} - T_{m_2}) + N\lambda \quad (14)$$

$$k_m = \varepsilon k_a + (1 - \varepsilon)k_s \quad (15)$$

where  $k_m$  is the effective thermal conductive of the membrane (solid material and air in the pores),  $d$  is the membrane thickness,  $\lambda$  is the latent heat of evaporation,  $\varepsilon$  is the membrane porosity,  $k_g$  is the thermal conductivity of the air and  $k_s$  is the thermal conductivity of the solid material [75].

**(3) Heat transfer from the permeate side of the membrane to the condensation layer/film on the condensing plate**

The gas reduces its temperature by exchanging with its surroundings and condensing ( $N\lambda$ ) in the condensing plate, which creates a condensation layer/film. This process is described as follows [110, 111]:

$$Q_3 = \left( \frac{k_g}{b} + N \cdot C_g \right) (T_{m_2} - T_{c_1}) + N\lambda \quad (16)$$

$C_g$  is the specific heat at constant pressure in the gas phase of water,  $k_g$  is the gas phase thermal conductivity and  $b$  is the air-gap width.

**(4) Heat transfer from the permeate side of the membrane to the condensation layer/film on the condensing plate**

At the condensation layer interface to the cold bulk liquid, the heat transfer rate can be described by [110, 111]:

$$Q_4 = h_f(T_{c_1} - T_{c_2}) - NC_p(T_{me} - T_{c_1}) = \frac{k_p}{e}(T_{c_2} - T_{c_3}) = h_m(T_{c_3} - T_{b_2}) \quad (17)$$

Where  $h_f$  is the heat-transfer coefficient of the condensing film,  $T_{c_1}$  is the temperature at the condensing film,  $T_{c_2}$  and  $T_{c_3}$  are the temperatures of inner and outer side of the cooling plate respectively;  $k_p$  is the thermal conductivity,  $e$  the thickness of the condensing plate, and  $h_m$  is the heat-transfer coefficient of the coolant.

**Mass transport through the membrane**

The transmembrane flux ( $N$ ) is usually expressed as a function of the vapor pressure difference across the membrane ( $\Delta P$ ) and the net mass transfer coefficient ( $C$ ).

$$N = C \cdot \Delta P \quad (18)$$

The vapor flux is controlled by diffusion through the membrane pores and natural convection through the air gap and can be expressed as [110]:

$$N = M_w \left[ \frac{C}{R} (P_{m_1} - P_{c_1}) \right] \quad (19)$$

Where  $C$  is defined as [110, 111]:

$$C = \frac{1}{\frac{1}{K_D} + \frac{1}{K_a}} \quad (20)$$

where  $M_W$  is molecular weight of the water,  $P_{m_1}$  is the partial pressure at  $T_{m_1}$ ,  $P_{c_1}$  is the partial pressure at  $T_{c_1}$ ,  $R$  is the ideal gas constant,  $K_D$  is the diffusive mass transfer coefficient through the membrane and  $K_a$  is the convective mass transfer coefficient through the air gap.

## Appendix 7. Energy Technologies theory

### Solar technology

Flat plate collectors(FPC) consist of a dark-colored absorber plate on the bottom, pipes where the fluid passes through, and a transparent glass on the top covering of the absorber, which reduces the calorific loss. The sides and the bottom are usually insulated to minimize the heat losses. It has many applications in a medium temperature range (100°C) [112], especially in sanitary hot water systems for commercial and domestic usages.

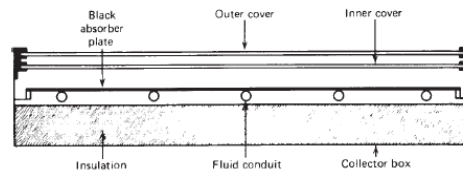


Figure 39 – cross-section of a basic flat-plate solar collector [113]

Evacuated tube collectors are made of several tubes (10-30 tubes), and one tube consists of a clear glass on the outer part, vacuum, a copper vacuum pipes where a fluid passes through and the absorber coating on the bottom. The pipes are usually U pipes. The tubes are connected on the copper header pipe placed at the top of the collector in an insulated box (manifold). The cold water passes through the manifold and exchange heat with the warm fluid inside the heat pipes. It can reach higher temperatures (100-300°C) compared to FPC [114].

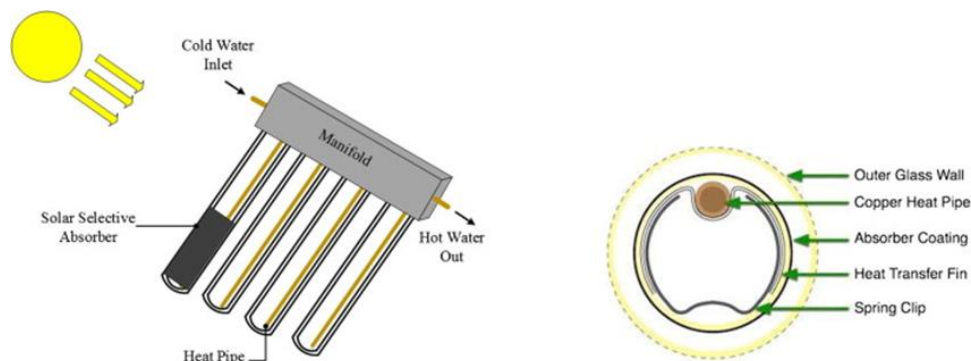


Figure 40 – cross section of an evacuated tube solar collector [115]

The thermal efficiency of the solar collectors is calculated by a quadratic efficiency curve. Manufacturers present the solar collectors efficiency as the sum of two terms, a constant factor ( $\eta_0$ ) known as the optical efficiency (depends on the materials: transmittance, absorptance of the glass and absorber, etc.), and a second term dependent on the temperature difference between fluid and ambient air. According to the standard EN 12975, the solar collector's efficiency is set as follows [113]:

$$\eta = \eta_0 - a_1 \frac{(t_m - t_a)}{G} - a_2 \frac{(t_m - t_a)^2}{G} \quad (21)$$

Where  $G$  the global solar irradiance,  $t_m$  the average fluid temperature in the collector ( $t_m = \frac{T_{out} + T_{in}}{2}$ ),  $t_a$  the air ambient temperature and,  $a_1$  and  $a_2$  are obtained by manufacturers in a specific steady-state conditions following the above-mentioned standards [116]. The optical properties depend on the incidence angle and it varies from one collector to another. In many manufacturers, especially for ETC, the incidence angle modifier (IAM) coefficient depending on the longitude  $K(\theta_t, 0)$ , and transversal coefficient  $K(0, \theta_l)$ , are given [117]. The IAM coefficient,  $K(\theta)$ , for beam and diffuse radiation, is calculated by:

$$K(\theta) = K_{\theta b}(\theta_t, \theta_l) = K(\theta_t, 0) \cdot K(0, \theta_l) \quad (22)$$

The useful output power ( $\dot{Q}$ ) of a solar collector for perpendicular incidence angle of the solar radiation during steady-state operating conditions can be written as:

$$\dot{Q} = \eta \cdot A_a \cdot G \quad (23)$$

For a different incidence angle, equation 12 and 13 are combined and the instantaneous thermal power delivered by the collectors is set as:

$$\dot{Q} = \eta_0 \cdot K(\theta) \cdot G \cdot A_a - a_1 \cdot (t_m - t_a) \cdot A_a - a_2 \cdot (t_m - t_a)^2 \cdot A_a \quad (24)$$

Ideally the tilt angle of the solar collectors should be optimized to maximize winter demand (tilt angle equal to latitude plus 10°) and summer demand (tilt angle equal to latitude minus 10°) [34]. This will be needed for FPC, as ETC tubular design is able to passively track the sun [118] and it can collect both direct and diffuse radiations, resulting in higher efficiencies than FPCs.

Another advantage it's that when a tube is broken it can be replaced, but in FPC a whole new collector is needed. One disadvantage is that ETC produces higher temperatures and it can have overheating problems [119]. The maximum equilibrium temperature can be estimated by making zero the useful energy power absorbed by the ETC or FPC (This means that all the heat absorbed by the collector is not being absorbed by other fluid, i.e., the tank):

$$T_m = T_{\max Q=0} = T_a + \frac{G(\tau\alpha)_n}{U_L}$$

A collector with  $(\tau\alpha)_n = 0.78$ , an ambient temperature  $T_a = 20^\circ\text{C}$ , solar irradiance of  $1000\text{W}/\text{m}^2$ , with  $U_L$  in the range of  $8.33\text{-}3.7\text{W}/\text{m}^2\text{C}$  (non-selective to highly selective absorbers) results in maximum equilibrium temperature ranges from  $114$  to  $230^\circ\text{C}$ . Extremely low temperatures must also be considered when freezing conditions can happen. This can be solved by using antifreeze fluids or arranging the system so that the collector will drain during periods that is not operating [120].

### Biogas technology

There are several technical solutions to produce electricity and heat from manure-based biogas. Most common engines are: sparkplug ignition (SI) or compression ignition (CI) [121]. CHP plants are more efficient than standalone engines or boilers. To produce the biogas that is used in the engines, a digester is needed.

Domestic biodigester consists of a semi-batch reactor that processes the organic compounds of the feed. The result is a mix of 50 to 70% of methane and 30 to 40% of carbon dioxide, among other gases. Biodigester vary in size and shape, depending on the manure that wants to be processed. The most common configuration in Africa and Asia are the fixed-dome digester (Figure 41).

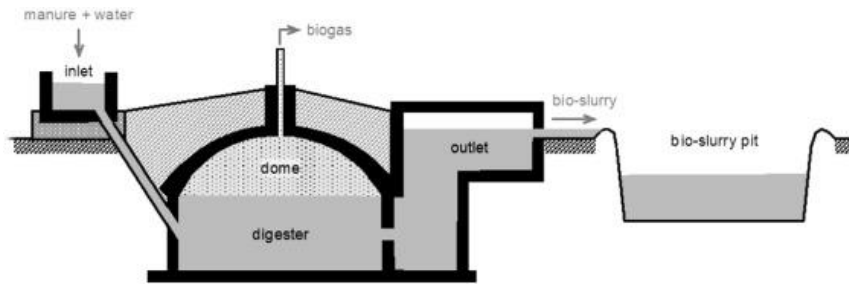


Figure 41 – Schematic of a fixed-dome biogas plant [62]

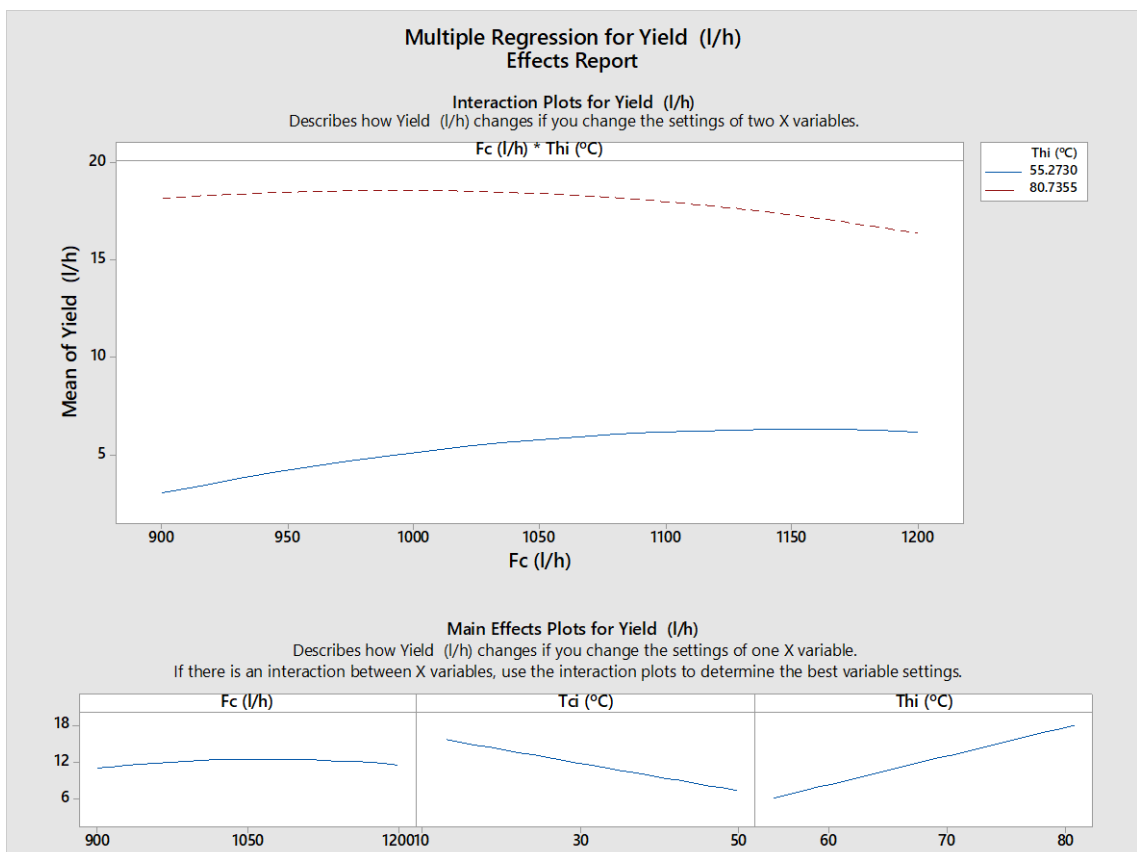
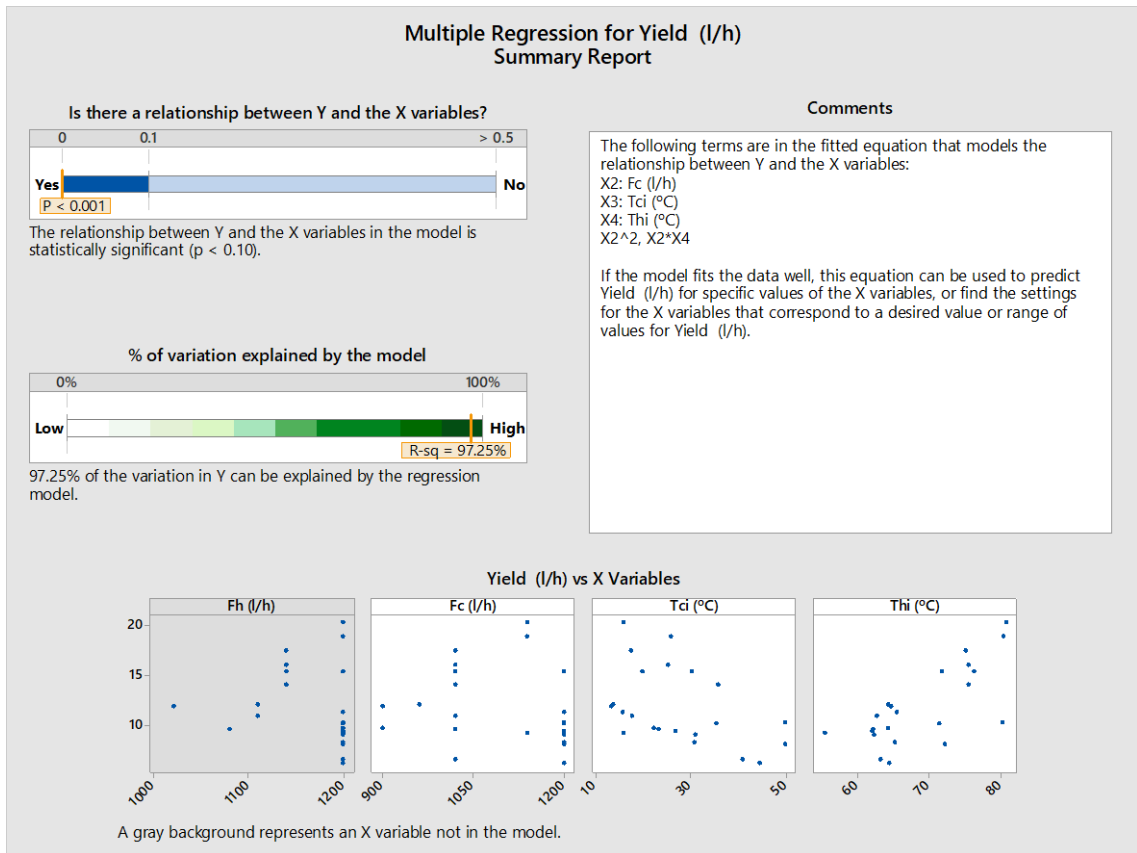
## Appendix 8. Regression analysis (Minitab 18)

Table 8 – Data used in the model, provided by Scarab Development AB and performed in [33]

Fh (L/h)	Fc (L/h)	Tci (°C)	Thi (°C)	Tco (°C)	Tho (°C)	Yield (L/h)
1200.0	1200.0	15.5	65.3	19.9	59.7	11.3
1200.0	1200.0	30.6	65.0	33.7	61.0	8.2
1200.0	1200.0	49.8	80.2	53.9	75.5	10.3
1200.0	1140.0	25.6	80.4	34.1	71.2	18.9
1200.0	1140.0	15.7	80.7	25.9	70.0	20.3
1140.0	1020.0	35.7	75.5	40.2	69.2	14.0
1140.0	1020.0	30.1	76.2	36.1	68.8	15.4
1140.0	1020.0	25.1	75.5	31.4	67.7	16.0
1140.0	1020.0	17.2	75.1	25.3	66.0	17.5
1200.0	1200.0	19.7	71.7	26.0	64.3	15.3
1200.0	1200.0	35.2	71.3	39.4	66.2	10.2
1200.0	1200.0	49.8	72.1	52.9	68.4	8.1
1200.0	1200.0	44.5	64.2	46.6	61.4	6.2
1200.0	1020.0	40.8	63.0	43.6	59.3	6.6
1200.0	1140.0	15.6	55.3	18.8	51.0	9.2
1200.0	900.0	22.2	64.1	28.2	59.2	9.7
1080.0	1020.0	23.0	61.9	28.6	56.2	9.6
1110.0	1020.0	17.5	62.6	24.1	56.2	10.9
1110.0	960.0	13.4	64.2	20.9	56.8	12.1
1020.0	900.0	13.0	64.5	20.5	57.1	11.9
1200.0	1200.0	30.8	62.2	34.3	57.7	9.0
1200.0	1200.0	26.6	61.8	30.6	57.3	9.4

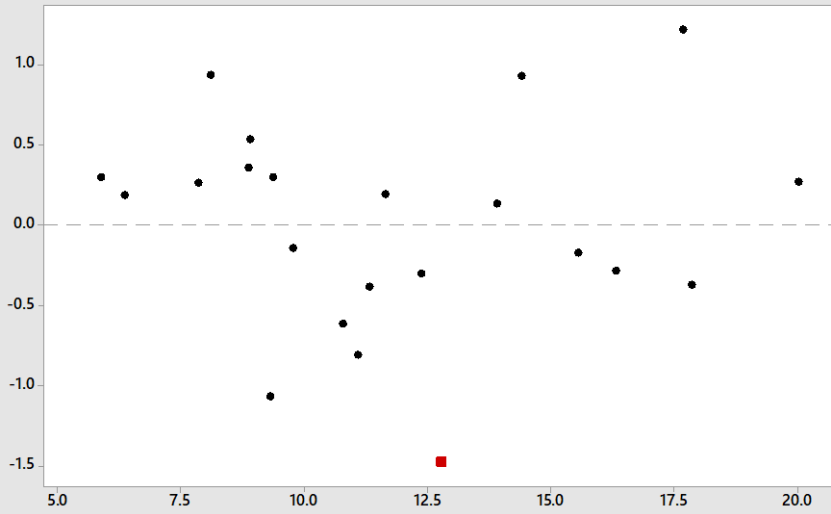
## Appendix 9. Multiple regression for Yield:

In the first step all data from Table 7 was used and the following model was obtained:



### Multiple Regression for Yield (l/h) Diagnostic Report

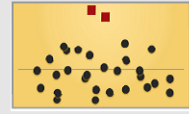
Residuals vs Fitted Values



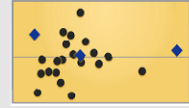
Look for patterns, such as strong curvature or clusters, that may indicate problems with the regression model. Ideally, the points should fall randomly on both sides of zero. Identify any large residuals that could have a strong influence on the model.

Look for these patterns:

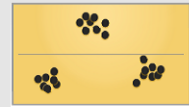
Large Residuals



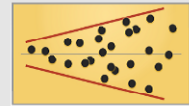
Unusual X Values



Clusters



Unequal Variation



### Multiple Regression for Yield (l/h) Model Building Report

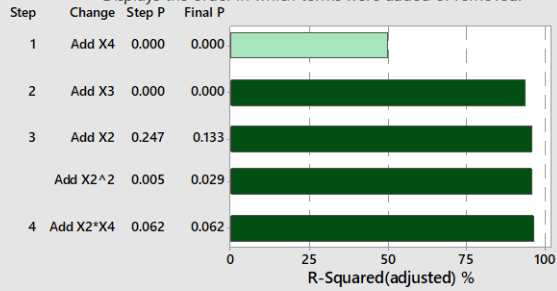
X1: Fh (l/h) X2: Fc (l/h) X3: Tci (°C) X4: Thi (°C)

Final Model Equation

$$\text{Yield (l/h)} = -121.4 + 0.1552 X_2 - 0.2230 X_3 + 1.174 X_4 - 0.000052 X_2^2 - 0.000645 X_2 X_4$$

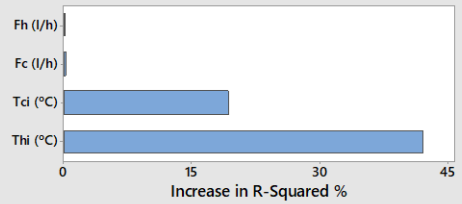
Model Building Sequence

Displays the order in which terms were added or removed.



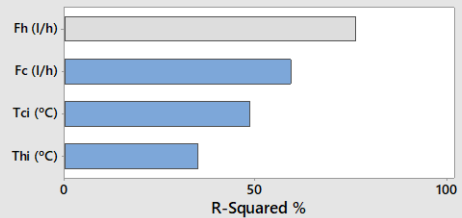
Incremental Impact of X Variables

Long bars represent Xs that contribute the most new information to the model.



Each X Regressed on All Other Terms

Gray bars represent Xs that do not help explain additional variation in Y.



A gray bar represents an X variable not in the model.

### Multiple Regression for Yield (l/h) Report Card

Check	Status	Description
Amount of Data		The sample size (n = 22) is not large enough to provide a very precise estimate of the strength of the relationship. Measures of the strength of the relationship, such as R-Squared and R-Squared (adjusted), can vary a great deal. To obtain a precise estimate, larger samples (typically 45 or more) should be used for a model of this size.
Unusual Data		One data point has a large residual and is not well fit by the equation. This point is marked in red on the Diagnostic Report and is in row 1 of the worksheet. Because unusual data can have a strong influence on the results, try to identify the cause for its unusual nature. Correct any data entry or measurement errors. Consider removing data that are associated with special causes and redoing the analysis.
Normality		Because you have at least 15 data points, normality is not an issue. If the number of data points is small and the residuals are not normally distributed, the p-values used to determine whether there is a significant relationship between the Xs and Y may not be accurate.

Summary:

Equations	R <sup>2</sup>	p-value	Independent variable that contributes the most
$Yield(l/h) = -121.4 + 0.1552 \cdot F_c - 0.2230 \cdot T_{ci} + 1.174 \cdot T_{hi} - 0.000052 \cdot F_c^2 - 0.000645 \cdot F_c \cdot T_{hi}$	97.95%	0.062	T <sub>hi</sub> and T <sub>ci</sub>

Even though the model can be explained 97.25% of the data, the p-value is too large (p-value>0.05). The data point that has a large residual and it's removed to see if the p-value and the R-squared can be improved. The result is the following:

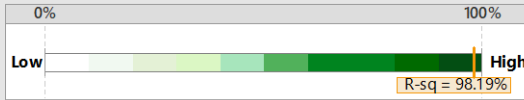
## Multiple Regression for Yield (l/h) Summary Report

Is there a relationship between Y and the X variables?



The relationship between Y and the X variables in the model is statistically significant ( $p < 0.10$ ).

% of variation explained by the model



98.19% of the variation in Y can be explained by the regression model.

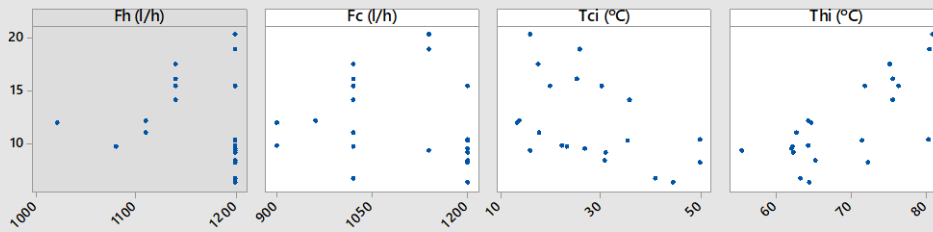
### Comments

The following terms are in the fitted equation that models the relationship between Y and the X variables:

X2: Fc (l/h)  
X3: Tci (°C)  
X4: Thi (°C)  
X2\*X3, X2\*X4

If the model fits the data well, this equation can be used to predict Yield (l/h) for specific values of the X variables, or find the settings for the X variables that correspond to a desired value or range of values for Yield (l/h).

### Yield (l/h) vs X Variables

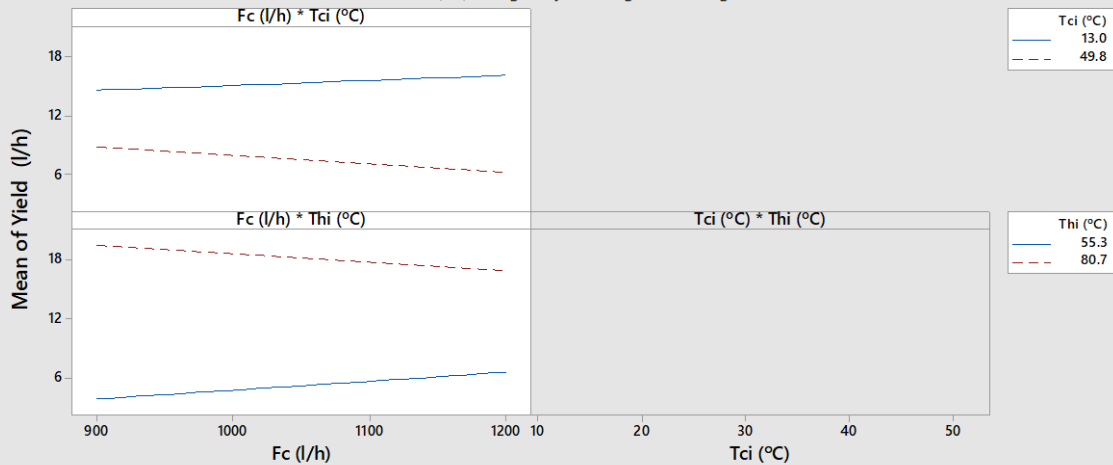


A gray background represents an X variable not in the model.

## Multiple Regression for Yield (l/h) Effects Report

### Interaction Plots for Yield (l/h)

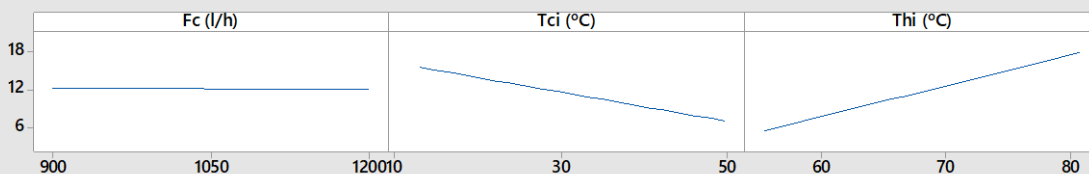
Describes how Yield (l/h) changes if you change the settings of two X variables.



### Main Effects Plots for Yield (l/h)

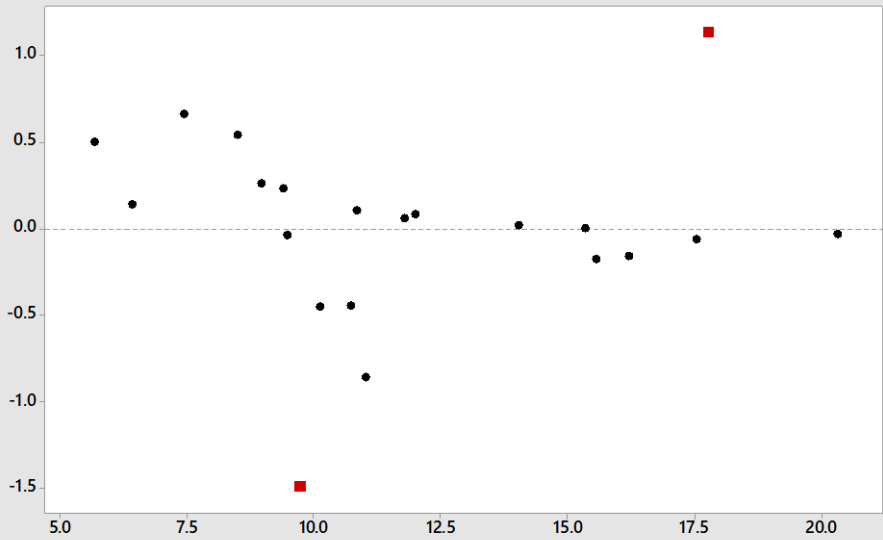
Describes how Yield (l/h) changes if you change the settings of one X variable.

If there is an interaction between X variables, use the interaction plots to determine the best variable settings.



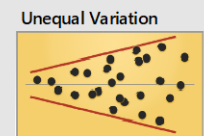
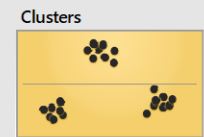
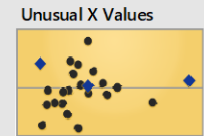
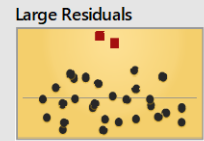
### Multiple Regression for Yield (l/h) Diagnostic Report

Residuals vs Fitted Values



Look for patterns, such as strong curvature or clusters, that may indicate problems with the regression model. Ideally, the points should fall randomly on both sides of zero. Identify any large residuals that could have a strong influence on the model.

Look for these patterns:



### Multiple Regression for Yield (l/h) Model Building Report

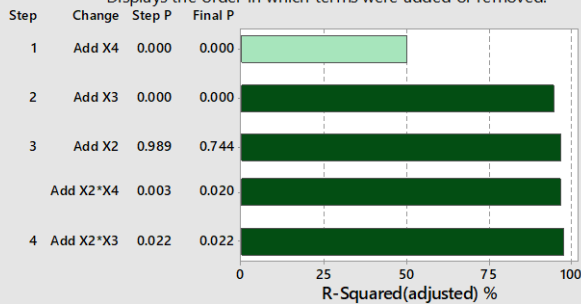
X1: Fh (l/h) X2: Fc (l/h) X3: Tci (°C) X4: Thi (°C)

**Final Model Equation**

$$\text{Yield (l/h)} = -78.2 + 0.0581 X_2 + 0.179 X_3 + 1.246 X_4 - 0.000372 X_2^*X_3 - 0.000701 X_2^*X_4$$

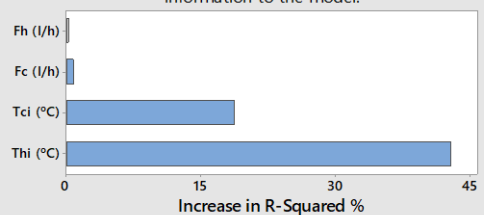
**Model Building Sequence**

Displays the order in which terms were added or removed.



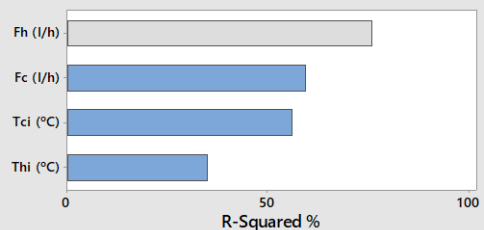
**Incremental Impact of X Variables**

Long bars represent Xs that contribute the most new information to the model.



**Each X Regressed on All Other Terms**

Gray bars represent Xs that do not help explain additional variation in Y.

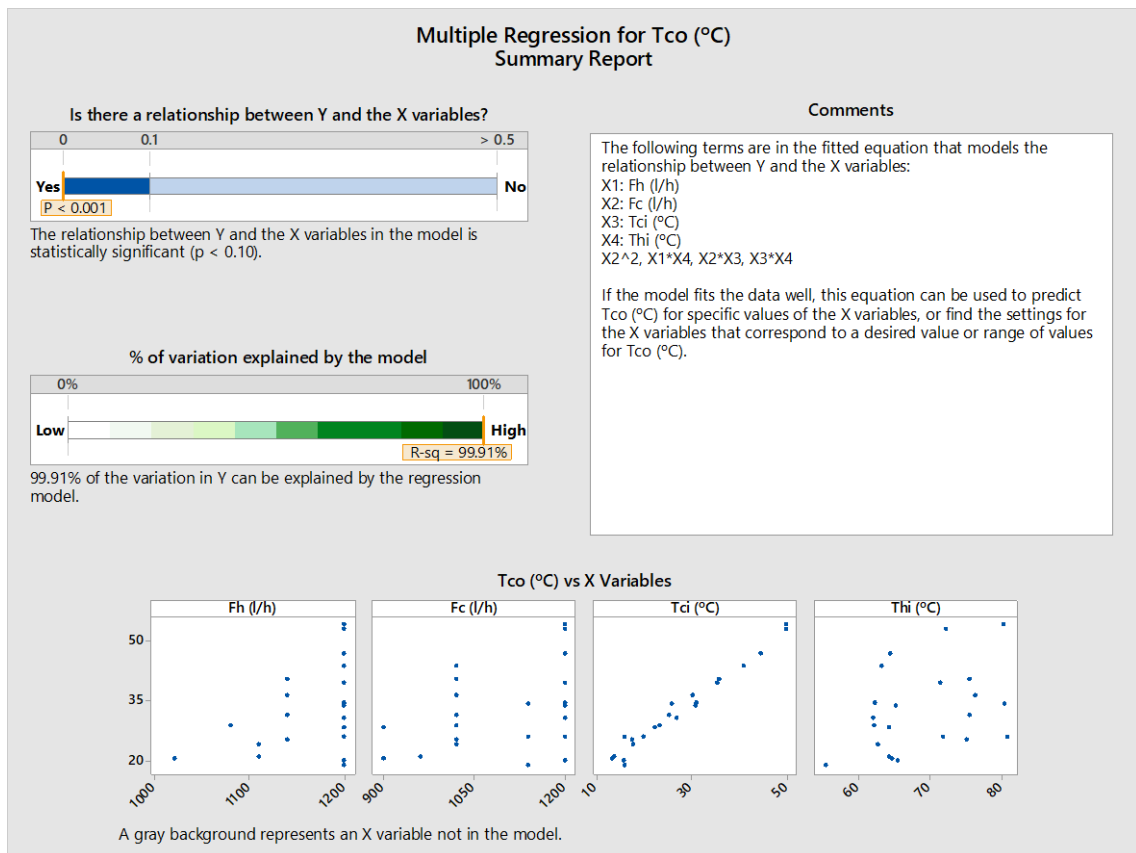


A gray bar represents an X variable not in the model.

Summary:

Equations	R <sup>2</sup>	p-value	Independent variable that contributes the most
$\text{Yield}(l/h) = -78.2 + 0.0581 \cdot F_c + 0.179 \cdot T_{ci} + 1.246 \cdot T_{hi} - 0.000372 \cdot F_c \cdot T_{ci} - 0.000701 \cdot F_c \cdot T_{hi}$	98.19%	0.022	T <sub>hi</sub> and T <sub>ci</sub>

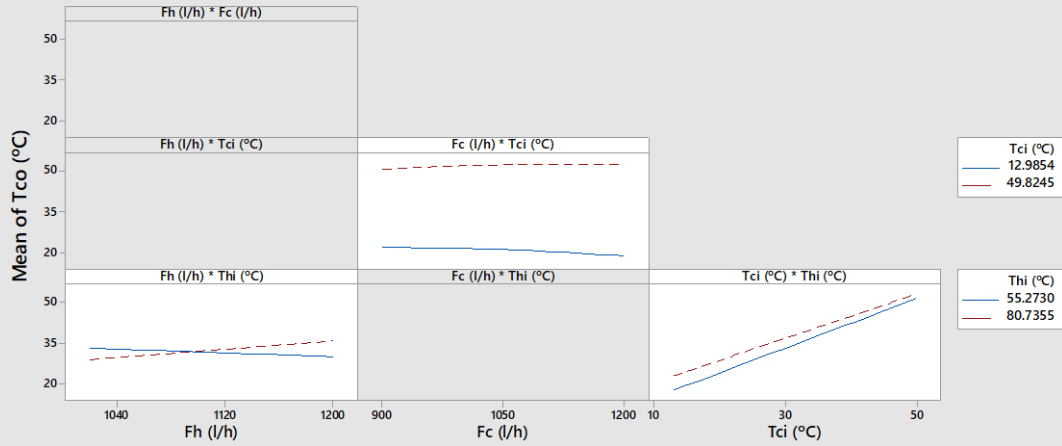
### Multiple regression for cold outlet temperature:



## Multiple Regression for Tco (°C) Effects Report

### Interaction Plots for Tco (°C)

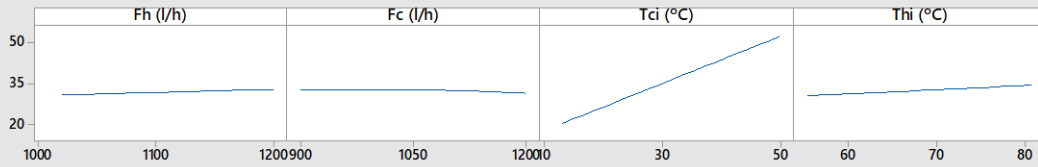
Describes how Tco (°C) changes if you change the settings of two X variables.



### Main Effects Plots for Tco (°C)

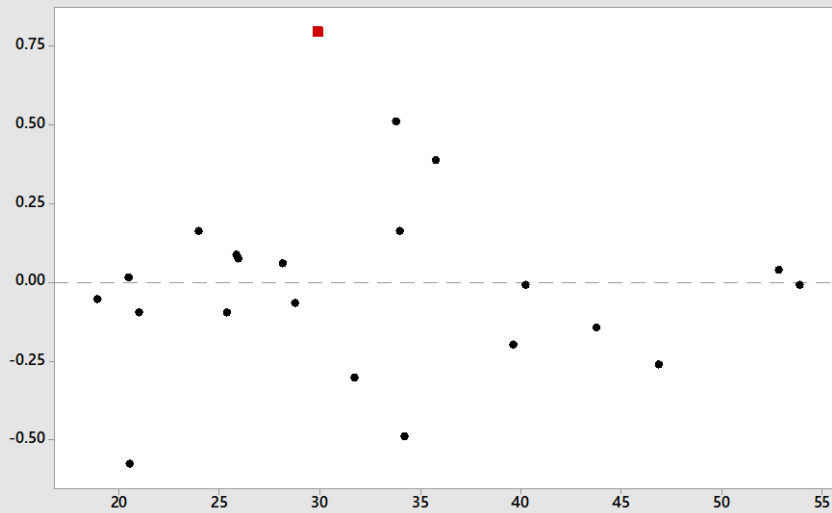
Describes how Tco (°C) changes if you change the settings of one X variable.

If there is an interaction between X variables, use the interaction plots to determine the best variable settings.



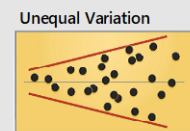
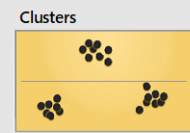
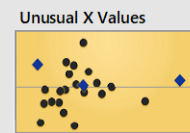
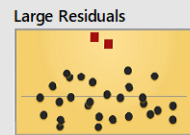
## Multiple Regression for Tco (°C) Diagnostic Report

### Residuals vs Fitted Values



Look for patterns, such as strong curvature or clusters, that may indicate problems with the regression model. Ideally, the points should fall randomly on both sides of zero. Identify any large residuals that could have a strong influence on the model.

Look for these patterns:

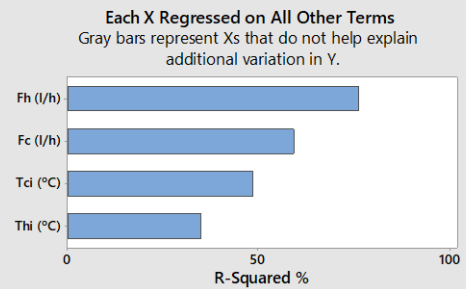
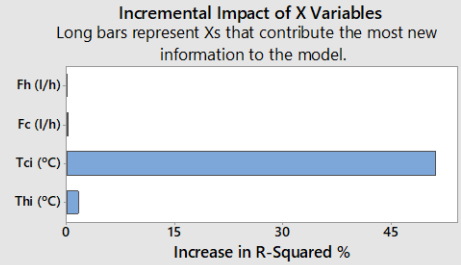
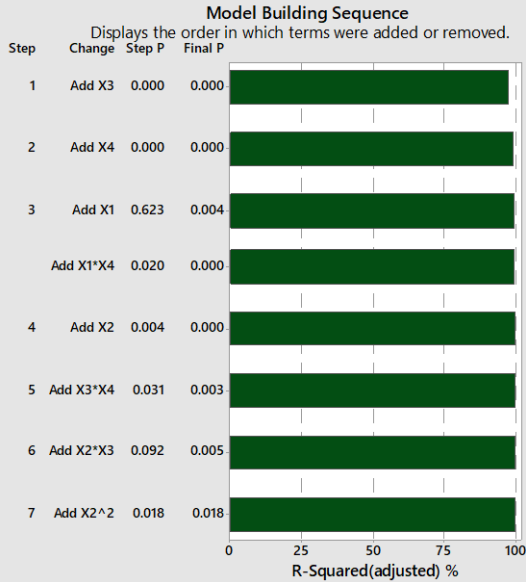


### Multiple Regression for Tco (°C) Model Building Report

X1: Fh (l/h) X2: Fc (l/h) X3: Tci (°C) X4: Thi (°C)

#### Final Model Equation

$$Tco (°C) = 124.6 - 0.1339 X1 + 0.0611 X2 + 0.673 X3 - 2.209 X4 - 0.000036 X2^2 + 0.002116 X1 * X4 + 0.000420 X2 * X3 - 0.00397 X3 * X4$$

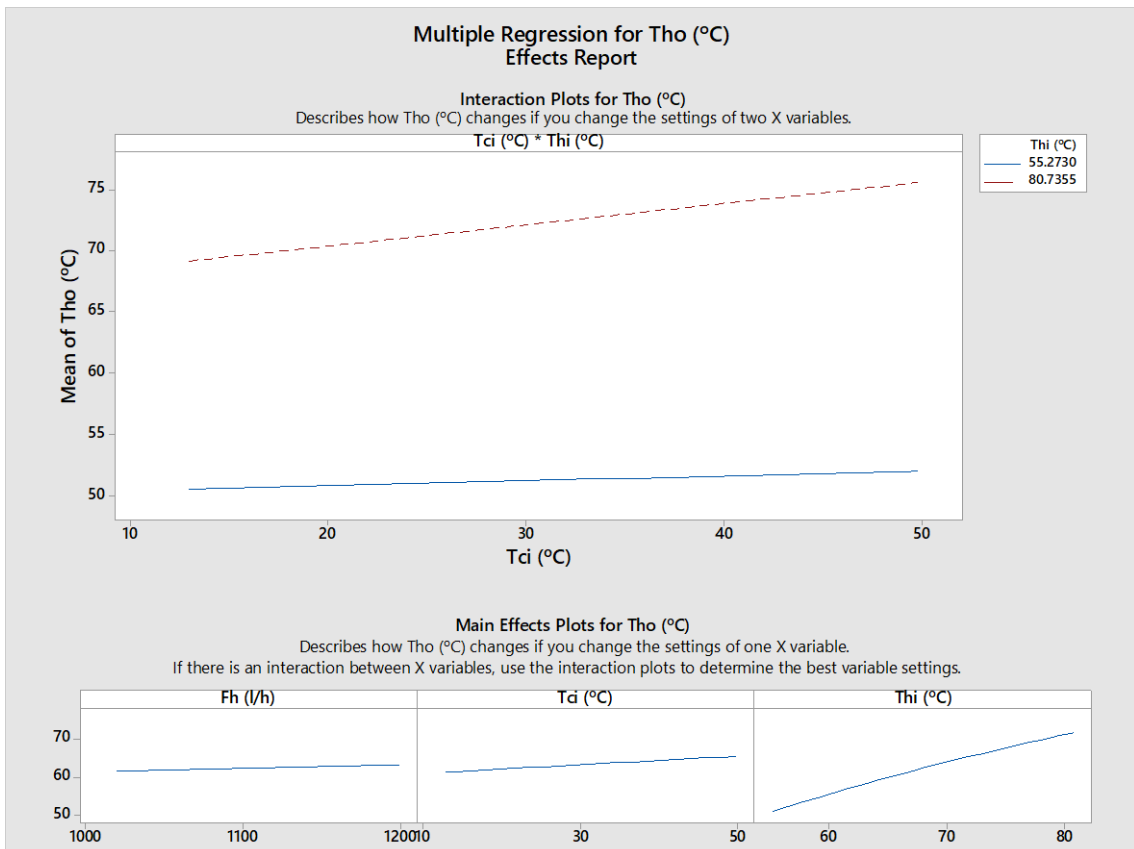
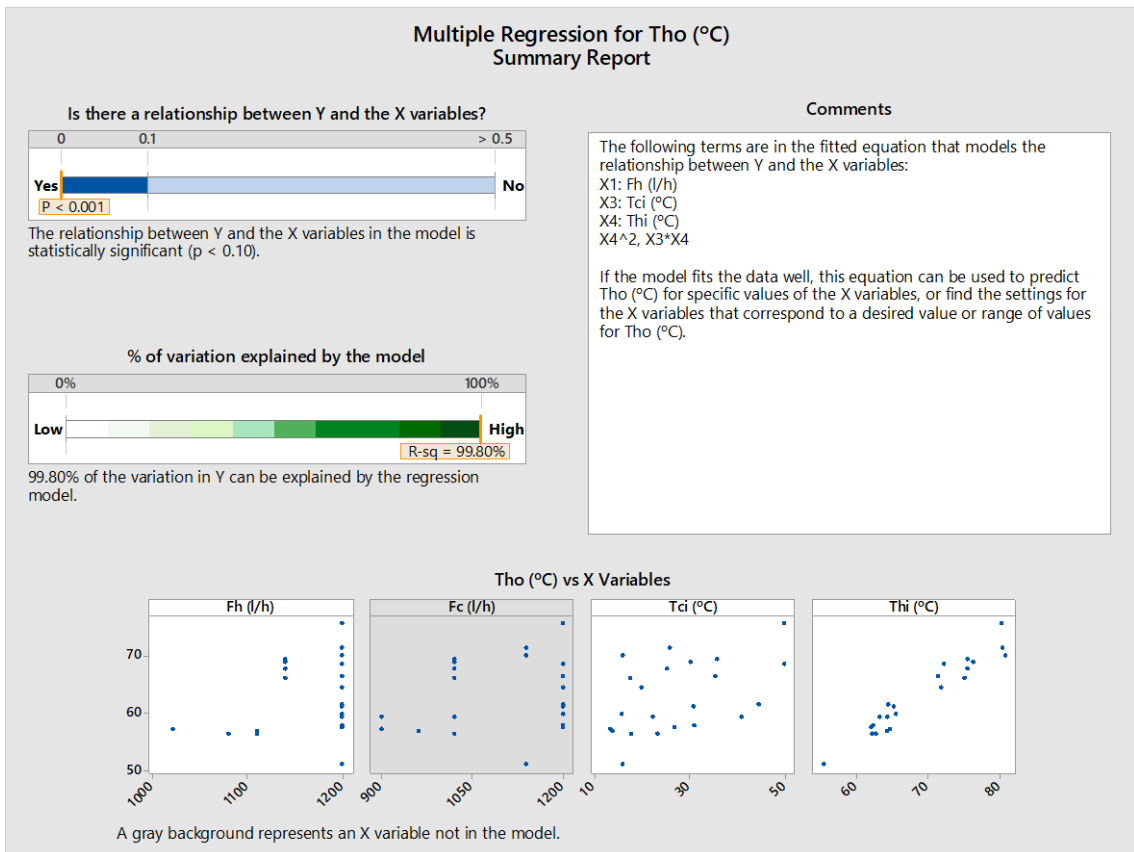


A gray bar represents an X variable not in the model.

### Multiple Regression for Tco (°C) Report Card

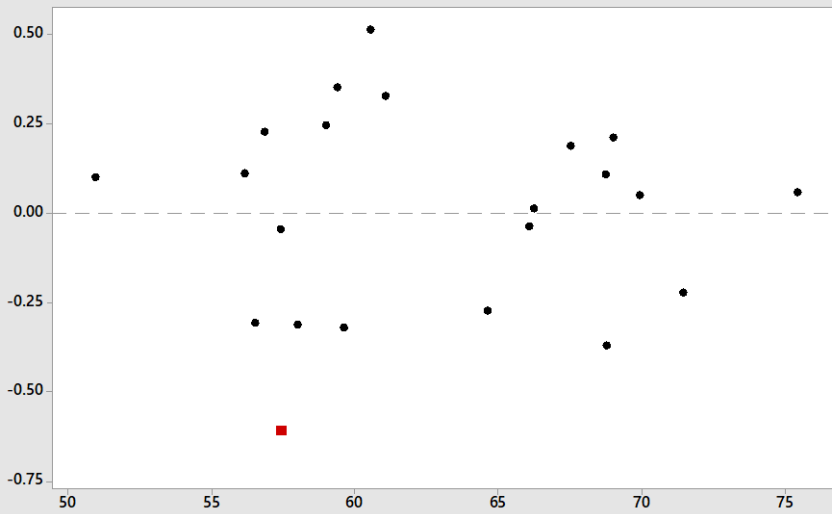
Check	Status	Description
Amount of Data		The sample size (n = 22) is not large enough to provide a very precise estimate of the strength of the relationship. Measures of the strength of the relationship, such as R-Squared and R-Squared (adjusted), can vary a great deal. To obtain a precise estimate, larger samples (typically 50 or more) should be used for a model of this size.
Unusual Data		One data point has a large residual and is not well fit by the equation. This point is marked in red on the Diagnostic Report and is in row 22 of the worksheet. Because unusual data can have a strong influence on the results, try to identify the cause for its unusual nature. Correct any data entry or measurement errors. Consider removing data that are associated with special causes and redoing the analysis.
Normality		Because you have at least 15 data points, normality is not an issue. If the number of data points is small and the residuals are not normally distributed, the p-values used to determine whether there is a significant relationship between the Xs and Y may not be accurate.

## Multiple regression for hot outlet temperature:



### Multiple Regression for Tho (°C) Diagnostic Report

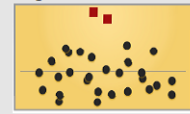
Residuals vs Fitted Values



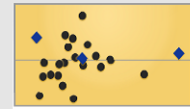
Look for patterns, such as strong curvature or clusters, that may indicate problems with the regression model. Ideally, the points should fall randomly on both sides of zero. Identify any large residuals that could have a strong influence on the model.

Look for these patterns:

Large Residuals



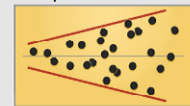
Unusual X Values



Clusters



Unequal Variation



### Multiple Regression for Tho (°C) Model Building Report

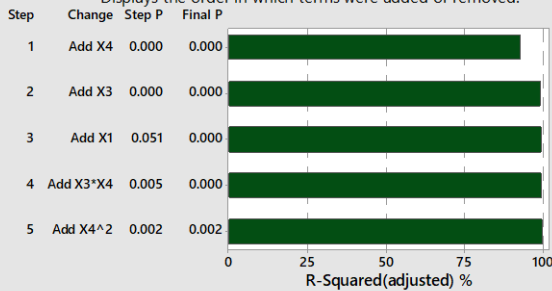
X1: Fh (l/h) X2: Fc (l/h) X3: Tci (°C) X4: Thi (°C)

Final Model Equation

$$\text{Tho (°C)} = -24.90 + 0.00914 X1 - 0.2507 X3 + 1.504 X4 - 0.00618 X4^2 + 0.005262 X3 \times X4$$

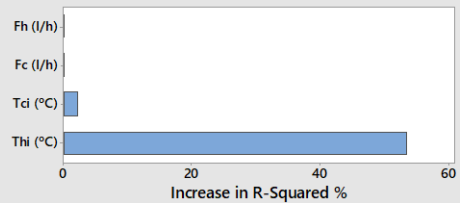
Model Building Sequence

Displays the order in which terms were added or removed.



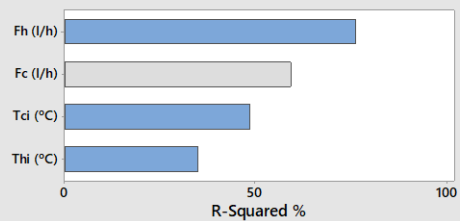
Incremental Impact of X Variables

Long bars represent Xs that contribute the most new information to the model.



Each X Regressed on All Other Terms

Gray bars represent Xs that do not help explain additional variation in Y.



A gray bar represents an X variable not in the model.

Model representation for constant flows (1200 L/h)

